

Revision of *Nicrophorus* in part: new species and inferred phylogeny of the *nepalensis*-group based on evidence from morphology and mitochondrial DNA (Coleoptera: Silphidae: Nicrophorinae)

Derek S. Sikes^{A,D}, Ronald B. Madge^B and Stephen T. Trumbo^C

^ADepartment of Biological Sciences, University of Calgary, 2500 University Drive NW, Calgary, Alberta, T2N 1N4, Canada.

^B1637 16 Street S. E., Calgary, Alberta, T2G 3P6, Canada.

^CDepartment of Ecology and Evolutionary Biology, University of Connecticut, Waterbury, Connecticut, 06710, USA.

^DCorresponding author. Email: dsikes@ucalgary.ca

Abstract. Carrion beetles of the genus *Nicrophorus* Fabricius, 1775 (Silphidae) are well known for their biparental brood care and monopolisation of small vertebrate carcasses in subterranean crypts. Although the taxonomy of New World species has received modern attention, the fauna of Asia, primarily of the *nepalensis*-group of species, has not. Herein we revise this species-group and describe as new the following seven species: *Nicrophorus charon* Sikes & Madge (Sulawesi), *Nicrophorus herscheli* Sikes & Madge (Sumatra), *Nicrophorus insignis* Sikes & Madge (Flores Island), *Nicrophorus melissae* Sikes & Madge (Nepal, Bhutan), *Nicrophorus reticulatus* Sikes & Madge (Guadalcanal), *Nicrophorus schawalleri* Sikes & Madge (Gansu, Shaanxi, Sichuan Province) and *Nicrophorus trumboi* Sikes & Madge (Nepal, Bhutan). We obtained a preliminary phylogeny using morphology and mtDNA (*COII*). This was inferred using maximum likelihood and Bayesian methods with the Mkv and GTR+I+G models (parsimony was rejected by the Akaike information criterion for being excessively parameter-rich). The phylogenetic signal in the morphological dataset was not strong and results were confounded by a ‘long-branch’ species, *N. reticulatus*. The signal was stronger in the combined dataset and the *COII*-only dataset. The molecular phylogeny supported the new status of species *N. trumboi* and *N. melissae*. Support was found for a mainland origin of the group with subsequent radiations into the Malay Archipelago.

Additional keywords: Bayesian phylogenetic inference, China, Himalayas, Malay Archipelago, maximum likelihood, Mkv model, Nepal.

Introduction

Beetles of the genus *Nicrophorus* Fabricius, 1775, (Silphidae: Nicrophorinae), commonly called burying beetles, are among the better-known insect lineages owing to their remarkable reproductive behaviours. Typically, parent beetles work together to attempt to monopolise, bury, encrypt and guard a small vertebrate carcass as a food resource for their larval brood throughout development. These biparental care and nesting behaviours displayed by the parents have been the focus of intense behavioural ecological research over the last few decades (e.g. Anduaga and Huerta 2001; Trumbo *et al.* 2001; Nisimura *et al.* 2002; Rauter and Moore 2002; Smiseth *et al.* 2003). Although the taxonomy of the 21 New World silphid species was revised relatively recently (Peck and Anderson 1985; Sikes and Peck 2000), that of the Old World, particularly Asia, has seen little comprehensive attention since the world revisions of Portevin (1926) and Hatch (1927). Three new Asian species in the subfamily

Nicrophorinae were described by Háva, Schneider and Růžička in two publications (Háva *et al.* 1999; Růžička *et al.* 2000). The most recent taxonomic work including Asian nicrophorine species was the world catalogue of Sikes *et al.* (2002), in which numerous synonymies and nomenclatural changes affecting described species were introduced. In the current paper we focus on inference of the phylogeny and descriptions of new species in the *nepalensis* species-group *sensu* Sikes (2003) of Asia. Species of this group are primarily found in montane regions of eastern Asia and the Malay Archipelago (Fig. 1), ranging in longitude from 73°E (Pakistan) to 149°E (Papua New Guinea) and latitude from 51°N (Ussuri, Russia) to 9°48'S (Papua New Guinea). If the species we are naming *N. reticulatus* belongs to this group, its range will encompass the Solomon Islands and thus extend to 160°E. This is not the only species-group of *Nicrophorus* in Asia – members of at least six other species-groups, of the nine listed in Sikes (2003), occur in Asia.

Although there have been no formally published phylogenetic analyses that have attempted to infer the interrelationships of the species in the *nepalensis*-group, various taxonomists have proposed hypotheses of monophyly in the form of traditional Linnaean classifications. This species-group was first described by Hatch (1927), to contain the following five currently recognised valid species: *Nicrophorus nepalensis* Hope, 1831; *N. podagricus* Portevin, 1920; *N. heurni* Portevin, 1926; *N. quadripunctatus* Kraatz, 1877; and *N. maculifrons* Kraatz, 1877. Hatch (1927) apparently based this grouping on the keys of Portevin (1926, couplets 28 to 36) and Portevin (1923, couplets 14 to 18), who presumably united these species based on their shared possession of a few distinctive morphological traits, most obviously an orange spot on the frons and/or black spots within the orange elytral fascia. He chose the most common and widely occurring species, *N. nepalensis*, for the name of the group. Semenov-Tian-Shanskij (1933), one of the few workers to propose formal subgeneric groupings within *Nicrophorus*, apparently restricted this group to only two species: *N. heurni* and *N. podagricus*, calling it the subgenus *Nesonecrophorus*. He placed the remaining *nepalensis*-group species of Hatch's concept, along with ~40 other species, into *Necropter* – a very heterogeneous subgenus. This arrangement was followed in the species listing by Nishikawa (1986). Růžička *et al.* (2000) included the same

five species that Hatch (1927) had listed, but brought the total to seven by the addition of *N. montivagus* Lewis, 1887 and their newly described species *N. sausai* Růžička, Háva & Schneider, 2000. Based on a morphological phylogenetic analysis, Sikes (2003) concluded that the similarities of *N. sausai* to the *nepalensis*-group species were a result of parallelism (possibly mimicry-driven) and excluded this species from the *nepalensis*-group. Included, however, were *N. apo* Arnett, 1950 and *N. insularis* Grouvelle, 1893, bringing the total valid species count to eight as of 2003.

An adequate test of the monophyly of this species-group requires an analysis of the entire subfamily (D. S. Sikes and S. T. Trumbo, unpublished data). Preliminary phylogenetic analyses of the subfamily, based on morphology and sequence data from the mitochondrial genes *COI* and *COII*, supported the *nepalensis*-group *sensu* Sikes (2003) as monophyletic with a Bayesian posterior probability of 100% (Sikes 2003). Morphologically, all of the included species except *N. reticulatus*, sp. nov. share a unique elytral microsculpturing pattern (Fig. 2), among some other, but homoplastic, character states (see group diagnosis below). Ambiguity, however, was seen with the placement of the species *N. reticulatus*, sp. nov., which was found infrequently as a basal member of the *nepalensis*-group, but most often as a sister-species to the sympatrically distributed *N. kieticus* Mroczkowski, 1959, with this pair together being a sister-

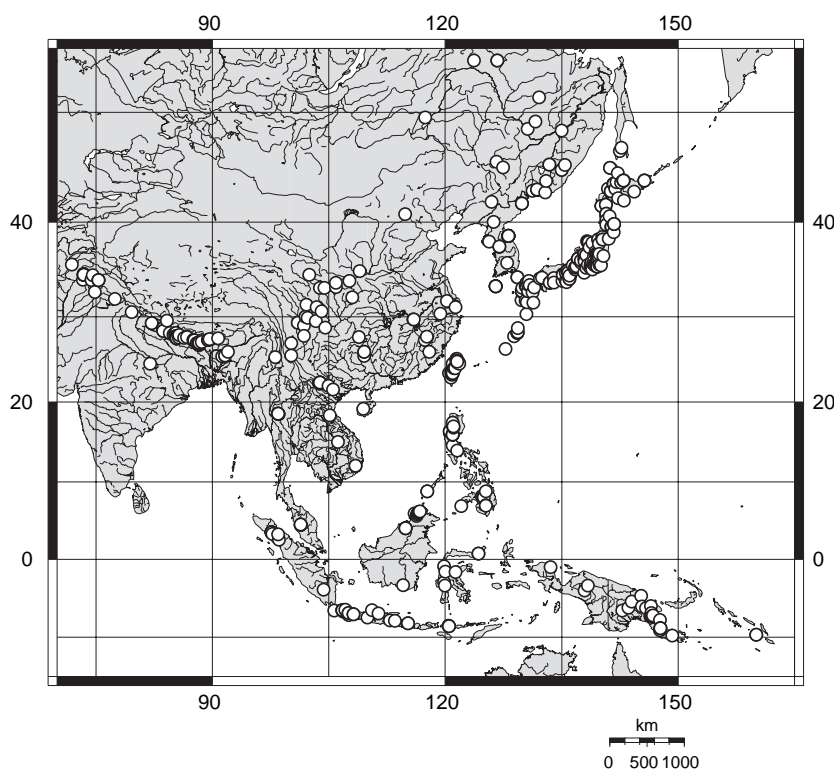


Fig. 1. Distribution of all geo-referenced specimens of the *nepalensis*-group in the genus *Nicrophorus*.

lineage to the *nepalensis*-group (Sikes 2003). Unfortunately, DNA data were not available for the species *N. reticulatus*, sp. nov. and *N. kieticus*, both from the Solomon Islands, so these results were based on morphological data alone. We hypothesise, however, that molecular data, once obtained for these species, will demonstrate that many of the morphological similarities between these two species are a result of parallelism and that *N. reticulatus*, sp. nov., but not *N. kieticus*, will join within the *nepalensis*-group proper.

Some of these species described as new herein had been noted by prior workers and have a history in the literature before their formal naming. Portevin (1926), in describing the distribution of *N. nepalensis* as including Flores Island, had indicated in a footnote (p. 208) 'Le seul spécimen que j'ai vu de cette provenance (collection Oberthur) offre une coloration remarquable'. This is the first known reference to the species we are naming *N. insignis*. This species, and the species we are herein naming *N. charon*, *N. reticulatus* and *N. herscheli*, were also mentioned as undescribed species in

the following three papers (Hanski and Krikken 1991; Hanski and Niemelä 1990; Peck 2001). Emetz and Schawaller (1975) had noted and described as an aberration (and thus an unavailable name) the species we are herein naming *N. melissae*. None of the other species described herein had been previously mentioned in the literature with the exception of their inclusion in the dissertation of Sikes (2003).

The primary goal of this publication is to describe and make names available for several new species of *Nicrophorus*. In addition, the phylogenetic analyses presented herein, which should be considered no more than preliminary, were undertaken to answer the following questions: (1) what is the relationship of the members of the *nepalensis*-group species to one another? (2) do the morphology based species demarcations within this group correspond to discrete mtDNA lineages? and (3) are the conclusions of Portevin (1926) and Emetz and Schawaller (1975), regarding

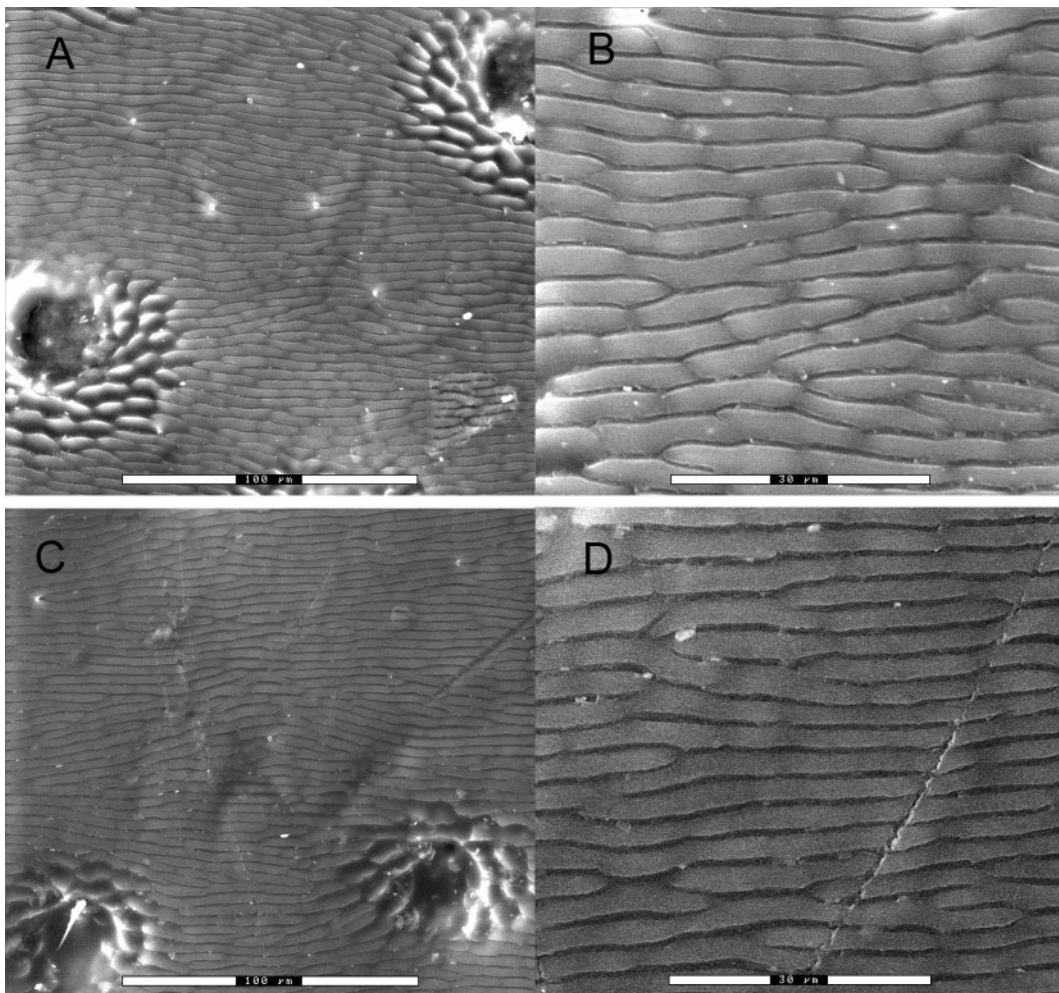


Fig. 2. Environmental scanning electron micrograph of elytral microsculpture of two specimens of *Nicrophorus nepalensis*. A, C, 500 \times . B, D, 1500 \times .

the degree of polymorphism within *N. nepalensis*, supported by molecular data?

Materials and methods

Taxon sampling

All 15 known species of the *nepalensis*-group *sensu* Sikes (2003) were included in analyses. In addition, the species *N. sayi* Laporte, 1840 (eastern North America) and *N. humator* (Gleditsch, 1767) (Europe) were included as outgroups because of their frequent appearance at the base of the *nepalensis*-group in preliminary analyses of the subfamily. The phylogenetic proximity of these outgroup taxa to the *nepalensis*-group is supported by the following morphological characters: posterior margin of the elytron bearing 5–10 clusters of long, dark to light-brown setae; and first abdominal spiracle lobed with a small bulb projecting posteriorly. Finally, the new species *N. reticulatus*, endemic to the Solomon Islands, was included because this species was hypothesised to belong to the *nepalensis*-group by the second author, based on the enlarged male metatibiae typical of this group of species. DNA data were obtained for nine of these 17 species (Appendix 1).

Specimens examined for coding of morphological data and for recording of locality data, belonged to 45 institutions or private collections (430 specimens are part of the first author's research collection) (Appendix 2). A total of 2187 specimens in the *nepalensis*-group was databased. With the exception of private collections, the codens listed in Appendix 2 and used throughout this work are derived from the index prepared by Arnett *et al.* (1993).

The first author studied primary or secondary type specimens of six of the eight described species in the *nepalensis*-group (two type series – those of *N. maculifrons* Kraatz and *N. quadripunctatus* Kraatz – are considered lost). These were used to confirm species diagnostic characters, phylogenetic characters and to test species status for questionable names. Lectotypes and paralectotypes were designated for all names that we considered valid and for which we had studied the syntype series. Details of these type specimens, including label data for lectotype and paralectotype designations, type depositories, sex and number of specimens etc. are presented in the taxonomic catalogue of Sikes *et al.* (2002).

Specimen preparation and examination

All DNA vouchers are kept one beetle per vial in 95–100% ethanol in an ultracold –80°C freezer. To investigate within-species genetic variation and to help prevent laboratory errors, such as tube mix-ups or misidentifications, an effort was made to sample two or more specimens for each species, preferably taken from distant portions of the species' range (Appendix 1). Extractions of these extra samples were made on different days.

Morphological data were scored based on examination of all known specimens for rare species (~1–30 specimens known), with the exception of characters that required dissection, which were studied on fewer individuals as deemed sufficient. For non-rare species, variable numbers of specimens were examined depending on the character. Characters that showed signs of polymorphism within a species were examined on numerous specimens for each species. Characters requiring dissection were examined on few specimens, as were characters that showed no signs of polymorphism. A synoptic set of specimens that had been brought to Europe and compared side-by-side with type specimens was used extensively for character coding.

Some specimens were dissected to allow observations of the genitalia, wings or metasternal apophysis (metendosternite). Dissection of the genitalia was accomplished after softening the posterior of a beetle in almost boiling water for 5–10 min. Dissected genitalia were mounted on stiff cards using glue. These cards were placed below the beetle, but above the labels on the pin. Observation of the metendosternite required

destruction of the thorax and abdomen of the beetle so this feature was not studied for all species. Observations were made with a Wild M3C stereo dissecting microscope (maximum 80× magnification, Heerbrugg, Switzerland). Measurements are given as mean ± standard deviation.

Few specimen labels included geocoordinate data. Three major sources were used to geo-reference records (associate geocoordinates with names of localities): The Getty Thesaurus of Geographic Names On Line (www.getty.edu/research/tools/vocabulary/tgn/, verified March 2006), The Alexandria Digital Library Gazetteer Server (<http://middleware.alexandria.ucsb.edu/client/gaz/adl/index.jsp>, verified March 2006) and the GEOnet Names Server (<http://gnswww.nga.mil/geonames/GNS/index.jsp>, verified March 2006). In some cases, localities could not be found with these gazetteers or the localities had too many possible matches. All label data are listed in the material examined, but only confidently georeferenced data are plotted on the maps. Any data not present on specimen labels, but listed here, are placed in square brackets (e.g. country name, lat / long). Asterisks (**) indicate material found at the same higher locality. The country for some label data localities could not be determined, these are listed as 'country not found'. Complete specimen label data are provided for species newly described herein. A complete list of material examined is available as 'Accessory Material' on the *Invertebrate Systematics* webpage, it includes material examined data for previously described species. A label bearing a unique alphanumeric code was placed on the pin of each specimen examined. These codes are listed in the material examined data for type specimens to provide unambiguous association of specimens with data. Each code has a three or four letter prefix that is the abbreviation for the depository of the specimen. Synonymy lists are not provided for each species because this information is available in the world catalogue of Sikes *et al.* (2002).

Collecting and breeding

We used two protocols to collect beetles depending on whether the specimens were intended for DNA extraction or museum preparation. Details of the trap design are the same for both methods with the exception that specimens intended for DNA extraction must be kept alive in the traps before their removal. Specimens trapped for museum preparation can be killed in the traps using a preservative such as propylene glycol. This latter method allows traps to remain unemptied for over two weeks, whereas the live-trapping protocol requires the traps be emptied within 48 h, preferably within 24 h, or the beetles will die in the traps. If the beetles die in the traps, even within 24 h of collection, their DNA usually degrades sufficiently to make extraction and sequencing more trouble-prone.

For forest-dwelling species, traps suspended at head-height from tree trunks or similar structures are the most efficient means to trap microphorines (efficiency meaning maximisation of microphorines caught per 'unit' trap set-up effort). Suspending traps in trees has at least two major advantages over the traditional ground-level pitfall trap. The bait (rotten meat) is attractive to vertebrates and scavengers more often destroy ground-level traps than tree-suspended traps. Another advantage is that tree-suspended traps are simple to set up because they do not require digging. A possible disadvantage is that tree-suspended traps catch few non-microphorine beetles (few to no scarabs, carabids, etc.) that are typically present in ground pitfalls. Microphorine beetles, however, show equal or greater persistence in accessing the bait in tree-suspended traps as they do the bait in ground-level pitfalls. The traps themselves can be of any convenient material or size (2 L plastic bottles with a wide (10+ cm) opening work quite well) and may be hung using wire or string, or simply nailed to trees. The bait must be rotten meat of some sort (chicken or fish work well).

Although generalisations about habitat types preferred by microphorines are of questionable value, when faced with a diversity of habitats it is best to select cooler, moister habitats with deeper humus

layers (e.g. north-facing rather than south-facing slopes and forested rather than open habitat). Note, however, that some species are grassland specialists, although no members of the *nepalensis*-groups appear to be so.

To rot the bait (chicken or fish), place raw meat inside ziplock bags and then put these bags inside a tightly sealed PVC bucket or a larger garbage bag. The bait usually smells terrible within 3–5 days when kept at 20°C or higher. The use of individual bags allows the bait to be moved into the traps without touching it. Numerous holes in the bottom of the traps, or some form of rain-roof, helps prevent rain from drowning live-trapped beetles.

For best preservation of DNA for later extraction, specimens must be trapped alive. Upon removal from the traps, each live specimen is placed into its own 15–35+ mL vial (5–10+ drams) of 95–100% ethanol. *Nicrophorus* beetles are challenging to preserve because they appear to have a lot of water and/or lipids in their bodies and these substances degrade or inhibit DNA extraction so rapid dehydration is important. There are two methods to facilitate dehydration: before placing a live beetle into a vial of ethanol, remove one or both hind legs and place them in the vial first, then add the rest of the beetle. This procedure allows the muscle tissues of the hind legs to be quickly dehydrated. In addition to this, replacing the ethanol (which will have become diluted by the water in the beetle's body) after 24 h also facilitates dehydration. Obviously, having too small a vial or too little ethanol (which could result from putting multiple beetles in the same vial) is less effective. Keeping the vials as cold as possible also improves the chances of successful DNA extraction. Finally, into each vial should be placed a data label written in permanent ink or pencil with as much information as possible, especially geocoordinate data.

Larvae are most easily obtained by breeding microphorines in the laboratory. Descriptions of breeding protocols can be found in myriad papers on *Nicrophorus* (especially in the behavioural and ecological literature). Laboratory colonies of adults of most species are easy to maintain but require constant attention. All microphorines that we have kept alive are cannibalistic and will eat each other if they run out of food (or, sometimes, for unknown reasons). Thus, it is best to keep adults separated, although this may be impractical for large colonies. Heat and moisture are the two variables that seem to have the greatest influence on keeping these beetles alive. They do best in cool temperatures (< 18°C) and seem to be unable to survive for even short periods without a constant supply of water (and/or high humidity). We found that using damp paper towels inside large plastic boxes with small air holes works well. The towels absorb the beetles' faeces and can be easily replaced every few days. They can be fed small pieces of old chicken liver or large meal worms every few days.

Breeding the beetles was accomplished by putting a male and a female with a freshly killed mouse inside a large, sealed container filled with potting soil. The container was left in a dark place and if the beetles were going to breed they would typically bury the mouse within 24 h. Oviposition takes place during the first few days and first instars appear at the carcass in the subterranean chamber approximately five days after burial. Third (final) instars are available between Days 8 and 14. Larvae are best preserved by killing them in subboiling water and storing them in vials of 70% ethanol.

Gene choice

Although the gene sequenced was mitochondrial, the nuclear genome was not unsampled – the morphological data represent a wide sampling of unspecified regions of the nuclear genome. Hillis and Wiens (2000) provide a nice contrast of the use of both morphology and molecular data for phylogenetic inference and emphasise, as we do here, the advantages of using both together.

Mitochondrial DNA sequence data have been shown repeatedly to be of value in phylogenetic inference of closely related species (e.g.

Simon *et al.* 1994; Stepan 1998; Serb *et al.* 2001), but saturation of these relatively fast genes reduces their value for reconstructing ancient divergences (e.g. Liu and Beckenbach 1992). Having data representing the nuclear genome is important because mtDNA genes are inherited as a single linkage group and thus any mismatch between gene and population histories will affect all mtDNA markers (Moore 1995; Maddison 1997). However, despite this concern, as pointed out by Moore (1995) and reiterated by Wiens and Penkrot (2002), because the mitochondrial genome's effective population size is effectively one-fourth that of a nuclear-autosomal gene, mtDNA of a given species will become monophyletic (i.e. coalesce) four times more quickly than the variation in a nuclear gene (given certain assumptions). Thus, a mtDNA gene has a significantly greater chance of accurately reflecting the population history on a short internode than does a nuclear gene (Moore 1995). Moore (1995) estimated that one would need to sample 16 nuclear genes to achieve the same confidence in accuracy of phylogenetic inference as one mtDNA gene. The gene cytochrome oxidase II was chosen because preliminary work with this marker indicated that it provided a considerable number of phylogenetically informative sites and it was relatively trouble-free to amplify and sequence.

Morphological characters

All morphological data were managed using MacClade 4.04 OSX (Maddison and Maddison 2001) in one NEXUS file. Species descriptions were prepared by editing the output generated by use of the 'export descriptions' menu option of MacClade.

Characters selected included all those used in prior phylogenetic analyses of these taxa, although these characters were all re-assessed and in many cases changed (usually by increasing the number of character states). The majority of characters, however, are novel. Internal morphology was not well evaluated, for example the proventriculus, alimentary canal, glands, soft reproductive organs and other components of the internal anatomy were not studied. Additionally, no characters of the eggs or pupae were included. Characters were given weight = 1 for analyses if the character showed discontinuous variation within the ingroup and the states were largely invariant within species. Some characters with polymorphic states in certain species were used, however.

Often, numerous characters may be coded from a structure that is absent from various taxa. For example, we have coded various characters based on the shape of the fascia of the elytra; however, there are species that lack fascia altogether (they are 100% black). These different characters would be 'inapplicable' (Maddison 1993) to these all-black species. Inapplicable character states were assigned a gap value '-' and treated equivalent to missing data ('?') during computer analyses. This method of handling inapplicables has been termed 'reductive coding' (Strong and Lipscomb 1999) and is considered by many investigators who have dealt with inapplicables in phylogenetic inference, including us, to be the best solution to handling such characters (Strong and Lipscomb 1999). Readers interested in the issue of how to handle inapplicable characters are directed to the following additional papers on this topic: Nixon and Davis (1991), Platnick *et al.* (1991), Maddison (1993), Wilkinson (1995a, 1995b) and Hawkins *et al.* (1997). The issue of how to code inapplicables in morphological data is almost identical to the issue of how to treat indels (insertion/deletion events, gaps) in molecular data, particularly whether to code each site of an indel as a fifth state or as missing data. There is a rich literature on this subject (e.g. Giribet and Wheeler 1999, Lutzoni *et al.* 2000, Simmons and Ochoterena 2000) and the same concerns apply – coding gaps as a fifth state can result in these states being found apomorphic, which can lead to overestimated support for certain branches or even inaccurate phylogenetic reconstructions. The effects of coding as a 'fifth state' are dependent on how many characters are so coded and whether they take apomorphic or plesiomorphic polarities. If a single apomorphic deletion event resulted in the loss of hundreds of sites and

each site is coded as a fifth state, the taxa with the deletion would be held together based on hundreds of characters rather than a more appropriate single character that represents a single deletion event.

All character codings before analyses represent primary homology statements that are hypotheses to be tested during the analysis (Patterson 1982; de Pinna 1991). The single origin of a character state on an inferred phylogeny is consistent with a hypothesis of homology, whereas multiple originations of a character state are inconsistent with a hypothesis of homology.

The descriptions of morphological characters (Table 1) attempt to explain the homology statements we have made with some discussion based on prior studies in the literature and minor post-analysis discussion. States were not polarised before tree searching, which was conducted on unrooted networks (Nixon and Carpenter 1993). All characters were unordered and weighted either 1 or 0. Characters weighted 0 were included either for descriptive purposes or for later mapping on final trees, but, obviously, did not influence the topology. Table 2 includes only characters of weight = 1. The decision to weight a character 0 was based on either pre- or post-analysis assessment of that character's value to corroborative homology assessment. Most investigations that involve the construction of a new dataset (i.e. one not assembled from previously published characters) include at least two stages of selection: an initial pre-analysis selection of potentially useful characters, which involves the rejection of constant and apparently hypervariable characters, and a second selection after a matrix has been made and the data have been explored. This second, post-analysis selection is used to reject characters that show excessive homoplasy (some of these characters can be re-evaluated and new state assignments and/or homology assessments can eliminate obvious mistakes or excessive homoplasy). Some homoplasy is unquestionably 'real' in that actual convergence on the same state has occurred (these characters, after re-evaluation, were not changed), other homoplasy is the result of mistaken state assignment (these characters, after re-evaluation, were changed), and some characters were simply ambiguous. These ambiguous homoplastic characters were not clearly the former or latter of these cases, and because they showed major conflict with other, less ambiguous characters, the safest way to handle them was to assign them zero-weights.

For many characters the outgroup taxa show the state assigned 'zero'; however, this is not the case for all the characters and state 'zero' should not be assumed to represent the ancestral state.

We coded many autapomorphic characters for several reasons. These are characters that are not parsimoniously informative because they change only once and do so on a terminal branch, thus not uniting any branches. We used the same matrix for management of both descriptive and phylogenetic characters, and autapomorphies are important for descriptions and diagnoses of taxa. In addition, we consider branch length, i.e. the estimated amount of change that has occurred on a branch, to be important to phylogenetic inference. Some terminal taxa have relatively high numbers of autapomorphies and thus are long branches, suggesting that they may be relics (most close relatives are extinct), lineages with higher rates of change, or unusual in other ways. If these numerous autapomorphies were ignored, the atypical status of these taxa might be missed and would not be illustrated on the topologies produced. This branch length information can be used to better assess the confidence one has in the placement of these taxa. Seeing, for example, an extremely long branch connect within a derived clade of short branches immediately suggests that although it may belong within the clade, it is clearly different in many respects from other members of that clade.

Although the parsimony optimality criterion ignores autapomorphies while choosing topologies, maximum likelihood, which can now be used to infer phylogenies from morphological data using Bayesian Inference (Lewis 2001), does not. Unlike equally weighted

parsimony, likelihood does not consider all possible changes equally likely – it allows synapomorphies to be more or less likely depending on various other types of information, such as the amount of change within the lineages in question. Parsimony attempts to explain all shared states as synapomorphies, returning a verdict of homoplasy only when conflict among characters results from numerical dominance of some characters over others. The logic of likelihood's behaviour is based on the notion that a randomly chosen pair of lineages that have each shown many changes relative to other taxa, are more likely to share some of their states due to chance than a randomly chosen pair of taxa that each have amounts of change close to the average for other taxa. Because likelihood expects a higher probability of convergence events between such high-rate lineages, it requires a proportionally greater amount of evidence to overcome the hypothesis of convergence, i.e. it effectively downweights potential synapomorphies among longer lineages to help account for the greater than average possibility that they are not synapomorphies but are convergent. Likelihood thus assesses, not only the quantity of evidence for competing topologies but the quality of the evidence as well. The assessment of quality is based on the accumulated understanding of how evolution proceeds, for example the well documented observation that transition events in nucleotide sequence data are generally more common than transversion events (reviewed in Simon *et al.* 1994). Some systematists contend that assessing the quality of characters introduces bias into an analysis and the topology should be determined only by the quantity of characters supporting a given topology. Their logic is simple: there should be more characters that agree with the true topology than characters that agree with a false topology. Misleading, or homoplasious, characters should conflict not only with truthful characters, but among themselves as well. The debate in the systematics community over this issue is an old one. We contend that complete removal of quality assessment of characters in the hope of obtaining a perfectly objective science is impossible. Most morphologists, for example, consciously decide which characters to include in their matrices – ignoring in many cases hypervariable, highly homoplasious, or sexually selected characters. By doing so they have implicitly employed character weights of 0 and 1 as we have done, although explicitly, in this study.

In the character discussion in Table 1, there appear a few cases that are best explained by a general protocol. In these cases we divided a character into what might appear to be an excessive number of states. Our justification for this is based on our preference for erring on the side of loss of information rather than the addition of misinformation to the matrix. When homologies among distantly related taxa, that, for example, span the basal splits of the tree, are questionable, we find it safer to consider the taxa as possessing separate states (presuming the taxa do indeed show differences of some sort in the character in question) than to risk coding them as homologous in error (and thus introducing homoplasy to the dataset). In addition, for a small set of characters, species could not be confidently assigned to a state (due to inaccessibility of the structure on species known from few specimens or due to variability in the structure and other reasons). These taxa were coded as inapplicable (–) or missing (?) based on the same logic – that is, letting the remaining characters determine the value that belongs in the empty cell of the matrix.

DNA extraction, amplification and sequencing

DNA was extracted from beetle hind legs using Qiagen DNeasy Tissue Kits (www.qiagen.com, verified May 2006), although some earlier samples were extracted using a cationic detergent cetyl-trimethylammonium bromide (CTAB)/dodecyltrimethylammonium bromide (DTAB) (Gustincich *et al.* 1991), or a phenol/chloroform protocol (Sambrook *et al.* 1989). The protein-coding mitochondrial gene cytochrome oxidase II (*COII*) was successfully sequenced, including portions of the tRNAs flanking *COII* (tRNA leucine, tRNA lysine, and

Table 1. Character descriptions for morphological data used in phylogenetic analysis of the *nepalensis*-group of species in the genus *Nicrophorus*

All characters were weighted equally and unordered, thus state 0 is not always the ancestral state. State numbers are not in all cases contiguous (e.g. 0, 1, 2, etc.) because this dataset is a subset of a larger dataset in which all intermediary states are included, and of which some states were not present among members of the species analysed herein. See Table 2 for data matrix. Despite the poor resolution of the preliminary phylogenetic estimates for this species-group we discuss the inferred evolution of these characters below where it is possible.

Head

- (1) *Antennal club colour*: 0, entirely orange; 1, basal segment black, apical three orange; 2, basal three segments black, apical orange.
All included species have the basal antennal club segment black and the apical three segments orange with *N. trumboi* being polymorphic and showing in most specimens a distinct pale, almost entirely orange basal segment of the club. Having only the apical segment of the club orange is an autapomorphy of *N. montivagus*.
- (2) *Frons*: 0, black, with orange spot; 1, black, without orange spot.
An orange spot on the frons seems to be a basic feature of the group. Rarely the spot is absent in *N. montivagus* and *N. nepalensis*. The outgroup species, *N. sayi* and *N. humator*, lack an orange spot on the frons which is shared by *N. reticulatus* – a lineage questionably reconstructed as a member of the basal polytomy of the species-group (Fig. 4). The majority of the species in the *nepalensis*-group have an orange spot on the frons with the exception of a derived clade of three species: *N. insularis*, *N. charon*, and *N. heurni*. Their derived placement on the trees of all three analyses (Figs 4, 6, 7) suggests this character has undergone a reversal to the ancestral state. These three derived species are biogeographically close, being found on Sumatra, Sulawesi, and New Guinea respectively. *Nicrophorus reticulatus*, based on the branch length reconstructions in Figs 4 and 6, has experienced considerable morphological evolution relative to other members of the species-group. This species is endemic to the island of Guadalcanal of the Solomon Islands and is thus geographically closest to *N. heurni* of New Guinea. This character alone, plus geographic proximity, suggests that the placement of this species in Figs 4, 6, and 7 is incorrect.
- (3) *Post-ocular bulge of large males*: 0, larger than females; 1, equal to size of females.
Two species show polymorphism for this character: *N. humator* and *N. montivagus* whereas in all other species the post-ocular bulge of the largest males is larger than in the largest females.

Thorax

- (4) *Mean pronotal width*: 0, greater than 4.5 mm; 1, less than 4.5 mm.
Only one *Nicrophorus* species is of equal or smaller size as species of the genus *Ptomascopus*, and that is *N. montivagus*, with an average pronotal width of 4.2 mm. Excepting this species, the average pronotal widths of *Nicrophorus* species range from 4.6 mm to 11.2 mm (Sikes 2003). State 1 is thus an autapomorphy for *N. montivagus* in this analysis.
- (5) *Pronotum of large males*: 0, orbicular; 1, subquadrate.
With the exception of *N. reticulatus* and *N. quadripunctatus* a subquadrate pronotum of large males appears to be ancestral, being shared by the outgroup and most of the basal taxa and an orbicular pronotum of large males is seen only in the more derived species.
- (6) *Setae on posteroventral portion of hypomeron*: 0, absent; 5, long, erect, sparse filling region extending a third or less of the length between trochantin and posterior margin, restricted to upper region of sclerite.
All species have setae in this region as described for state 5 with the exception of *N. reticulatus*, which is autapomorphic in being glabrous.
- (7) *Epipleuron*: 0, entirely orange; 1, not entirely orange.
The majority of species in the group including all the basal species excepting *N. reticulatus* have the presumably ancestral state of having entirely orange epipleura. One outgroup species *N. humator*, and three ingroup species, *N. reticulatus*, *N. charon*, and *N. heurni*, have epipleura that are not entirely orange. This is another character, like characters 5 and 2, which suggests *N. reticulatus* may be more closely related to *N. charon* and *N. heurni* than its current placement (Figs 4, 6) suggests, as the second author hypothesises (Fig. 3).
- (8) *Epipleuron (if not entirely orange)*: 1, entirely black; 4, black throughout, medial (dorsal) half orange.
All species with state 0 for character 7 were coded inapplicable (–) for this character. An entirely black epipleuron is shared by *N. reticulatus* and *N. humator*, whereas state 4 is shared by the sister species *N. charon* and *N. heurni*. However, two of the three paratypes of *N. reticulatus* show a small region of dark orange in the posterior dorsal portion of their epipleura and thus this species was coded as polymorphic for this character.
- (9) *Posterior epipleural ridge*: 0, with isolated single-file row of contiguous preapical setae; 2, without isolated single-file row of contiguous preapical setae.
All species have setae as described for state 0 with the exception of *N. reticulatus* which is autapomorphic in lacking this row of setae. This species is atypical in showing numerous losses and reductions of setae throughout the body.
- (10) *Epipleural ridge*: 0, short, to tip of scutellum; 1, long, to middle of scutellum.
All ingroup species have an epipleural ridge that is considered short in reaching only to the tip of the scutellum whereas both outgroup species have a long ridge which reaches to the middle of the scutellum.
- (11) *Epipleuron*: 0, glabrous, or with very sparse, extremely small setae (approximately the size of a puncture); 5, with sparse, short, recumbent, yellow setae throughout.
All species have sparse setae on their epipleura with the exception of *N. reticulatus* which is autapomorphic in being glabrous. This species is atypical in showing numerous losses and reductions of setae throughout the body.
- (12) *Elytra*: 0, entirely black; 1, bicoloured and bifasciate.
All species have bicoloured and bifasciate (or bimaculate) elytra with the exception of the outgroup species, *N. humator*, which is autapomorphic in having solid black elytra.
- (13) *Region adjacent to apex of elytral suture*: 0, black; 1, orange or yellow.
All species have this region black with the exception of *N. quadripunctatus* which is autapomorphic in having this region solid orange.

(continued next page)

Table 1. (continued)

- (14) *Anterior fascia of elytron*: 0, with black spot completely surrounded by fascia; 1, without black spot; 2, with black spot incompletely surrounded by fascia, joined to basal band.
A complex character. An incompletely surrounded black spot is seen in three species: the sister species pair *N. maculifrons* and *N. montivagus* (which are polymorphic for this state and state 1) and *N. podagricus* which shows only state 2. This latter species thus is inferred to have evolved from a ancestor with a complete black spot and undergone a change to an incomplete black spot. A complete black spot is seen in the most derived species: *N. insularis*, *N. nepalensis*, *N. charon*, and *N. heurni* including *N. quadripunctatus*. This indicates that this character state, although present in the namesake of the species-group, *N. nepalensis*, is representative of only the more derived members of the group and an anterior fascia lacking a black spot is the ancestral condition. These conclusions are supported by all three analyses: *COII*, morphology, and combined (Figs 4–7).
- (15) *Anterior fascia of elytron*: 0, passing first costa but not reaching the suture; 1, reaching suture; 2, stopping at or just before first costa as a wide band; 6, small, triangular-square, just reaching 2nd costa (6).
Most species show state 0. *Nicrophorus quadripunctatus* is autapomorphic for state 1, *N. melissae* is polymorphic – the western specimens from Nepal show state 0 but the eastern specimens from Bhutan show state 2. The last state, 6, is one of many autapomorphies of *N. reticulatus*.
- (16) *Anterior fascia between costae, anterior margin*: 1, u-shaped between costae 1 and 2 (with bottom of u towards posterior); 2, u-shaped between costae 3 and 4 (with bottom of u towards posterior). All species show state 1 with the exception of *N. reticulatus*, which is autapomorphic for state 2.
- (17) *Posterior fascia*: 0, not touching lateral or posterior margins of elytron; 1, touching lateral and posterior margins of elytron.
Most species show state 0, however, three species show state 1: *N. nepalensis*, *N. insignis*, and *N. quadripunctatus*.
- (18) *Black spot of elytral posterior fascia near anterior margin of fascia*: 0, present on callus; 1, absent.
This character is almost evenly split among the species of the *nepalensis*-group.
- (19) *Black spot of elytral posterior fascia near anterior margin of fascia*: 0, complete, surrounded by fascia; 1, incomplete, joining black elytral disc.
This character is either inapplicable, or is typically seen as state 1. Only *N. nepalensis* and *N. quadripunctatus* show state 0 (although rarely *N. nepalensis* shows state 1, but we did not code this species as polymorphic because > 99% of specimens show state 0).
- (20) *Black spot of elytral posterior fascia near posterior margin of fascia*: 0, absent, region black; 1, present between costa 1 and 2 and incompletely surrounded by fascia; 4, absent, region within fascia.
Most of the basal species show state 0 and most of the derived species show state 1. Only *N. quadripunctatus* and *N. insignis* show state 4.
- (21) *Elytral posterior fascia*: 0, reduced, interrupted before suture; 1, enlarged, not interrupted; 2, greatly reduced, far from suture, jagged.
This character may be correlated with the previous. All species show state 0 except *N. reticulatus* which shows state 2, and *N. insignis* and *N. quadripunctatus* which show state 1.
- (22) *Elytral microsculpture*: 0, isodiametric; 7, transverse straight, narrow with breaks.
All species show state 7 except *N. reticulatus* which is autapomorphic for state 0.
- (23) *Posterior margin of elytron*: 1, with some or all setae in distinct clusters; 2, glabrous.
Although *N. trumboi* shows a reduction in the number and size of the setae on the posterior margin of the elytra, only *N. reticulatus* is totally glabrous (state 2).
- (24) *Metanotal subalare*: 1, with gradually rising ridge along anteriomedial edge; 3, with sharply rising, internally margined ridge along anteriomedial edge.
This sclerite can only be viewed if an elytron and wing are removed – it is located just posterior to the wing hinge. All species of the ingroup show state 3 except *N. reticulatus* which shows the state of the outgroup (1). This character may be responsible for some of the ‘rogue’ behaviour of *N. reticulatus* and further study is warranted.
- (25) *Metasternal pubescence medially*: 0, short, fine; 1, long, well developed.
All species show state 1 except *N. heurni* which is autapomorphic for state 0.
- (26) *Metasternal pubescence*: 0, dark brown; 1, golden; 2, light brown.
Nicrophorus charon and *N. heurni* are the only species that show state 0 and *N. maculifrons* and *N. montivagus* are the only species that show state 1 (although *N. schawalleri* is polymorphic with some individuals showing light brown pubescence and others showing golden pubescence).
- (27) *Metapimeral posterior lobe*: 1, with long brown setae throughout lobe; 3, with short brown setae throughout lobe.
All species show state 1 except *N. reticulatus* which is, again, autapomorphic for a setal reduction character (state 3).
- (28) *Stridulatory files*: 0, parallel; 1, diverging anteriorly.
All ingroup species show state 0 and both outgroup species show state 1.
- (29) *First abdominal spiracle*: 0, lobe normal size or absent; 1, lobe large.
All species show state 0 except *N. charon* which is autapomorphic for state 1. This is one of the best characters indicating the allopatric, but closely related forms, *N. heurni* and *N. charon*, are distinct species.
- (30) *Setae cluster on centre of sternite 3 between metacoxae*: 0, dark brown; 2, light brown; 4, absent in centre but with long erect setae lateral of centre under coxae.
The outgroup species show state 0 and most ingroup species show state 2. Three apparent independent originations of state 4 are seen: *N. apo*, *N. heurni*, and *N. reticulatus*.
- (31) *Tergite 9 of males (pygidium)*: 0, with golden setae; 1, with brown setae.
All ingroup and outgroups species show state 1, *N. reticulatus* is autapomorphic for state 0.

(continued next page)

Table 1. (continued)

Legs

- (32) *Anterior face of protrochantin*: 1, with sparse, long setae along outer margin, glabrous inner face; 3, with regions of dense pubescence composed of short, recumbent golden setae.
Both outgroup species show state 1 and all ingroup species show state 3.
- (33) *Lateral margin of anterior of procoxae*: 0, smooth, without ridge or bump, or with elongate low ridge; 1, with distinct bump-like, short, raised ridge.
All ingroup and outgroup species show state 0, however, *N. podagricus* is polymorphic and shows state 1 also.
- (34) *Meso- and metatibia apical angle*: 0, not produced into spine or lobe; 2, produced into lobe.
The outgroup species and *N. maculifrons* + *N. montivagus* show state 0 whereas all the remaining ingroup species show state 2.
- (35) *Inner margin of metatibia of large males* (Fig. 15): 0, straight or gradually curved inwards; 1, gradually curved outwards (Fig. 15C, D, E); 2, with a prebasal bump (Fig. 15A, B).
Both outgroup species show state 0 and most ingroup species show state 2. State 1 apparently originated independently at least three times (*N. trumboi*, *N. quadripunctatus*, the derived clade of *N. charon*+*N. heurni*+*N. podagricus*+*N. insularis*+*N. reticulatus*). Although *N. reticulatus* does not always join within the indicated clade, this character is further evidence for its placement therein.
- (36) *Middle of outer margin of metatibia*: 1, not swollen; 2, slightly swollen in large males.
State 1 is seen in the outgroup and the basal lineages of the ingroup: *N. trumboi*, *N. schawalleri*, *N. maculifrons*, and *N. montivagus*. State 2 is seen in the remaining, derived members of the ingroup (further evidence that *N. reticulatus* is not basal).
- (37) *Middle of inner face of metatibia (large males)*: 0, not greatly widened (less than 2 × width at base); 1, greatly widened (2.5 × width or greater at base).
This character shows almost the same pattern of evolution as character 35. All ingroup and outgroup species show state 0 with the exception of *N. trumboi*, *N. quadripunctatus*, and most of the derived clade of *N. heurni*+*N. podagricus*+*N. insularis*+*N. reticulatus*, however, *N. charon*, of this clade, shows a reversal to state 0.
- (38) *Metatibia*: 0, curved; 1, straight.
All species show state 1 except for the outgroup species *N. sayi* which shows state 0.
- (39) *Metatrochanter spine of males*: 0, short and subapical; 4, long, round and thin, pointing parallel to leg, and subapical.
Like character 38, this character is an autapomorphy of *N. sayi*. All species show state 0 except for *N. sayi*, which shows state 4.
- (40) *Metatrochanter spine of males*: 0, apex pointing parallel (or almost parallel) to leg; 1, apex pointing perpendicular to leg.
All species show state 0 except the closely related *N. maculifrons* and *N. montivagus*, which shows state 1.
- (41) *Metatrochanter spine of males*: 0, straight, not recurved dorsally; 3, recurved dorsally without acute angle ventrally, with a sharp apex.
The outgroup species show state 0 and this state is also seen in the derived species *N. charon*, *N. heurni* and the possibly derived *N. reticulatus*. The species *N. melissae* is polymorphic for this character.

Genitalia

- (42) *Paramere apicolateral setal patch*: 0, reaches apical curve; 1, does not reach apical curve.
This character describes how far the apicolateral setal patch extends apically on the parameres. All ingroup species show state 1 whereas the outgroup species *N. sayi* shows state 0.
- (43) *Paramere flange*: 0, absent; 1, present.
A small flange on the parameres is absent from all species but the outgroup species *N. humator*, which is polymorphic for this character.
- (44) *Parameres*: 0, evenly curved (e.g. Figs 16A, B, D, E); 1, sinuate (e.g. Figs 16C, 17I, J).
All species show state 0 except the basal ingroup species *N. maculifrons*, *N. montivagus*, *N. trumboi*, and *N. schawalleri* (the last of which is polymorphic).
- (45) *Spatula on proctiger (T10) apex*: 0, narrow; 1, wide.
All ingroup species show state 0 except the basal species *N. trumboi*. This and the next character could not be coded for *N. reticulatus* because female specimens have not been obtained.
- (46) *Valvifer claw* (Figs 10, 11): 0, lobed with round apex (e.g. Fig. 11B); 2, dentate (e.g. Fig. 11D).
The outgroup and basal ingroup species (*N. trumboi*, *N. maculifrons*, *N. schawalleri*) show state 0 with the exception of *N. montivagus* which shows minor dentation of the valvifer claw (Fig. 11F) and thus was coded state 2 along with the remaining ingroup species.

tRNA aspartic acid). We obtained 20 sequences of the *COII* gene for nine nicrophorine species.

Amplification and sequencing of the *COII* region was accomplished using two primers: forward: TL2-J-3034 (5' AAT ATG GCA GAT TAG TGC A 3') (Simon *et al.* 1994) and reverse: A8-N-3914 (5' TCA TAT TAT TGG TGA TAT TTG AGG 3'). The reverse (3') primer (3914) would sometimes not work, so TK-N-3785 (5' GTT TAA GAG ACC AGT ACT TG 3'), which sits in the lysine tRNA (Simon *et al.* 1994), would be used instead. This alternative primer amplified a smaller portion of the region but was usually more reliable.

Polymerase chain reaction (PCR) for these sequences was usually accomplished using a 'touchdown' programme in which the annealing temperature is gradually lowered to decrease specificity that included

5 steps: (1) 60 s at 94°C (denaturing); (2) 60 s at 54–49°C (annealing, 7 cycles); (3) 60 s at 48°C (annealing, 23 cycles); (4) 90 s at 72°C (extension); and (5) a final 7 min extension at 72°C. In addition to this programme, the following 30-cycle, 3-step cycling profile was used: (1) 30 s at 92°C (denaturing); (2) 60 s at 47°C (annealing); and (3) 60 s at 72°C (extension).

ABI PRISIM® BigDye™ kit terminators (Perkin-Elmer Applied Biosystems, www2.appliedbiosystems.com, verified May 2006) were used under recommended conditions to cycle sequence these PCR products. Cycle sequencing was done using the original PCR primers for each amplification product. An ABI 377 DNA automated sequencer (www2.appliedbiosystems.com, verified May 2006) was used to visualise sequences.

DNA sequence editing and alignment

Each sequence was amplified in both directions to verify accuracy. These double-stranded sequence data were assembled and aligned with each other to create a single consensus sequence using the software Sequencher™ version 3.0 (Gene Codes Corp., www.genecodes.com, verified May 2006).

Data were aligned by eye with reference to codon position and the amino acid sequence based on Liu and Beckenbach (1992). Alignment was not difficult as a result of the absence of indels within the protein-coding sequence.

Base frequencies

The null hypothesis of homogeneity of base frequencies across taxa for the *COII* data was not rejected either for all characters ($\chi^2 = 11.822$ (d.f. = 57), $P = 1.000$ or for just parsimony-informative characters ($\chi^2 = 56.075$ (d.f. = 57), $P = 0.509$). However, the application of this test assumes independence of taxa, which is clearly violated due to their shared evolutionary history.

Data partition combinability

The incongruence length difference (ILD) test (Farris *et al.* 1994) was used to determine if the morphological and DNA datasets were consistent with the same underlying phylogenetic signal (and thus appropriate to combine). The test was performed using 100 maximum parsimony (MP), heuristic searches, swapping to completion 20 optimal length trees per replicate. Darlu and Lecointre (2002) critically evaluated the ILD test using simulations and concluded that its interpretation is not straightforward but depends on a complex set of factors. Two confounding factors that made test results questionable were large differences in rate heterogeneity between or within data partitions.

Model selection

A critical preliminary step, following alignment, in parametric phylogenetic inference, is the selection of a process model that is complex enough to capture much of the observed complexity in the data, but not so complex that it overwhelms the data's ability to provide precise esti-

mates of parameter values. The selection of a 'best-fitting' model with realistic assumptions concerning the evolutionary process that generated the data is recognised as our best hope of avoiding systematic errors (Buckley and Cunningham 2002; Posada and Buckley 2004). Systematic errors can result from use of an overly simple model (e.g. model misspecification), leading to errors resulting from statistical bias, or conversely from the mistake of model 'over-fitting', in which too many parameters are included leading to errors resulting from increased variance (Buckley and Cunningham 2002; Posada and Buckley 2004). Methods commonly used to select best fitting models, in general, reward models for complexity that improves the likelihood of seeing the observations but penalise models for unnecessary complexity that does not significantly improve the likelihood of seeing the observations. These issues are nicely reviewed in a recent paper by Posada and Buckley (2004).

To select a model with the best fit to the data we employed a variety of measures: the Akaike information criterion (minimum theoretical information criterion, AIC (Akaike 1974)); the Bayesian information criterion (BIC) modified by Minin *et al.* (2003) to include a decision-theory framework; and Bayes factors (Nylander *et al.* 2004). The hierarchical likelihood ratio test (hLRT) can only be used to compare nested models, so this method was used for some but not all comparisons. The AIC score of a model is calculated as follows:

$$\text{AIC} = -2 \ln L + 2k$$

Where $\ln L$ is the log-likelihood and k is the number of parameters estimated by the model. Smaller AIC scores indicate better fitting models. MODELTEST version 3.6 (Posada and Crandall 1998) was used to select the best fitting model for the *COII* dataset using the AIC and hLRT methods. MODELTEST does not compare the parsimony model so this was done manually as follows. The $-\ln L$ of a tree, based on a DNA dataset, under the Tuffley and Steel (1997) parsimony model is:

$$-\ln L = (\text{nsites} + \text{nsteps}) (\ln 1/4)$$

with the number of estimated parameters:

$$\text{nparameters} = \text{nsites} \times \text{nbranches}$$

and there being $2(\text{nOTUs}) - 3$ branches in a tree.

Table 2. Morphological dataset

This dataset contains 46 equally weighted, unordered characters and is a subset of a larger matrix applicable to all species of the subfamily, thus, some character states that do not apply to species in this matrix are missing (i.e. not all states included below are contiguous); characters scored – are inapplicable. Refer to Table 1 for character descriptions

| Taxa | Characters | | | | | |
|---------------------------|------------|------------|------------|------------|--------|--|
| <i>N. humator</i> | 1AA0151101 | 500-----0 | -011121100 | 1100010100 | 0AA010 | |
| <i>N. sayi</i> | 1100150-01 | 51010101-0 | 00111E1100 | 1100010040 | 000010 | |
| <i>N. trumboi</i> | A000150-00 | 51010101-0 | 0713121002 | 1302111100 | 310110 | |
| <i>N. schawalleri</i> | 1000150-00 | 510101AA1D | 07131E1002 | 1302210100 | 310A00 | |
| <i>N. maculifrons</i> | 1000150-00 | 510BA10011 | 0713111002 | 1300210101 | 310100 | |
| <i>N. montivagus</i> | 2AA1150-00 | 510E010011 | 0713111002 | 1300210101 | 310102 | |
| <i>N. herscheli</i> | 1000150-00 | 51010101-0 | 0713121002 | 1302220100 | 310002 | |
| <i>N. apo</i> | 1000150-00 | 51010101-0 | 0713121004 | 1302220100 | 310002 | |
| <i>N. insignis</i> | 1000050-00 | 51010111-4 | 1713121002 | 1302220100 | 310002 | |
| <i>N. nepalensis</i> | 1000A50-00 | 5100011001 | 0713121002 | 1302220100 | 310002 | |
| <i>N. melissae</i> | 1000050-00 | 510EB10011 | 0713121002 | 1302220100 | C10002 | |
| <i>N. quadripunctatus</i> | 1000150-00 | 5110111004 | 1713121002 | 130B121100 | 310002 | |
| <i>N. insularis</i> | 1100050-00 | 5100010011 | 0713121002 | 1302E21100 | 310002 | |
| <i>N. podagricus</i> | 1000050-00 | 5102010011 | 0713121002 | 13A2121100 | 310002 | |
| <i>N. charon</i> | 1100051400 | 5100010011 | 0713101012 | 1302120100 | 010002 | |
| <i>N. heurni</i> | 1100051400 | 5100010011 | 0713001004 | 1302121100 | 010002 | |
| <i>N. reticulatus</i> | 1100001F20 | 010162-1-0 | 2021123004 | 0302121100 | 0100?? | |

A, polymorphism (01); B, polymorphism (02); C, polymorphism (03); D, polymorphism (04); E, polymorphism (12); F, polymorphism (14).

The general time reversible (GTR) + proportion of invariable sites (I) + gamma distribution (G) model had the best AIC score for the DNA data (AIC for GTR+I+G = 5944; AIC for T&S97 = 65 688). A branch-and-bound parsimony search using PAUP* 4.0b10 resulted in three shortest trees of length 405 steps for the *COII* data (making the $-\ln L = (841+405)(-1.3863) = -1727.3$ with $k = 841 \times 37 = 31\,117$ therefore the $AIC = -2(-1727.3) + 2(31\,117) = 65\,688$). The hLRT implemented in MODELTEST and the decision theory (DT) method as implemented in the program DT-ModSel (Minin *et al.* 2003) also chose this model.

The Markov k-state 1 parameter (Mkv) model (Lewis 2001) had the best AIC score for the morphology data, although the scores were close between the Mkv and the Mkv+G models (AIC for Mkv+G = $-2(-373.11) + 2(2+69) = 888.22$; AIC for Mkv = $-2(-370.44) + 2(1+69) = 880.88$; AIC for T&S97 = $-2((47+73) \times -1.3863) + 2(47 \times 69) = 6819$). Because the Mkv model is, to date, only available in Bayesian software, the AIC scores for these models were generated using the estimated harmonic mean of the marginal likelihood. These values used to calculate the AIC score were themselves means of 10 independent runs of MrBayes version 3.0b4 (Huelsenbeck and Ronquist 2001). Although this comparison of the Mkv to the T&S97 model may be slightly improper because maximum likelihood values were not used, the comparison works as a rough approximation – if actual maximum likelihood scores had been available for the Mkv model these would only improve its AIC score, and thus lead to the same conclusion. Because the parsimony model (T&S97) estimates a separate parameter for every branch by character combination, this model was rejected by its extreme AIC score as being too complex relative to the common-mechanism model, Mkv, of Lewis (2001).

Nylander *et al.* (2004) demonstrated the use of Bayes factors as an alternative means of model selection, specific to Bayesian analyses. Bayes factors can be interpreted as providing a comparison of the predictive likelihoods of the models (Kass and Raftery 1995; Nylander *et al.* 2004). An advantage of this method of model comparison over indices such as the AIC or hLRT is that it incorporates uncertainty in the parameter estimates rather than being based on point estimates (Nylander *et al.* 2004). To use Bayes factors, we followed the procedure of Nylander *et al.* (2004) and compared the estimated harmonic mean of the marginalised likelihood scores of competing models. The absolute difference between these scores was doubled to yield the Bayes factor, which was interpreted following the guidelines presented by Kass and Raftery (1995) (see also Nylander *et al.* 2004: table 1). The Bayes factor for the model with the highest score for the morphological data (which surprisingly was the less parameter-rich model), Mkv, was 5.36 – a value that suggests this model has ‘positive’ but not strong, nor very strong, support in preference to the alternative two-parameter model, Mkv+G. The addition of the parameter to allow for among-site rate variation appears to not significantly improve the fit of the model to the morphological data. The estimate for the value of the α shape parameter from ten runs using the Mkv+G model was between 4.5 and 6 – values that indicate there is little rate heterogeneity among characters in the morphological data and that support the conclusion of the Bayes factor analysis that this parameter is superfluous.

Phylogenetic analysis

Multiple analyses were run. The morphological dataset (Tables 1 and 2) was analysed separately using the Mkv model (Lewis 2001) with MrBayes 3.0b4. The *COII* dataset, with multiple sequences per species, but representing only nine *nepalensis*-group species of the 15 known, was analysed separately using the GTR+I+G model in both a Bayesian and maximum likelihood framework using both MrBayes 3.0b4 (Huelsenbeck and Ronquist 2001) and PAUP* 4.0b10 (Swofford 2002). And finally, the combined mtDNA *COII* plus morphology dataset (236 parsimony-informative characters) was analysed using a different model for each data partition (GTR+I+G for mtDNA, Mkv for morpho-

logy) using MrBayes 3.0b4. These separate analyses were intended to detect potential areas of strongly supported incongruence as indicated by conflicting clade support values (> 0.91 posterior probability, $> 84\%$ bootstrap; Erixon *et al.* 2003). All characters used in phylogenetic inference were equally weighted and unordered before analyses.

The combined analysis provides the most valuable means of inference for these data because it joins the hundreds of informative characters from the mtDNA dataset (but for only nine species) with the complete taxon-set of all ingroup taxa and the morphological ‘backbone’ dataset. Either analysis alone has problems absent from the combined analysis: the mtDNA data lacks almost half of the ingroup taxa and thus provides an estimate of the phylogeny with gaps for many species; the morphology dataset, although it includes all ingroup species, shows signs of questionable arrangements probably resulting from homoplasy among morphological states or simple lack of phylogenetic signal. The combined analysis appears to have eliminated most of these problems: all taxa are included and many additional informative characters are brought to bear on the inference problem. The question of whether to combine datasets or perform separate analyses has a considerable presence in the literature (Kluge 1989; Bull *et al.* 1993).

Based on a qualitative, non-algorithmic study of the morphology and geographic distributions of these species, the second author proposed the hypotheses of relationships depicted in Fig. 3. The hypotheses of relationships implied by the tree in Fig. 3 were tested with the DNA and morphological based algorithmic analyses presented herein.

This combined dataset includes considerable missing data (42%) because not all of the OTUs in the matrix have DNA data. The effects of missing data on phylogenetic inference have been investigated by numerous authors, some (e.g. Livezey 1989; Kress 1990; Hufford 1992) advocating an elimination of characters or taxa with missing data (use of ‘safe deletion rules’ e.g. Wilkinson 1995b), others advocating total inclusion (Kluge 1989) and many advocates of positions in between these two extremes. We favour inclusion of all characters, based primarily on recurrent conclusions from numerous investigations of the effects of missing data (e.g. Wiens and Reeder 1995; Wiens 1998; Anderson 2001; Kearney 2002). One of the conclusions arrived at independently by these investigators is that the amount of missing data seems not to be as important to the accuracy of phylogenetic inference as the quality of the present data; that is, missing data becomes more of a problem as the signal in the present data weakens, and less of a problem as the signal in the present data strengthens. Under most circumstances studied, inclusion of characters with incomplete data is more likely to increase phylogenetic accuracy than decrease it (Wiens 1998). Exclusion of taxa or characters based only on an arbitrary cut-off of data completeness is shown frequently in the abovementioned studies to be unwise because the stability resulting from an incomplete taxon or character is not correlated with its completeness (e.g. Anderson 2001).

Bayesian inference was performed with MrBayes 3.0b4 (Huelsenbeck and Ronquist 2001). Bayesian phylogenetic inference is a relatively new method (Huelsenbeck *et al.* 2001, 2002) that was pioneered by Li (1996), Mau (1996), Rannala and Yang (1996), Mau and Newton (1997), Yang and Rannala (1997), Larget and Simon (1999), Mau *et al.* (1999) and Newton *et al.* (1999). The program MrBayes uses the Metropolis–Hastings–Green algorithm for Markov Chain Monte Carlo (MCMC), which allows the approximation of the posterior probabilities of parameters of interest (Metropolis *et al.* 1953; Hastings 1970; Green 1995). All prior probabilities were left at the default values set by the program’s authors. As explained in the ‘Model selection’ section above, the least parameter-rich models with the best fit to the data were chosen for analyses. The Mkv model was used for the morphological data (Lewis 2001) and the general time reversible model with allowances for among site rate variation (GTR+I+G; Yang 1993, 1994; Gu *et al.* 1995) was used for the mtDNA data with all parameters estimated from the data during the tree searching process. The gamma

distribution was approximated using a setting of 4–8 rate classes. All searches were initiated with random starting trees and were run for 1–2 million cycles. Samples of trees from the cold chain of 2–6 MCMC chains were taken every 100 cycles, which resulted in 10000–20000 trees depending on the total number of cycles.

All MCMC run results were examined to identify when the run had reached stationarity (i.e. converged) as indicated by a plateau of the log-likelihood scores of sampled trees. Prior to stationarity, all parameter values are essentially random, but once stationarity has been reached, these values are thought to be sampled in proportion to their posterior probabilities (Huelsenbeck and Ronquist 2001). In all cases, stationarity had been reached before the 50000th cycle, so the first 5000 trees and parameter estimates sampled were discarded as ‘burn-in’ samples. As occurs with standard exploration of tree-space using MP or maximum likelihood (ML), it is possible for an MCMC Bayesian search to become stuck in suboptimal parameter space (analogous to a suboptimal ‘tree island’), as occurred in Leaché and Reeder’s (2002: fig. 4a) investigation of eastern fence lizards. To assess whether this had happened, we ran multiple MCMC runs from random starting trees as is advised by Huelsenbeck and Bollback (2001). Additionally, two to six MCMC chains were used for each run to improve the exploration of parameter space. Default heating values were used for these chains. Mixing among different regions of parameter space was evaluated by examination of value plots for all parameter values (Nylander *et al.* 2004).

Finally, to check for incongruence among results of different MCMC runs, the actual 50% consensus topologies of all post-burn-in trees and clade posterior probabilities were compared visually across different runs. This was done because different analyses might converge on the same log-likelihood values while actually preferring incongruent topologies (Leaché and Reeder 2002).

Results and discussion

DNA sequence characteristics

The final alignment of the DNA sequences (nine species, 20 sequences), including gaps, was 840 bp long (tRNA^{Leu}: 1–27 (27 bps); *COII*: 28–715 (687 bps); tRNA^{Lys}: 718–779 (61 bps); tRNA^{Asp}: 780–840 (60 bps)). Of these, 199 sites were parsimony informative (164 ingroup parsimony informative). The morphology data partition (15 ingroup species) contained 46 characters; 27 were parsimony informative (19 ingroup parsimony informative). The majority of the parsimony-informative DNA sites, 143 (72%), are third codon position; 2 (1.0%) are second position, 34 (17%) are first position and 16 (8%) are non-coding positions. On the insect *COII* sequences presented by Liu and Beckenbach (1992: fig. 1) the *COII* data we sequenced start at their site 1 (our site 28), the first codon position of the *COII* start codon, and end at their site 688 (our site 715) with apparently only a single T of the stop codon.

As is typical of insect mtDNA, the sequences showed a strong A–T bias (72%). The complete mtDNA dataset was found to be comprised of 34.3% A, 14.9% C, 13.2% G and 37.6% T. These values are typical of those reported from other insects for *COII* (Liu and Beckenbach 1992). For the *COII* data, PAUP*, reported the following average frequencies for nucleotides by codon position: A (33%, 27%, 42%),

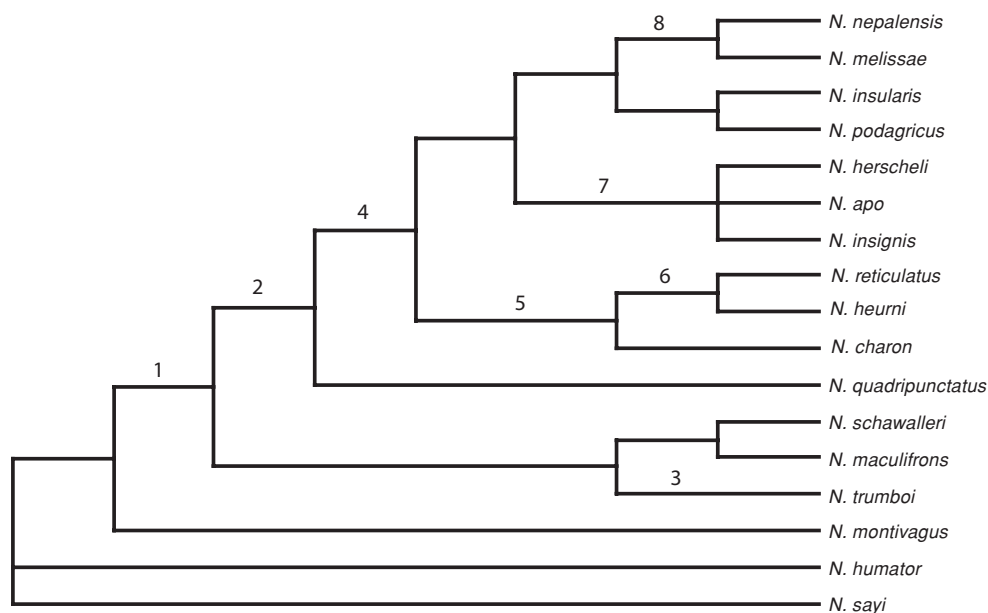


Fig. 3. Hypothesis of relationships among *nepalensis*-group species proposed by second author. Topology is the result of non-algorithmic reconstruction methods and is based on information from morphology and biogeography. Parsimony tree length (based on data in Table 2): 89 steps, consistency index (*CI*): 0.573, retention index (*RI*): 0.519. Number above nodes correspond to the following hypothesised evolutionary events: (1) body size increases to moderately large; (2) male metatibia swollen dorsally, female valvifer claw toothed; (3) several aberrant characters including meso- and metatibia with apical emargination large, semicircular; (4) dispersal to southern Asia; (5) first invasion of Malay Archipelago, dark epipleuron; (6) inner face of male metatibia widened; (7) second invasion of Malay Archipelago; (8) inner face of male metatibia widened, third invasion of Malay Archipelago.

C (17%, 20%, 9%), G (23%, 14%, 3%), T (28%, 40%, 45%). These results show that, as expected (Simon *et al.* 1994), the majority (87%) of the A–T richness in these sequences occurs at the third codon position. Uncorrected ingroup genetic distances (p) for *COII* ranged from 0.0 to 0.125 (Table 3). When corrected using the GTR+I+G ($\alpha = 1.8$) model, the maximum ingroup distances for *COII* was 0.252 (Table 3).

Data partition combinability

To determine if the morphological and DNA datasets were consistent with the same underlying phylogenetic signal (and thus appropriate to combine), the ILD test (Farris *et al.* 1994) as implemented in PAUP* was used. The partitions were estimated to be not significantly incongruent, the null hypothesis of congruence failing to be rejected at $P = 0.1$. However, because the DNA partition was considerably larger than the morphology partition, the test may have been biased towards accepting these partitions as similar. Alternatively, the signal in the morphological dataset appears to be much weaker than that in the DNA dataset, which would also result in no strong incongruence.

Separate analysis of the morphological data

Figure 4 shows the 50% majority rule consensus phylogram obtained from the Bayesian analysis of the morphological data. The posterior probabilities were low for most nodes of interest with the exception of the *N. maculifrons* and

N. montivagus clade (100%) and the clade representing the entire *nepalensis*-group (96%). This figure also shows the extreme length of the branch leading to *N. reticulatus*, sp. nov., indicating this species differs markedly in its morphology from its apparent close relatives in the *nepalensis*-group.

Separate analysis of the molecular data

Maximum likelihood and Bayesian analyses of the *COII* data resulted in the ML phylogram shown in Fig. 5. In contrast to the morphological analysis, the tree is well supported by both ML bootstrap values and Bayesian posterior probabilities, with only two branches that received weak support. One of these poorly supported branches (labelled branch A in Fig. 5) suggests the species *N. nepalensis* is paraphyletic with respect to *N. podagricus* (see section below on Biogeography).

Combined analysis

Figure 6 shows the 50% majority rule consensus phylogram of the combined data analysis. Some of the node posterior probabilities are slightly higher than the pure morphology analysis (Fig. 4) but all are considerably lower than those of the pure molecular analysis (Fig. 5). The long-branch taxon, *N. reticulatus*, sp. nov., joins in the most derived clade of the tree in this analysis, contrary to its placement at the base of the species-group in the pure morphology tree (Fig. 4).

Investigating the possibility that this long-branch taxon was acting as a ‘rogue’ lineage or ‘floater’ and weakening the

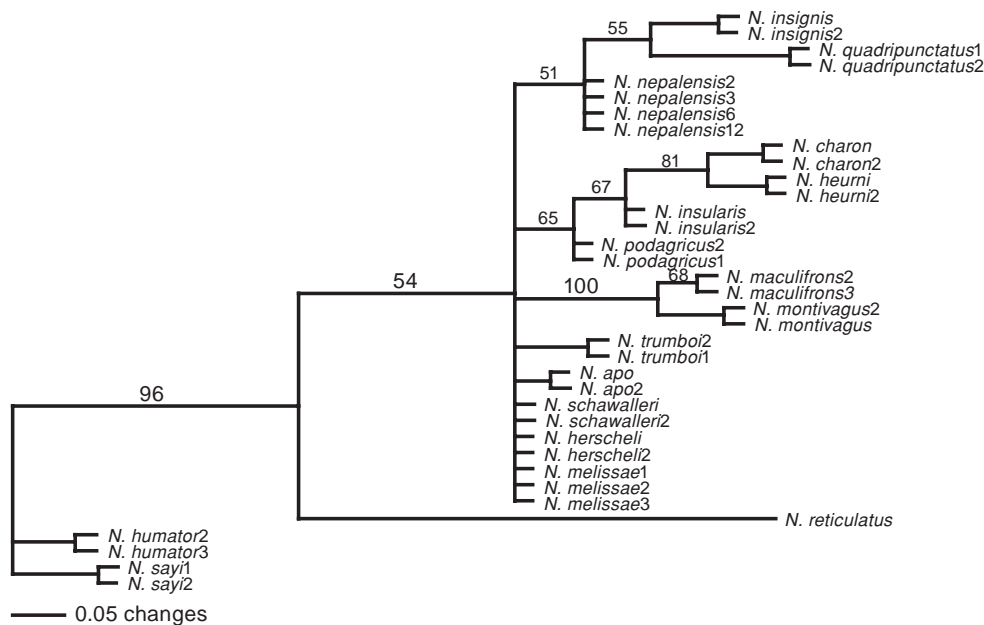


Fig. 4. 50% majority rule consensus phylogram of 15 000 post-burn-in trees of MrBayes 3.0b4 Metropolis-coupled Markov chain Monte Carlo (MCMCMC; 6 chains) search based on morphological data using the Markov k-state 1 parameter (Mkv) model of Lewis (2001). Chains were run for 2 million iterations with every 100th tree sampled. Values above branches are estimated posterior probabilities. Branches without values shown are all > 85%.

signal in the data of the remaining species, we removed this taxon from the matrix and re-analysed the combined data (Fig. 7). Without the long-branch taxon, *N. reticulatus*, sp. nov., as suspected, node support values increased throughout the tree (Fig. 7). Although few node support values increased to 95% or above, most increased by 10% to 20% over those of the analysis of Fig. 6. The only exception being a slight drop from 73% (Fig. 6) to 68% (Fig. 7) for the *N. insignis*, sp. nov. + *N. quadripunctatus* clade.

New species

Schawaller (1982) described the carrion beetle fauna of the Himalayas, primarily that of Nepal. He described the species *N. nepalensis* as highly polymorphic and illustrated some examples of elytral patterns that he proposed represented variation within *N. nepalensis*. One of these patterns had been described as an aberration (infrasubspecific category, and thus not an available name according to the ICZN (1999)) by Emetz and Schawaller (1975) using the name *immaculatus* (a name preoccupied by Portevin (1923)). One of us, R. Madge, based on examination of museum specimens from Nepal, had proposed that one of these elytral pattern variants recognised by Schawaller (1982) was a distinct species. During an expedition to Nepal the first author

was able to collect fresh material of some of these variants and later use their mtDNA (*COII*) sequences to test Schawaller's and Madge's hypotheses.

Figures 4–7 shows the results of these tests. Two of the elytral pattern variants proposed by Schawaller were sampled. One of these, which Madge had earmarked as a distinct species and we are naming *N. trumboi*, sp. nov., was inferred to be near the base of the *nepalensis*-group, at least three speciation events removed from *N. nepalensis* and showing an uncorrected 'p' distance for the *COII* sequences of 11% from *N. nepalensis* (corrected distance of 23% from *N. nepalensis* (Table 3)). The elytral pattern of this lineage is quite distinct from that of *N. nepalensis* (compare Fig. 8F with 8H), and other morphological characters, including genitalia, separate these lineages (see key and description).

The elytral pattern assigned the aberrational name *immaculatus* by Emetz and Schawaller (1975) was sampled from two widely separated regions of Nepal (Mustang and Solu Khumbu districts). All *COII* sequences of this elytral pattern (*N. melissae*, sp. nov.) grouped together with an estimated posterior probability of 100%, and branched off within a derived position of this species-group at least two speciation events away from sympatric *N. nepalensis* samples that were collected from the same two locations in

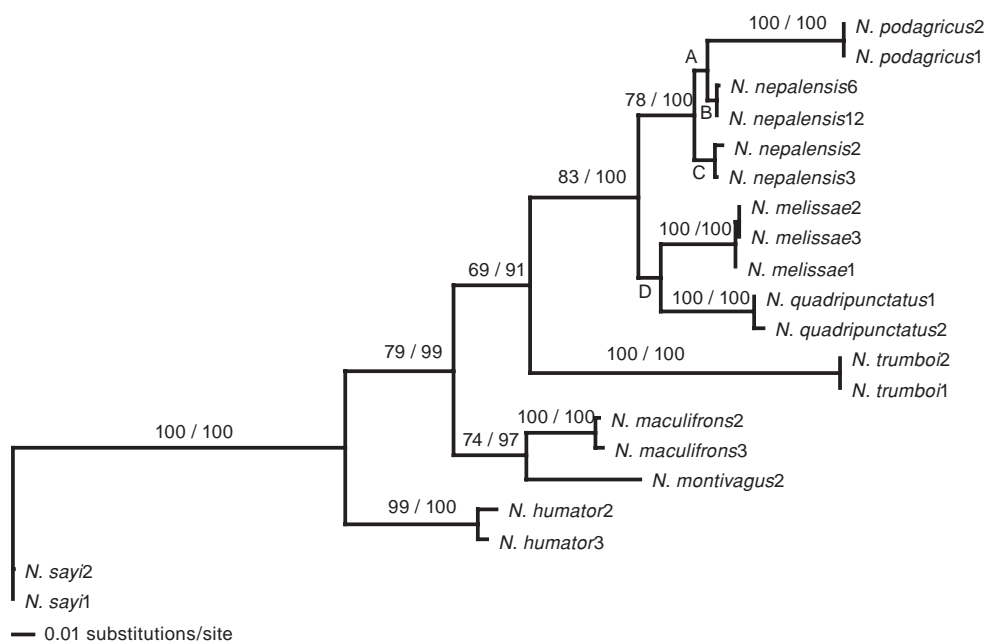


Fig. 5. Maximum likelihood phylogram, $-\ln L = 2959.247$ found in each of 3 independent runs of 10–12 random addition sequence, tree-bisection reconnection (TBR) heuristic searches with maximum likelihood (ML) parameters estimated from the data for the general time reversible (GTR) + proportion of invariable sites (I) + gamma distribution (G) model (using eight categories for the α shape parameter of the gamma distribution). Branch support, first value = recovered in 1000 ML bootstrap searches (parameters set using values from ML search). Second value = estimated posterior probability of clade based on 20 million iteration Metropolis-coupled Markov chain Monte Carlo (MCMCMC; eight chains) search using MrBayes 3.0b4. The 95% credible set from the Bayesian analysis contained 55 trees. Values for lettered branches as follows: A (55/76), B (86/92), C (98/100), D (51/61).

Nepal. The uncorrected 'p' genetic distance for this lineage was 5.5% from *N. nepalensis* (average corrected distance of 8.41% from *N. nepalensis* (Table 3)). The elytral pattern is distinct from *N. nepalensis*, but less so than that of *N. trumboi* (Fig. 8C, D, H), as might be expected based on the much closer genetic distance. Additional morphological characters diagnosing this lineage are listed in the key and the description.

Schawaller (1982) based his assessment of elytral pattern polymorphism on his understanding of the European species, some of which have been shown to display considerable elytral pattern variation (e.g. European *N. interruptus*, *N. germanicus*, *N. vespilloides*). Based on the *COII* analysis and the examination of hundreds of specimens of *nepalensis*-group species, it appears that species in the *nepalensis*-group differ from species common to Europe by showing little to no elytral pattern polymorphism. Elytral patterns in the *nepalensis*-group that differ by small degrees seem to correspond to distinct species, as corroborated by other morphological characters, particularly the valvifer claw of the ovipositor.

Biogeography

The results of these phylogenetic analyses are too preliminary, lacking in both sufficient molecular data and taxa, for

confident inference of biogeographic history. However, some useful biogeographic comments on the hypothesis of the second author (Fig. 3) can be made. In all trees (Figs 4–7), the species *N. schawalleri*, *N. montivagus*, *N. maculifrons* and *N. trumboi* appear near the base of the *nepalensis*-group, similar to their placement in Fig. 3. These species occur in mainland Asia from Japan through northern, central and southern China, and west to the Himalayas. As such, they support a mainland origin of the group with subsequent radiations and/or invasions of the Malay Archipelago.

The close, and biogeographically parsimonious, relationship hypothesised (Fig. 3) between *N. charon* of Sulawesi, *N. heurni* of Papua New Guinea and *N. reticulatus* of the Solomon Islands, is not recovered in the analyses presented here (Figs 4–7). This is most likely a result of *N. reticulatus* being a long morphological branch, i.e. this species bears numerous autapomorphies and few synapomorphies. We are actively seeking DNA of *N. reticulatus* and expect that, once obtained, it will help resolve the placement of this species. The species *N. charon* and *N. heurni* are, however, recovered as sister-species in all analyses (Figs 4, 6, 7), which agrees with the second author's hypothesis and is biogeographically parsimonious.

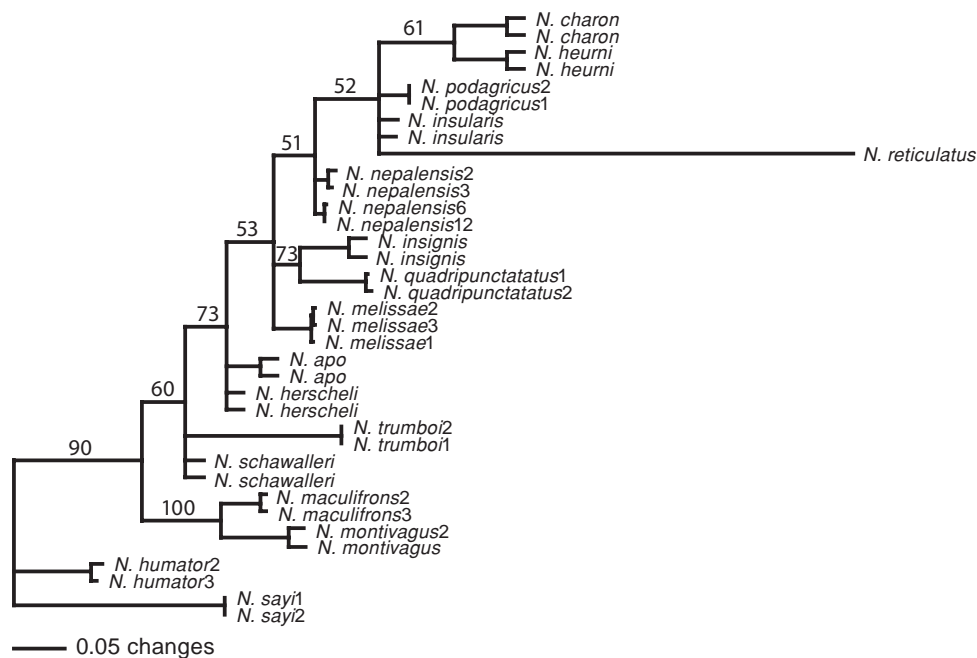


Fig. 6. Combined dataset analysis with *Nicrophorus reticulatus* included. 50% majority rule consensus phylogram of 15000 post-burn-in trees of MrBayes 3.0b4 Metropolis-coupled Markov chain Monte Carlo (MCMCMC; 6 chains) search based on two partition dataset: morphological data fit by the Markov k-state 1 parameter (Mkv) model of Lewis (2001) and mtDNA sequences of the *COII* gene fit by the general time reversible (GTR) + proportion of invariable sites (I) + gamma distribution (G) model with the α shape parameter for the gamma distribution estimated using 8 rate categories. Chains were run for 2 million iterations with every 100th tree sampled. Values above branches are estimates of posterior probabilities. Branches without shown values are all > 85%. Samples with numbers at the end of their names were represented by both DNA and morphological data, samples without numbers were represented by only morphological data.

The second author proposed a close relationship between the island species *N. insignis* of Flores, *N. apo* of Mindanao and *N. herscheli* of Sumatra, all of which share a similar elytral pattern (Fig. 8E, G, K) in lacking any isolated black spots in the fascia. This relationship is not recovered in any analysis (Figs 4, 6, 7), although a polytomy allowing a close relationship between the latter two species is common. We lack DNA of these species and hope that, once it is obtained, we will be able to better test the proposed close relationship among these island species.

The proposed sister-species relationship between *N. podagricus* and *N. insularis* (Fig. 3) is contradicted by all analyses (Figs 4, 6, 7), although these species repeatedly appear as close relatives in a paraphyletic grade. In major contrast to Fig. 3, which proposes multiple invasions and/or radiations of the Malay Archipelago, the analyses presented here (Figs 4, 6, 7) indicate the sister-species pair *N. charon* and *N. heurni* are most closely related to *N. insularis*, supporting a single archipelago radiation hypothesis for these species.

In partial agreement with Fig. 3, all analyses (Figs 4, 6, 7) support a close relationship between *N. nepalensis* and *N. podagricus*. However, the molecular data indicate the latter

species arose from within the former, making *N. nepalensis* paraphyletic (Fig. 5). This relationship is not unexpected owing to the widespread distribution of *N. nepalensis* – if *N. podagricus* originated relatively recently, as a result of peripheral isolation from island populations of *N. nepalensis*, we would expect this paraphyly. However, there are several other species for which we lack DNA samples that morphology indicates are potential close relatives of either or both *N. nepalensis* and *N. podagricus*. Three such species are *N. insularis*, *N. charon*, sp. nov. and *N. heurni*, all of which appear to be close relatives of *N. podagricus* (Fig. 4). Whether the paraphyly of *N. nepalensis* due to *N. podagricus* will remain after we have obtained DNA data from these other species is an open question.

The mid-basal placement of *N. quadripunctatus* of Japan and northern Asia in Fig. 3 is contradicted by all analyses (Figs 4–7), which place this species in a more derived position as sister to *N. insignis*, sp. nov. (morphology, Figs 4, 6, 7) or *N. melissae*, sp. nov. (DNA, Fig. 5). The basal placement in Fig. 3 agrees with a single, mainland, northern Asia origin of the group whereas the analyses presented herein require a more complex speciation pattern in which the northern fauna includes both basal and derived species.

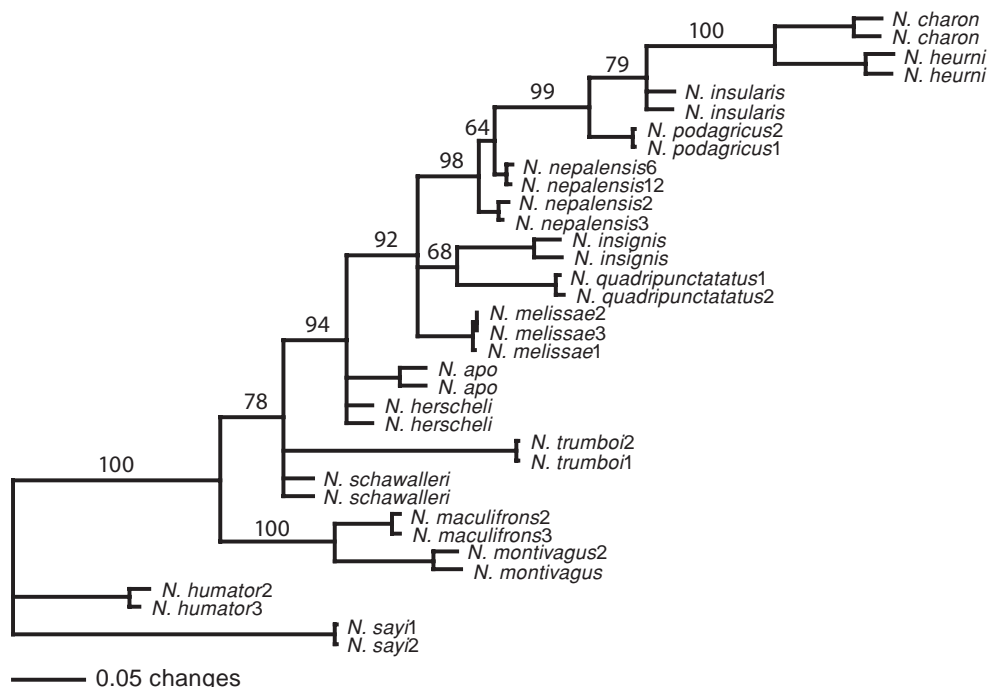


Fig. 7. Combined dataset analysis without *N. reticulatus*. 50% majority rule consensus phylogram of 15 000 post-burn-in trees of MrBayes 3.0b4 Metropolis-coupled Markov chain Monte Carlo (MCMCMC; 6 chains) search based on two partition dataset: morphological data fit by the Markov k-state 1 parameter (Mkv) model of Lewis (2001) and mtDNA sequences of the *COII* gene fit by the general time reversible (GTR) + proportion of invariable sites (I) + gamma distribution (G) model with the α shape parameter for the gamma distribution estimated using eight rate categories. Chains were run for 2 million iterations with every 100th tree sampled. Values above branches are estimates of posterior probabilities. Branches without shown values are all > 85%. Samples with numbers at the end of their names were represented by both DNA and morphological data, samples without numbers were represented by only morphological data.

Table 3. Genetic distances
 Maximum likelihood general time reversible (GTR) + proportion of invariable sites (I) + gamma distribution (G) corrected distances (Base = (0.3466 0.1325 0.1264), Rmat = (14.6181, 66.1630, 27.8476, 0.00001, 261.2247), Shape = 1.7999, Pinv = 0.6386) above the diagonal with uncorrected 'p' distances below the diagonal

| | 1 | 2 | 3 | 4 | 5 | 6 | 7 | 8 | 9 | 10 | 11 | 12 | 13 | 14 | 15 | 16 | 17 | 18 | 19 | 20 |
|-----------------|---------|---------|---------|---------|---------|---------|---------|---------|---------|---------|---------|---------|---------|---------|---------|---------|---------|---------|---------|----|
| 1 sayi1 | | | | | | | | | | | | | | | | | | | | |
| 2 sayi2 | 0 | | | | | | | | | | | | | | | | | | | |
| 3 humator2 | 0.10153 | 0.10153 | | | | | | | | | | | | | | | | | | |
| 4 humator3 | 0.09551 | 0.09551 | 0.01208 | | | | | | | | | | | | | | | | | |
| 5 podagricus2 | 0.1206 | 0.1206 | 0.11965 | | | | | | | | | | | | | | | | | |
| 6 podagricus1 | 0.1206 | 0.1206 | 0.12326 | 0.11965 | | | | | | | | | | | | | | | | |
| 7 melissae1 | 0.12553 | 0.12553 | 0.11948 | 0.11949 | 0.06993 | | | | | | | | | | | | | | | |
| 8 melissae2 | 0.12659 | 0.12659 | 0.12062 | 0.12063 | 0.0722 | 0.0722 | | | | | | | | | | | | | | |
| 9 melissae3 | 0.12659 | 0.12659 | 0.12062 | 0.12063 | 0.0722 | 0.0722 | 0.0012 | | | | | | | | | | | | | |
| 10 nepalensis2 | 0.11848 | 0.11848 | 0.11233 | 0.11474 | 0.05672 | 0.05544 | 0.05662 | 0.05662 | | | | | | | | | | | | |
| 11 nepalensis3 | 0.11715 | 0.11715 | 0.10985 | 0.11227 | 0.0543 | 0.0543 | 0.05301 | 0.05419 | 0.05419 | | | | | | | | | | | |
| 12 nepalensis6 | 0.11606 | 0.11606 | 0.10983 | 0.11107 | 0.04869 | 0.04869 | 0.05587 | 0.05704 | 0.05704 | 0.02315 | 0.02072 | | | | | | | | | |
| 13 nepalensis12 | 0.11339 | 0.11339 | 0.1074 | 0.10861 | 0.04813 | 0.04813 | 0.05421 | 0.05535 | 0.05421 | 0.02169 | 0.01928 | 0.00122 | | | | | | | | |
| 14 maculifrons2 | 0.11114 | 0.11114 | 0.09547 | 0.09427 | 0.09657 | 0.09657 | 0.09183 | 0.09292 | 0.09292 | 0.09794 | 0.09667 | 0.09047 | 0.08935 | | | | | | | |
| 15 maculifrons3 | 0.11475 | 0.11475 | 0.09908 | 0.09788 | 0.09415 | 0.09415 | 0.0894 | 0.0905 | 0.0905 | 0.10034 | 0.09663 | 0.09398 | 0.09173 | 0.00604 | | | | | | |
| 16 maculifrons2 | 0.11705 | 0.11705 | 0.10386 | 0.10146 | 0.111 | 0.111 | 0.10985 | 0.11095 | 0.11095 | 0.10396 | 0.10144 | 0.09877 | 0.09652 | 0.06157 | 0.06398 | | | | | |
| 17 trumboi2 | 0.13633 | 0.13633 | 0.11596 | 0.11476 | 0.1231 | 0.1231 | 0.11355 | 0.11464 | 0.11464 | 0.11367 | 0.11115 | 0.11466 | 0.11224 | 0.12556 | 0.12425 | 0.12425 | | | | |
| 18 trumboi1 | 0.13633 | 0.13633 | 0.11596 | 0.11476 | 0.1231 | 0.1231 | 0.11355 | 0.11464 | 0.11464 | 0.11367 | 0.11115 | 0.11466 | 0.11224 | 0.12556 | 0.12425 | 0.12425 | 0 | | | |
| 19 quadripunct1 | 0.11467 | 0.11467 | 0.11104 | 0.10984 | 0.07717 | 0.07717 | 0.06024 | 0.0614 | 0.0614 | 0.06388 | 0.06145 | 0.06072 | 0.059 | 0.09905 | 0.09965 | 0.09777 | 0.11351 | 0.11351 | | |
| 20 quadripunct2 | 0.11225 | 0.11225 | 0.10983 | 0.10863 | 0.07959 | 0.07959 | 0.06265 | 0.06381 | 0.06381 | 0.06629 | 0.06386 | 0.06319 | 0.06142 | 0.10147 | 0.09906 | 0.09897 | 0.11593 | 0.11593 | 0.00482 | |

Finally, the close relationship between *N. nepalensis* and *N. melissae*, sp. nov. in Fig. 3 is partially supported by the analyses presented herein, which either place these species as potentially paraphyletic relatives (in a polytomy based on morphology, Figs 4, 6, 7) or as neighbours in sister-clades (DNA, Fig. 5). If *N. melissae*, sp. nov. is a close relative of *N. nepalensis*, this raises the interesting possibility that *N. nepalensis* may be paraphyletic with respect to multiple lineages – one in the Himalayas and the other in the Malay Archipelago. Such a pattern of speciation would be challenging to identify and resolve.

In conclusion, the phylogenies presented here are clearly preliminary attempts to infer the evolutionary history of this species-group. Although complete resolution has not been obtained, these analyses provide sufficient information to support the general placement and validity of the new species described herein. Confident resolution of this history will require both a nearly complete DNA sample (all species represented) and a molecular dataset comprising multiple genes. We are currently pursuing these goals.

Taxonomy

The following description, but not diagnosis, of the *nepalensis*-group includes characters that vary within the *nepalensis*-group (i.e. no constant synapomorphies of the sub-family are included) but are constant within the *nepalensis* species-group – thus these characters are not repeated for each *nepalensis*-group species description because they apply to all the species of the group. Species descriptions, therefore, only contain characters that vary within the species-group.

Nicrophorus nepalensis-group

(Fig. 1)

Diagnosis

All members of the *nepalensis*-group (Table 4) except *N. reticulatus* and *N. trumboi* (which lack the first character state but have the second), and no other *Nicrophorus* species, share the following two character states: posterior margin of elytron with 5–10 clusters of long dark or light brown (but not golden) setae and epipleural ridge extending to tip of scutellum, but not beyond.

Although no single diagnostic trait works for all species of this group, they can be diagnosed from other members of the genus *Nicrophorus* based on a combination of the following character states (listed in decreasing order of value):

(1) Posterior margin of elytron with 5–10 clusters of long dark or light brown setae (unique to members of this group with the following exceptions: *N. reticulatus* lacks these setae, *N. trumboi* appears to have these setae greatly reduced to absent, and the two species used as outgroup taxa, and thus

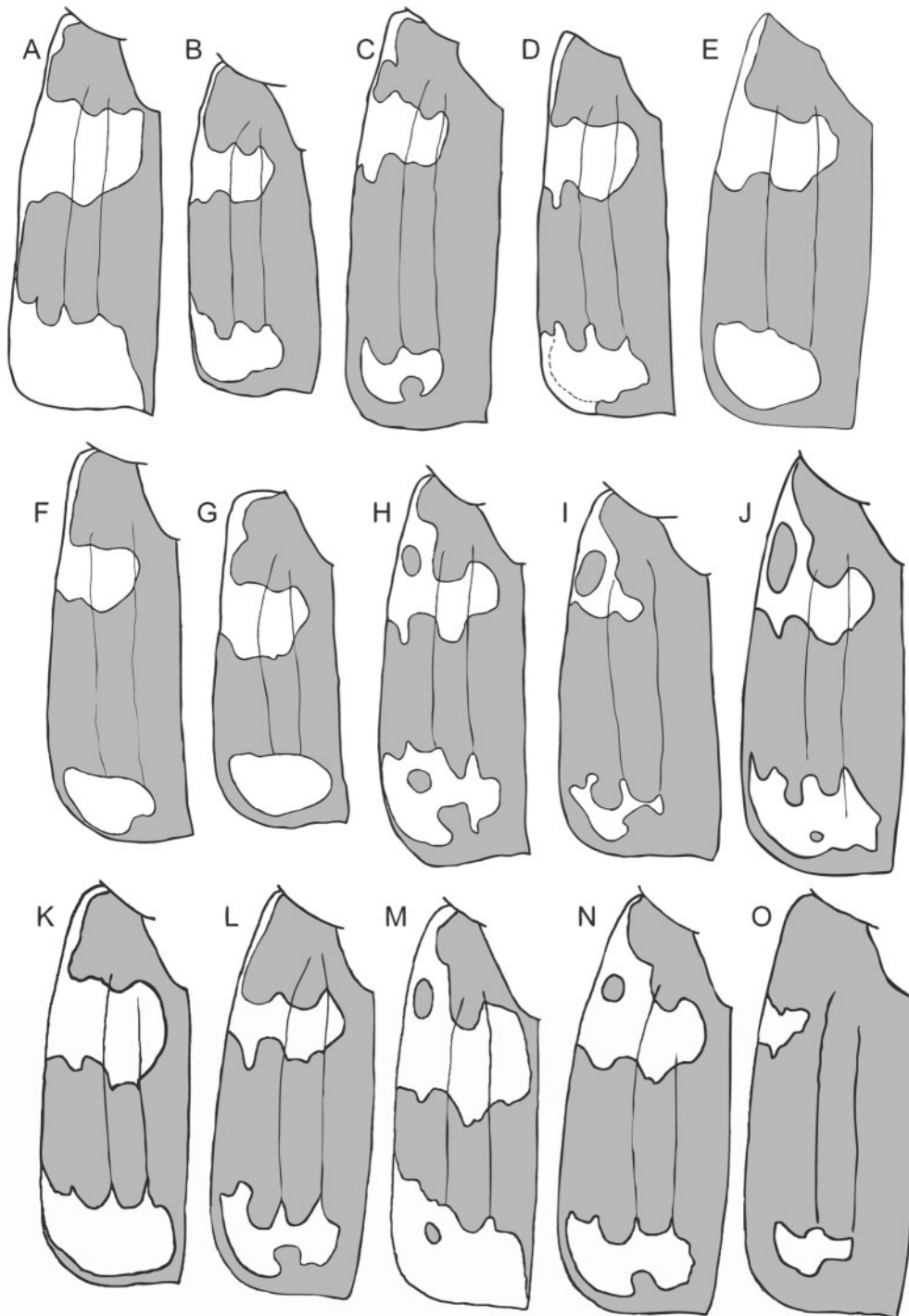


Fig. 8. Elytral patterns. *A*, *Nicrophorus schawalleri*. *B*, *N. schawalleri* (rare form, Sichuan China). *C*, *N. melissae* (Bhutan). *D*, *N. melissae* (Nepal). *E*, *N. apo*. *F*, *N. trumboi*. *G*, *N. herscheli*. *H*, *N. nepalensis* (typical form). *I*, *N. nepalensis* (rare melanistic form, Taiwan). *J*, *N. insularis*. *K*, *N. insignis*. *L*, *N. podagricus*. *M*, *N. quadripunctatus*. *N*, *N. charon*. *O*, *N. reticulatus*.

not members of the *nepalensis*-group as herein defined, *N. sayi* and *N. humator*, possess these setae; additionally, these setae are rarely broken off).

(2) Epipleural ridge extends to tip of scutellum but not beyond (all *nepalensis*-group species but also seen in six species not belonging to this species-group: *N. morio* Gebler, *N. germanicus* (L.), *N. satanas* Reitter, *N. antennatus* (Reitter), *N. dauricus* Motschulsky, *N. vestigator* Herschel).

(3) Frons with orange spot in centre (Fig. 9C) (only seen in members of this species-group, however the spot is typically, but not always, present in *N. montivagus* and *N. trumboi* and is absent from *N. insularis*, *N. charon*, *N. heurni*, and *N. reticulatus*).

(4) Valvifer claw of ovipositor dentate with dentition composed of small tooth or small rounded lobe, on small, curved lobe situated in the middle to distal third of the valvifer (Figs 10, 11) (dentition weak in *N. montivagus* and lacking in *N. maculifrons*, *N. trumboi*, and *N. schawalleri*).

(5) Elytral microsculpture transverse, narrow, with breaks (Figs 2, 12C, D, 13) (all *nepalensis*-group species except *N. reticulatus* which has isodiametric microsculpturing (Fig. 12A, B)).

(6) Clypeal membrane of female fasciform (transverse) rather than triangular or bell-shaped (all members of the *nepalensis*-group including outgroup species *N. sayi* and *N. humator* – also seen in eight *Nicrophorus* species external to the *nepalensis*-group).

(7) First abdominal spiracle with an apical lobe (Fig. 14) (all members of the *nepalensis*-group including outgroup species *N. sayi* and *N. humator* – also seen in ten *Nicrophorus* species external to the *nepalensis*-group).

(8) Middle of the outer margin of the metatibia slightly swollen in large males (Figs 15A, C, D) (restricted to members of the *nepalensis*-group but absent in *N. trumboi*, *N. maculifrons*, *N. montivagus*, and *N. schawalleri*). It differs from the greatly swollen metatibia of *N. germanicus*, *N. morio*, and *N. satanas*, which are swollen equally in males and females).

Description

Head. Dent receptive notch on right mandible present. Mandibles preapically wide, short, stout; with dorsal, ridged groove. Maxillary palpus not elongate, concealed beneath mandible when mandibles open. Clypeal membrane orange, yellow or brown, not black. Female clypeal membrane fasciform (transverse), male clypeal membrane campanulate (bell-shaped), produced posteriorly and laterally enclosed by clypeus. Gula bar of large males (Stickney 1923) reduced to thin strip, replaced by membrane, not contiguous with submentum. Antennal scape with posterior face flattened (fitting against eyes). Antennal club abrupt, large. Raised ridge on posterior of antennal club segments large, with sharp lateral edges. Basal antennomere of club oval, transverse, not circular. Epicranial sulci (grooves along inner

margin of eyes) long, reaching posterior of eyes and usually joining. Lateral margins of head of large males parallel, or subparallel, giving rear of head a square appearance. Width across postocular bulge of large males less than width across eyes. Posterior margin of eye of large males in lateral view sinuate. Width of eyes of large males wide (width greater than or equal to half length). Dorsum of neck with non-punctate band(s). Microsculpture of frons absent (smooth, polished).

Thorax. Pronotal anterior impressions complete, with distinct inner arcs. Setae on anterior corner of hypomeron absent. Triangular depression at midpoint posterior margin of pronotum absent. Pronotum disk black; posterior with flat margin or border; pair of 'v'-shaped bumps present. Medial groove of pronotum present. Antemesosternal sclerite cordiform, bilobate. Humeral setae present. Epipleural ridge short, to tip of scutellum, distinct. Elytral surface lacking many long setae. Elytra bicoloured and bifasciate. Elytron posterior margin sinuate. Elytral costae visible to naked eye (but not raised). Profile of elytra in lateral view raised posteriorly. Posterior fascia between costae, anterior margin u-shaped between costae 1 and 2 (with bottom of u towards posterior). Elytral colour variation – greatly increased orange forms unknown, all-black forms unknown. Ventral surface of elytron with golden sheen. Row of setae on inner lateral margin of elytra in posterior quarter along lateral ridge of elytron, setae facing inward or downward. Setae on inner lateral margin of elytra in posterior quarter present as distinct, single file row. Flange along mesepisternal anterior margin tapering gradually towards mesosternum. Metanotal subalare flat in posteriolateral quarter. Metepimeron constricted. Metepisternum with upper third impunctate and glabrous. Metasternal pubescence laterally long. Metasternum with long setae, bald patch posterior of mesocoxae absent. Metasternum posterior margin edge glabrous. Stridulatory file scraper on venter of elytron near elytral apex (< 0.2mm).

Abdomen. Stridulatory files parallel, separated by two or more file widths, touching posterior margin of tergite. First abdominal spiracle slit short, less than one third length of spiracle, in straight line with centre line of spiracle, spiracle lobed, with small bulb projecting anteriorly. Spiracle of tergite six elongate slit-like, parallel to lateral margin of tergite, or forming less than 30-degree angle with lateral margin. Tergite seven with short depressed setae.

Legs. Venter of protibia apex with lateral process. Anterior face of protochantin with regions of dense pubescence composed of short, recumbent golden setae. Anterior of procoxae with short setae on basal half. Outer margin of mesotibia straight or curved outwards. Inner margin of metatibia with inner face not forming wide channel entirely filled with dense long setae. Metatibia straight. Inner face of apex of metafemora with circular or oval cluster of short setae occupying one quarter to one half of apical region.

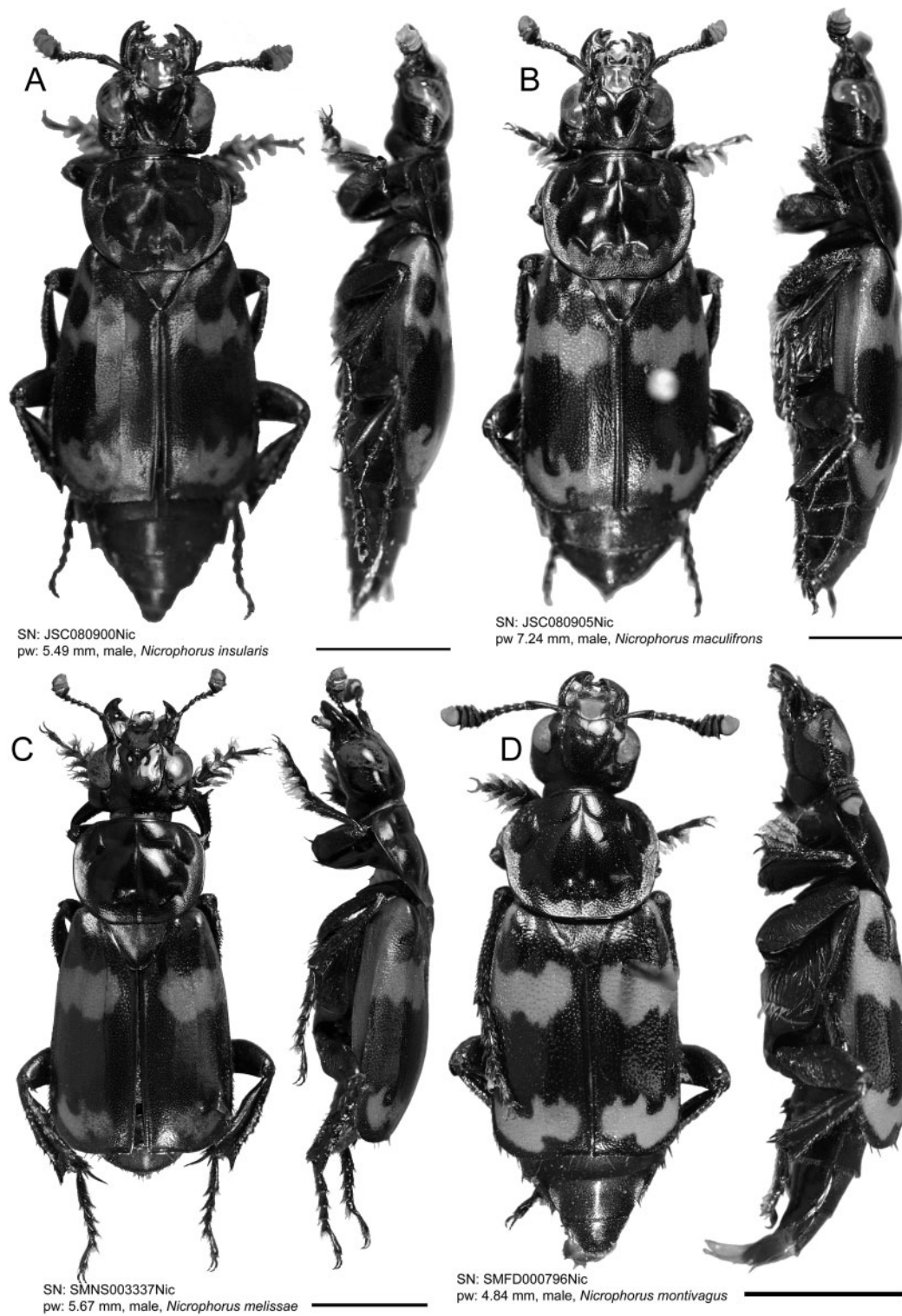


Fig. 9. Dorsal and lateral habitus. *A*, Male *Nicrophorus insularis* Grouvelle. *B*, Male *Nicrophorus maculifrons* Kraatz. *C*, Male *Nicrophorus melissae* Sikes (paratype). *D*, Male *Nicrophorus montivagus* Lewis. Scale bar = 5 mm.

Inner face of base of metafemora with single ridge separating medial setose area (area not depressed) from lateral half. Female metafemora slender (length ≥ 2.5 times greatest width). Metatrochanter spine of males short and subapical. Metacoxae wider than long. Metacoxal anterior line complete for half or more of metacoxa. Posterior margin of metacoxae without white microsetae. Tarsal empodium bisetose. Venter of metatarsomere 1 setae absent medially, esp. distally, leaving wide or narrow glabrous channel and with dense cluster of long setae at apex.

Aedeagus (Figs 16, 17). Paramere base not curved dorsally. Paramere apex with setae laterally, apicolateral setal

patch not reaching apical curve, apex rounded. Paramere ventral setal patch not composed of five evenly spaced setae of identical length. Paramere 3rd setal patch and flange absent. Parameres tapering towards apex but not constricted behind apex.

Ovipositor (Figs 10, 11). (Note: based on study of all species except *N. reticulatus*, sp. nov. of which females are unknown). Proctiger (T10) apex strongly lobed, spatulate; lobe apex not bifurcate; with pubescent apex, ventral setae. Proctiger (T10) venter of spatula apex smooth, lacking medial keel-like ridge. Gonocoxite terminal claw shorter than stylus or absent. Dorsal ridge on proctiger (T10)

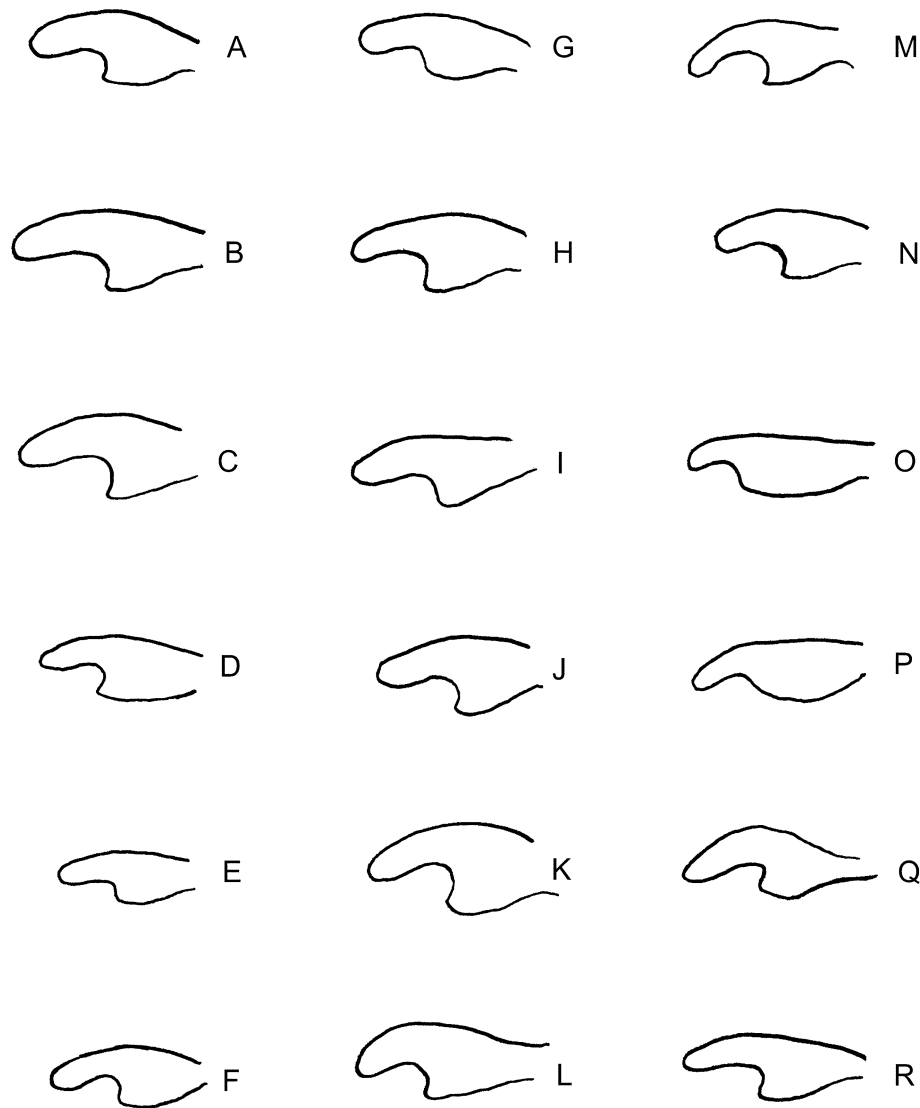


Fig. 10. Right valvifer claw of ovipositor, lateral view: *A*, *Nicrophorus nepalensis* (India: Kashmir). *B*, *N. nepalensis* (Japan: Ryukyu (Nansei)). *C*, *N. nepalensis* (Philippines: Luzon). *D*, *N. nepalensis* (Nepal: Mustang Dist.). *E*, *N. nepalensis* (Taiwan). *F*, *N. nepalensis* (Taiwan). *G*, *N. nepalensis* (Taiwan). *H*, *N. insularis* (Sumatra). *I*, *N. insularis* (Bali). *J*, *N. heurni* (Irian Jaya). *K*, *N. insularis* (Java). *L*, *N. podagricus*. *M*, *N. apo*. *N*, *N. quadripunctatus*. *O*, *N. maculifrons*. *P*, *N. schawalleri*. *Q*, *N. heurni*. *R*, *N. charon*.

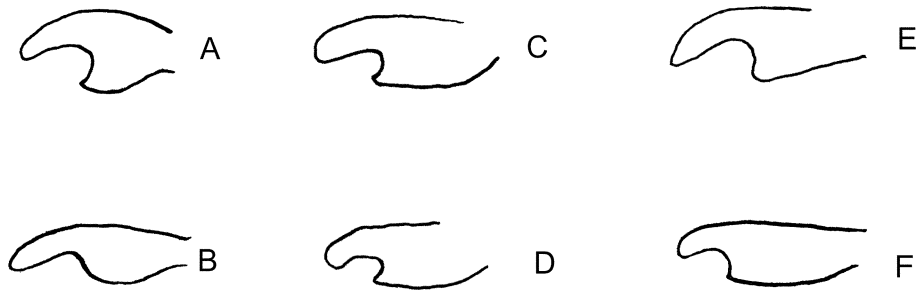


Fig. 11. Right valvifer claw of ovipositor, lateral view: *A*, *Nicrophorus herscheli*. *B*, *N. trumboi*. *C*, *N. melissae* (Nepal). *D*, *N. melissae* (Bhutan). *E*, *N. insignis*. *F*, *N. montivagus*.

absent. Paraproct (T9) apex glabrous, with well defined, raised ridge. Paraproct process absent. Valvifer claw dentition, when present, composed of small tooth or small rounded lobe, on a small, curved lobe situated in the middle to distal third of the valvifer. Valvifer claw lobe glabrous.

Larva. (Note: Based on study of specimens from only two species: *N. nepalensis* and *N. quadripunctatus*). Membrane at base of mandible of larva thickened centrally. Base of maxillary palp of larva without membranous process. Segment 2 of maxillary palp of larva with reduced sclerotization. Apical setae of galeal lobe of larva not pro-

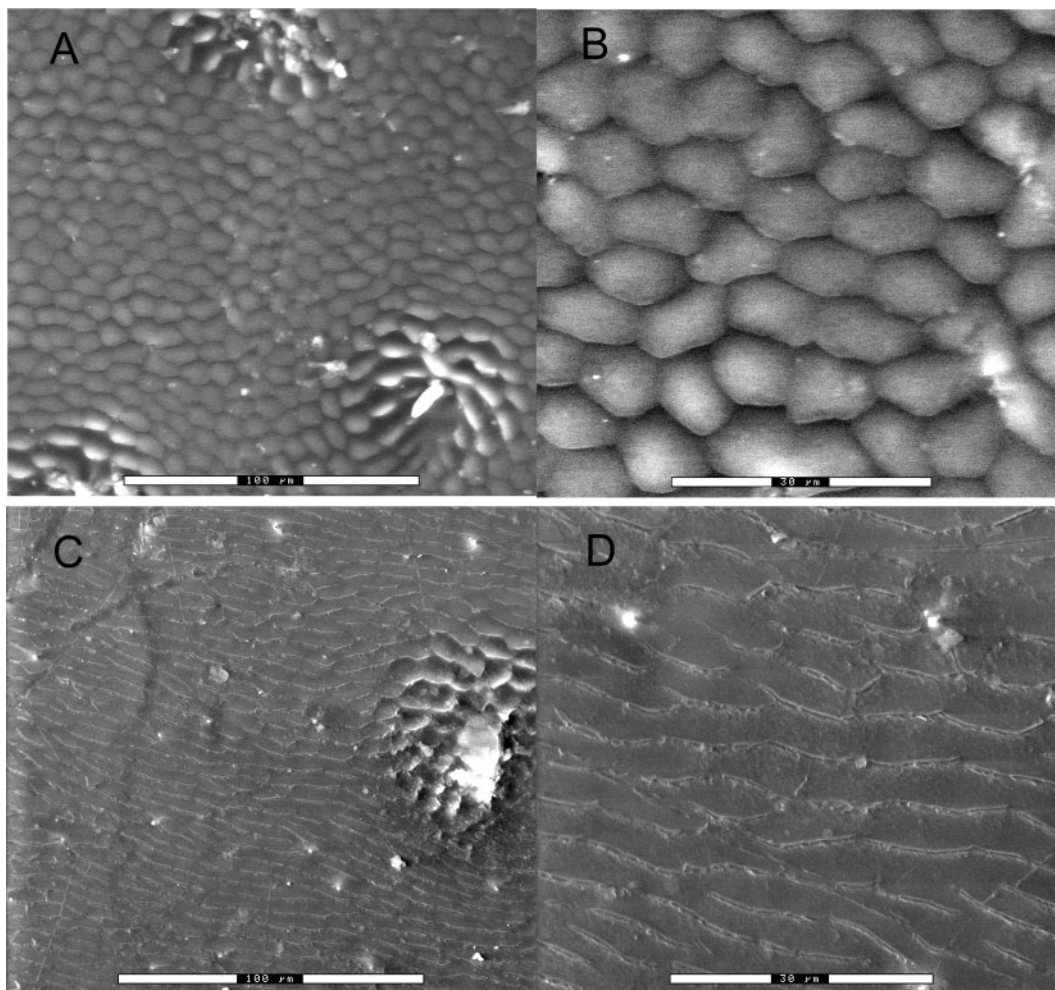


Fig. 12. Environmental scanning electron micrograph of elytral microsculpture. *A*, *Nicrophorus reticulatus* 500×. *B*, *N. reticulatus* 1500×. *C*, *Nicrophorus trumboi* 500×. *D*, *N. trumboi* 1500×.

longed towards base. Inner margin of lacinial lobe of maxilla of larva with numerous small spiculi throughout length. Labial palpus of larva segments 1 and 2 equal in length. Width across ligula of larval labium less than or equal to diameter of 1 palp base. Ventral surface of larval labial palpi sclerotised. Centre of ventral surface of larval prementum unsclerotised. Larval labium postmentum bearing pair of setae at anterior third. Larval labium base of mentum sclerotised heavily on outer angles only, weakly to not sclerotised medially. Sensory papilla margin of epipharynx of larva complete. Median sensory pegs of epipharynx of larva located anterolaterally of sensory papilla. Subantennal sclerite of larva not thickened or raised. Episterna of larval thorax heavily sclerotised. Mes- and metepimera of larval thorax distinct, elongate, triangular, separated from episterna by deep, heavily sclerotised sulcus. Tergites of larva small, not projecting, without lobes. Sternite 9 of larva entire. Base of ventrite 10 of larva sclerotised. Apex of ventrite 10 of larva sclerotised. Basal segment of urogomphus of larva short and

thick, 2–3 times length of segment 2. Lateral projection at base of urogomphus present. Unsclerotised suture at base of urogomphus incomplete medially.

Variation

Unlike most other *Nicrophorus* species-groups, some of which contain species ranging from all-black to fully maculated forms (e.g. Anderson and Peck 1986), there is relatively little evidence of elytral pattern variation in the *nepalensis*-group of species. Even the widespread *N. nepalensis* shows essentially the same elytral pattern from Pakistan to Malaysia and Japan (a single exception being a sole apparently melanistic specimen documented from Taiwan, Fig. 8I). Minor variation exists in some species (as discussed under each species below) in the darkness of pubescence, the presence or absence of the spot on the frons, and elytral pattern. As is true of most microphorines there is sexual dimorphism.

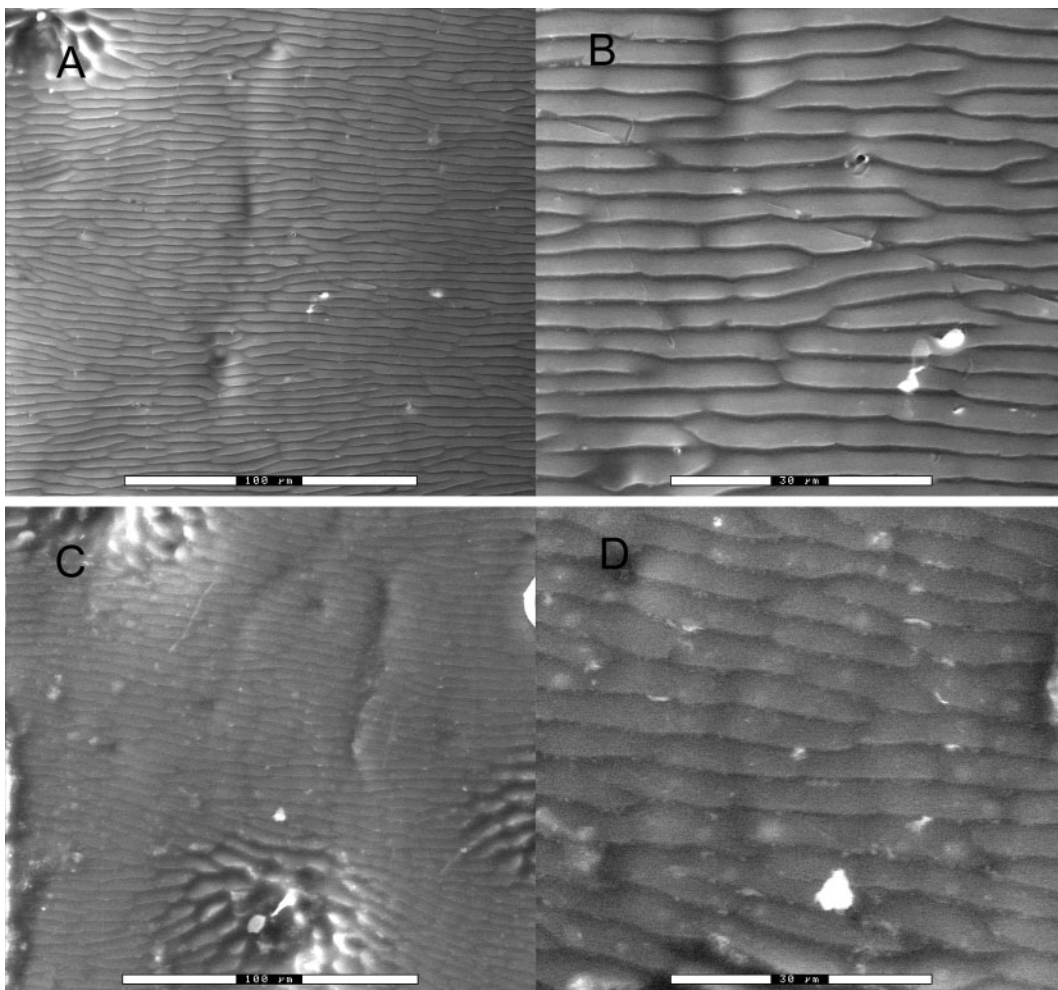


Fig. 13. Environmental scanning electron micrograph of elytral microsculpture. *A*, *Nicrophorus insignis* 500x. *B*, *N. insignis* 1500x. *C*, *Nicrophorus melissae* 500x (Nepal). *D*, *N. melissae* 1500x (Nepal).

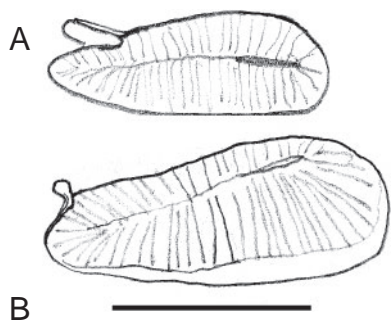


Fig. 14. First abdominal spiracle, lateral view. *A*, *Nicrophorus charon*. *B*, *Nicrophorus maculifrons*. Scale bar = 1 mm.

Bliss (1949) and Easton (1980) reported on sexually dimorphic features of *Nicrophorus* adults. Easton (1980) commented that the sexes of *Nicrophorus* adults can be distinguished by the number of visible abdominal segments because males have nine and females have eight (the ninth segment having become modified into the base of the ovipositor in females). There are at least four additional external traits that show sexual dimorphism in *Nicrophorus*, however, the degree to which these are expressed is dependent on body size and may represent an allometric relationship. Large males are strongly dimorphic but small males show female-like traits. Additionally, there is variation throughout the subfamily in the expression of dimorphism.

The clypeal membrane differs between the sexes in most microphorine species. All members of the *nepalensis*-group whose females are known, show a fasciform clypeal membrane in the female. The clypeal membrane of the male is cam-

panulate (bell-shaped, e.g. Fig. 9). Additionally, the postocular bulge of large males appears to be larger than that of females.

The tarsomeres of the foretarsi are longer and have longer setae on the males of most silphid species (Trumbo and Sikes 2000). The metatrochanter spur is also larger on males than on females, although again, small males look like females.

Ecology

Little is known of these species' ecology – few *nepalensis*-group species have been the subject of ecological investigations. The species that occur in Japan are the best known Asian *Nicrophorus* in general, with a variety of studies such as Kamimura *et al.*'s (1964) and Martin's (1989) altitudinal work, and numerous surveys of carrion beetle assemblages such as those by Ôhara (Ôhara and Higashi 1987; Ôhara 1992, 1994a, 1994b, 1995a, 1995b, 1997; Ôhara and Yabuki 1992; Ôhara *et al.* 1995). However, most autecological work has focused on *N. quadripunctatus* (e.g. Satou *et al.* 2001; Xu and Suzuki 2001; Nisimura *et al.* 2002). Less is known about the other *nepalensis*-group species of Japan, *N. maculifrons* and *N. montivagus*. The latter is the smallest-bodied *Nicrophorus* known and, in particular, how it survives among the speciose carrion beetle fauna of Japan remains unexplained. To supplement the sparse ecological literature we can attempt to infer aspects of species' ecology such as elevational or habitat preference from label data. However, this is challenging because elevation or habitat type are rarely indicated on labels.

Although some habitat preference diversity is seen in the genus (Anderson 1982; Scott 1998), all members of the *nepalensis*-group appear to be forest associated, primarily at higher (> 1000 m) elevations (Table 4). Some species are

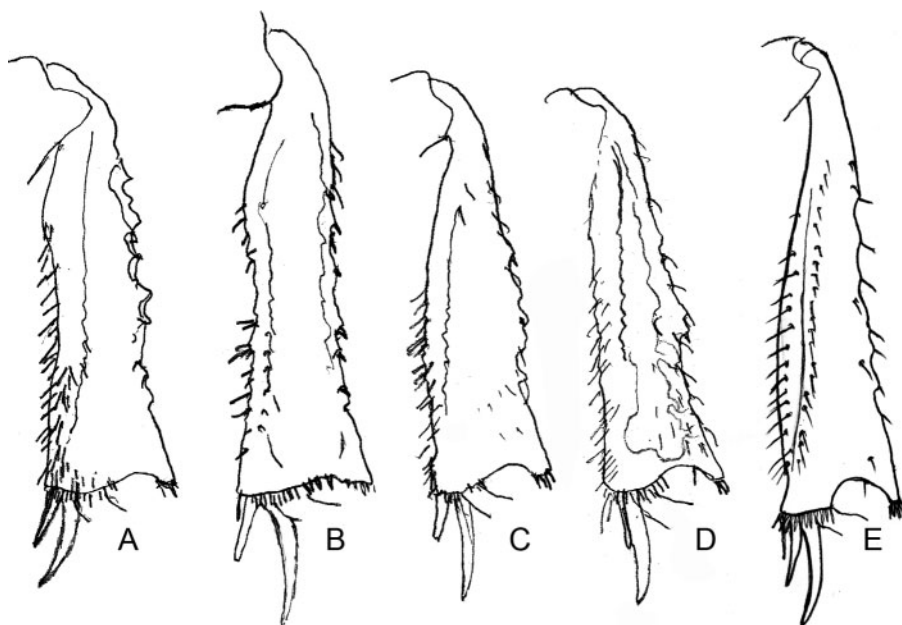


Fig. 15. Metatibia of large males. *A*, *Nicrophorus nepalensis*. *B*, *N. maculifrons*. *C*, *N. podagricus*. *D*, *N. insularis*. *E*, *N. trumboi*.

Table 4. Elevational ranges

Species of the *nepalensis*-group sorted by elevation data (in metres). Median values (rather than means) are reported to prevent single locations that were visited multiple times from influencing the results. Elevations given on specimen labels as a broad range (e.g. 1000–2000 m) were ignored. The median was used for individual records given on specimen labels as a narrow range (e.g. 1700–1900 m)

| Species | Author(s) | Median (minimum–maximum) elevation (m) | Number of specimens with elevation data | Number specimens studied (includes many specimens without elevational data) |
|--------------------------------------|---------------------|--|---|---|
| 1. <i>N. maculifrons</i> | Kraatz, 1877 | 500 (95–3000) | 19 | 248 |
| 2. <i>N. quadripunctatus</i> | Kraatz, 1877 | 800 (180–3744) | 33 | 599 |
| 3. <i>N. montivagus</i> | Lewis, 1887 | 1050 (720–1800) | 14 | 140 |
| 4. <i>N. insularis</i> | Grouvelle, 1893 | 1400 (36–2500) | 25 | 101 |
| 5. <i>N. reticulatus</i> , sp. nov. | Sikes & Madge, 2006 | 1471 (1341–1524) | 4 | 4 |
| 6. <i>N. podagricus</i> | Portevin, 1920 | 1560 (987–1800) | 19 | 137 |
| 7. <i>N. herscheli</i> , sp. nov. | Sikes & Madge, 2006 | 1630 (1630–1665) | 8 | 9 |
| 8. <i>N. charon</i> , sp. nov. | Sikes & Madge, 2006 | 1690 (1200–2200) | 10 | 18 |
| 9. <i>N. apo</i> | Arnett, 1950 | 1759 (914–1981) | 14 | 59 |
| 10. <i>N. insignis</i> , sp. nov. | Sikes & Madge, 2006 | 1829 (1200–1950) | 5 | 19 |
| 11. <i>N. heurni</i> | Portevin, 1926 | 1829 (1200–4000) | 25 | 162 |
| 12. <i>N. nepalensis</i> | Hope, 1831 | 2019 (150–3650) | 166 | 674 |
| 13. <i>N. schawalleri</i> , sp. nov. | Sikes & Madge, 2006 | 2550 (1524–3962) | 16 | 82 |
| 14. <i>N. melissae</i> , sp. nov. | Sikes & Madge, 2006 | 3025 (2400–3375) | 22 | 54 |
| 15. <i>N. trumboi</i> , sp. nov. | Sikes & Madge, 2006 | 3383 (2870–3383) | 7 | 23 |

occasionally encountered below this elevation: *N. insularis* (36–2500 m, six elevation records < 1000m of 25 total records), *N. maculifrons* (95–3000 m, 12 of 19 elevation records), *N. montivagus* (720–1200 m, four of 14 elevation records), *N. nepalensis* (150–3650 m, 17 of 166 elevation records), *N. quadripunctatus* (180–3740 m, 18 of 33 elevation records < 1000 m). It is probably not a coincidence that most of these species that occur below 1000 m have the

largest geographic distributions within the *nepalensis*-group. Additionally, the three species that occur at the lowest elevations (Table 4) are from northern latitudes in Asia where lower elevations have cooler temperatures than in tropical regions. Some species, not surprisingly the Himalayan endemics, occur typically above 2000 m: *Nicrophorus melissae* (2300–3375 m, 22 records) and *N. trumboi* (2870–3383 m, six records). Hanski and Niemelä (1990),

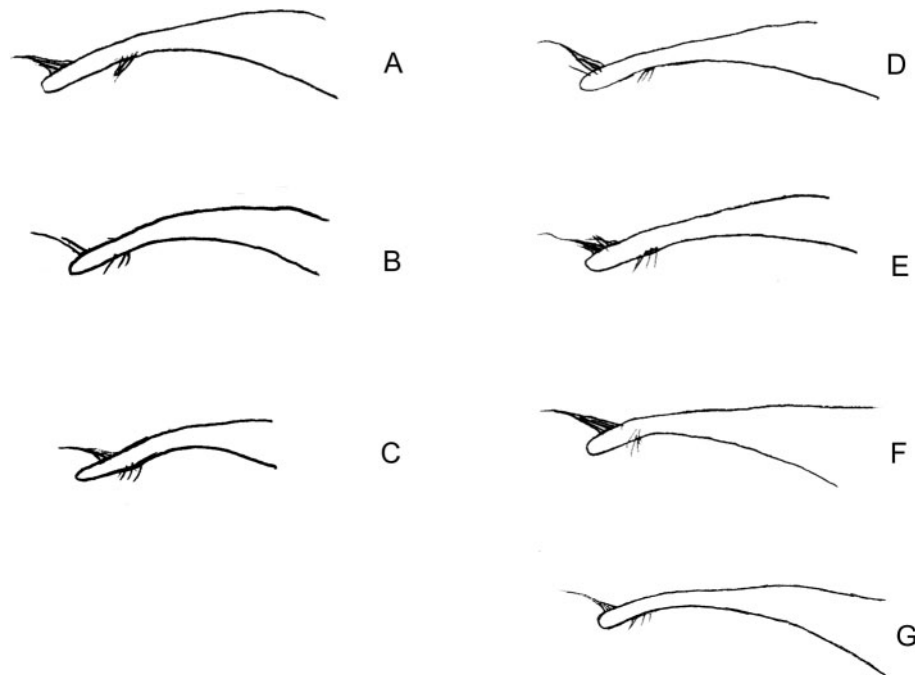


Fig. 16. Right paramere of aedeagus, lateral view: A, *Nicrophorus apo*. B, *N. quadripunctatus*. C, *N. montivagus*. D, *N. insularis*. E, *N. heurni*. F, *N. podagricus*. G, *N. herscheli*.

Hanski (1983) and Hanski and Krikken (1991) described dung and carrion beetle assemblages in Sulawesi and Borneo. They recorded elevational records for *N. charon* (as an undescribed species) and *N. podagricus*. We did not include their data in our analysis; however, their observations agree with ours (Table 4). We are concerned that populations of species restricted to the highest elevations of islands in the Malay Archipelago may go extinct if global temperatures increase as predicted (Root *et al.* 2003) – they will simply be unable to disperse upslope to higher and cooler habitats.

Key to adults of the species of *Nicrophorus* in the *nepalensis*-group

See also the flow-chart key (Figs 18, 19), which emphasises obvious characters. However, the flow-chart key is less likely to work for all cases of possible variation than the text key below. Given the number of species apparently endemic to particular islands, the use of geographic data will often simplify identification problems in this group.

The key includes the following characters that may be difficult to understand.

Microsculpturing of the elytral disc – this character cannot be seen without high-magnification, although it is visible using a strong dissecting microscope (often moving the specimen to achieve different angles of light reflectance helps).

Abdominal spiracle 1 is located in the basal pleuron of the abdomen; count anteriorly from the fifth tergum, which bears the stridulatory files; the elytron must be moved to see this character.

Moderate to large males – numerous secondary sexual characters are unique to moderate to large males, with small males showing the same states as females.

1. Elytra with epipleuron partially or entirely black 2
Elytra with epipleuron entirely red–orange 4
- 2(1). Abdominal sterna 3 to 6 with very short setae along posterior margins (these setae are 2–3 × longer than the distance between adjacent setae). Elytral disc with isodiametric microsculpturing (Fig. 12). Distribution: Solomon Islands: Guadalcanal (Fig. 20)
. *N. reticulatus* Sikes & Madge, sp. nov.
Abdominal sterna 3 to 6 with long setae along posterior margins (these setae are 5–8 × longer than the distance between adjacent setae). Elytral disc with strongly transverse microsculpturing (e.g. Figs 2, 13) 3
- 3(2). Metasternal pubescence short and fine medially. Males (moderate to large individuals only): metatibiae with inner face widened. Pale lunule at base of elytral epipleura large. Abdominal spiracle 1 with a small lobe at anterior end (e.g. Fig. 14B). Distribution: Indonesia: West Irian; Papua New Guinea (Fig. 21). *N. heurni* Portevin
Metasternal pubescence long and well developed medially. Males (moderate to large individuals only): metatibiae with inner face not widened. Pale lunule at base of elytral epipleura very small (Fig. 22B). Abdominal spiracle 1 with a large lobe at anterior end (Fig. 14A). Distribution: Indonesia: Sulawesi (Fig. 23)
. *N. charon* Sikes & Madge, sp. nov.
- 4(1). Moderate to large males: metatibiae with dorsal margin not swollen, simple as in female (Fig. 15B, E). Females: valvifer claw with outer margin lobed but not toothed (Figs 10O, P; 11B), or weakly toothed (Fig. 11F) 5
Moderate to large males: metatibiae with dorsal margin swollen near middle (e.g. Fig. 15A, C, D). Females: valvifer

- claw with outer margin obviously toothed (Figs 10M; 11A, C, D, E) 8
- 5(4). Antennal club with basal three segments black or reddish black, apical segment orange. Frons with or without orange spot. Distribution: Japan (Fig. 24) . . . *N. montivagus* Lewis
Antennal club all orange or with only basal segment black, apical three orange. Frons with orange spot 6
- 6(5). Antennal club usually all orange, sometimes basal segment darkened. Meso- and metatibiae with apical emargination very large, semicircular; the apical process thus very narrow; lower part of emargination without a row of setae (Fig. 15E). Posterior fascia with anterior margin smooth. Moderate to large males: metatibiae with inner face convex (Fig. 15E). Distribution: Nepal, Bhutan (Fig. 25)
. *N. trumboi* Sikes & Madge, sp. nov.
Antennal club with basal segment black, apical three orange. Meso- and metatibiae with apical emargination smaller, not semicircular; the apical process thus broader; lower part of emargination with a row of setae (e.g. Fig. 15B). Posterior fascia with anterior margin irregular. Moderate to large males: metatibiae with inner face bearing a prebasal bump and then concave (Fig. 15A, B) 7
- 7(6). Elytra with middle black band usually not reaching the dorsal ridge of the epipleuron (Figs 8A, B; 26A). Pubescence of metasternum golden (when middle black band shortened, e.g. Fig. 8A) or dark brown (when middle black band reaches or almost reaches the dorsal ridge, and sometimes when it almost does, e.g. Fig. 8B). Dorsal ridge of epipleuron with posterior setae golden in palest forms but grading to dark brown in others. Metafemora with apical setae golden in palest forms but grading to dark brown – apparently the first sign of darkening. Distribution: China: Sichuan, Gansu, and Shaanxi Provinces (Fig. 27)
. *N. schawalleri* Sikes & Madge, sp. nov.
Elytra with middle black band always reaching dorsal ridge of epipleuron (Fig. 9B). Metasternum with golden pubescence. Dorsal ridge of epipleuron with posterior setae dark brown. Metafemora with apical setae dark brown. Distribution: North-east China, far eastern Russia (Ussuri region, Sakhalin Island), Korea, Japan (Fig. 28)
. *N. maculifrons* Kraatz
- 8(4). Elytra with posterior margin of middle black band without a dark finger projecting over the callus (bump near posterior of elytron); never with a completely surrounded black spot near humerus (e.g. Figs 8E, G, K; 22A, C, D) 9
Elytra with posterior margin of middle black band with a dark finger (rarely an isolated dark spot) projecting over the callus; humeral spot completely surrounded or not (e.g. Figs 8C, D, H, I, J, L, M) 11
- 9(8). Third abdominal sternum on basal half with a patch of long, semi-erect setae on either side of midline (area may be partially hidden by metacoxae) but glabrous medially. Distribution: Philippine Islands: Mindanao (Fig. 29)
. *N. apo* Arnett
Third abdominal sternum on basal half with band of long, semi-erect setae across middle, not interrupted at midline 10
- 10(9). Elytra with posterior maculae usually widely separated at suture. Posterior fascia not touching lateral or posterior margin of elytron (Fig. 8G). Pronotum of large males subquadrate. Metasternum with dark to light brown pubescence. Apical procoxal setae very short, straight and very sparse. Distribution: Indonesia: northern Sumatra (Fig. 30)
. *N. herscheli* Sikes & Madge, sp. nov.

- Elytra with posterior fascia typically not interrupted at suture, or if interrupted, then fascia narrowly separated. Posterior fascia touching lateral and posterior margins of elytron (Fig. 8K). Pronotum of large males orbicular. Metasternum with light brown to golden pubescence. Apical procoxal hairs long, curved and somewhat more abundant. Distribution: Indonesia: Flores Island (Fig. 23)
 *N. insignis* Sikes & Madge, sp. nov.
- 11(8). Shoulder area of elytra with a completely surrounded black spot, separated from end of basal black band (e.g. Fig. 8H, I, J, M, N) 12
 Shoulder area of elytra with black spot connected to basal black band, not separated (e.g. Fig. 8C, D, L) 14
- 12(11). Elytra with posterior fascia not interrupted at suture (Fig. 8M). Metasternum with golden pubescence. Shoulder area of elytra with a row of long erect setae. Moderate to large males: metatibiae expanded laterally, inner face convex, without a prebasal bump (Fig. 15C, D). Distribution: Japan, Korea, far eastern Russia, north-east China (Fig. 31)
 *N. quadripunctatus* Kraatz
- Elytra with posterior fascia interrupted at suture (Fig. 8H, I, J). Metasternum with dark brown pubescence. Shoulder area of elytra with a row of short setae. Moderate to large males with metatibiae expanded laterally, or not, with inner face convex (Fig. 15 C, D), or not convex but with a prebasal bump (Fig. 15A, B) 13
- 13(12). Frons without an orange spot. Elytra with posterior fascia not reaching dorsal ridge of epipleura (Fig. 8J). Moderate to large males with metatibiae expanded laterally, inner face convex, without a prebasal bump (Fig. 15C, D). Distribution: Indonesia: Sumatra, Java, Bali (Fig. 32)
 *N. insularis* Grouvelle
- Frons usually with an orange spot. Elytra with posterior fascia usually reaching dorsal ridge of epipleura (Fig. 8H, 33A). Moderate to large males with metatibiae not expanded laterally, inner face not convex but with a prebasal bump (Fig. 15A). Distribution: Pakistan, Himalayas, India, China, Laos, Burma, Malaysia, Japan: Ryukyu; Philippines, Taiwan, Thailand, Vietnam (Fig. 34) *N. nepalensis* Hope
- 14(11). Moderate to large males with metatibiae expanded laterally, with inner face convex (Fig. 15C, D). Distribution: northern Borneo – east Malaysia (Sarawak, Sabah) (Fig. 35)
 *N. podagricus* Portevin
- Moderate to large males with metatibiae not expanded laterally, with inner face not convex but with a prebasal bump (e.g. Fig. 15A, B). Distribution: Nepal, Bhutan (Fig. 36)
 *N. melissae* Sikes & Madge, sp. nov.

Nicrophorus apo Arnett

(Figs 8E, 10M, 16A, 22A, 29)

Nicrophorus apo Arnett, 1950: 67.

Material examined

See Accessory Publication on *Invertebrate Systematics* website.

Measurements

(19 ♂, 22 ♀), pronotal width: ♂ 4.24–6.35, 4.94 ± 0.75 mm, ♀ 3.57–6.04, 4.92 ± 0.59 mm.

Diagnosis

Nicrophorus nepalensis-group taxon with third abdominal sternum on basal half with a patch of long, semi-erect setae on either side of midline (area may be partially hidden by metacoxae) but glabrous medially; elytra with posterior margin of middle black band without a dark finger projecting over the callus (bump near posterior of elytron); never with a completely surrounded black spot near humerus (Figs 8E; 22A); moderate to large males: metatibiae with dorsal margin swollen near middle (e.g. Fig. 15A, C, D). Females: valvifer claw with outer margin obviously toothed (Fig. 10M); elytra with epipleuron entirely red-orange.

Description

Head. Antennal club basal segment black, apical three orange. Antennomeres of club weakly emarginate. Frons black, with orange spot. Post-ocular bulge of large males larger than that of females.

Thorax. Microsculpture of pronotum disc composed of many parallel transverse lines. Pronotum of large males sub-square. Setae on posteroventral portion of hypomeron long, erect, sparse; filling region extending a third or less length between trochantin and posterior margin, restricted to upper region of sclerite. Pronotum with brown to light-brown, short (approximately < 0.1 mm), sparse, setae restricted to margins. Humerus immediately dorsal of epipleural ridge orange. Humeral setae short, not forming row. Epipleuron entirely orange. Posterior epipleural ridge with isolated single-file row of contiguous preapical setae. Epipleuron and lateral margin of elytron with sparse, short, recumbent, yellow setae throughout. Region adjacent to apex of elytral suture black. Anterior black band (or spot) not reaching 3rd costa. Anterior fascia of elytron without black spot, passing first costa but not reaching suture, anterior margin u-shaped between costae 1 and 2 (with bottom of u towards posterior), posterior margin u-shaped between costae 1 and 2 (with bottom of u towards posterior). Posterior fascia not touching lateral or posterior margins of elytron. Black spot of elytral posterior fascia near anterior margin of fascia absent. Black spot of elytral posterior fascia near posterior margin of fascia absent, region black. Elytral posterior fascia reduced, interrupted before suture. Elytral microsculpture transverse straight, narrow with breaks (e.g. Figs 2, 13). Posterior margin of elytron with 5–10 clusters of long, dark or light brown setae. Metanotal subalare with sharply rising, internally margined ridge along antero-medial edge. Metasternal pubescence medially long, well developed, light brown. Metapimeral posterior lobe with long brown setae throughout lobe.

Abdomen. Posterior margin of abdominal ventrite 5 with long setae. Setae cluster on centre of sternite 3 between metacoxae absent in centre but with long erect setae lateral of centre under coxae. Abdominal setae dark brown. Tergite 9 of males (pygidium) with brown setae.

Legs. Lateral margin of anterior of procoxae smooth, without ridge or bump. Meso- and metatibia apical angle produced into lobe. Inner margin of metatibia of large males with a prebasal bump. Middle of outer margin of metatibia slightly swollen in large males. Middle of inner face of metatibia (large males) not greatly widened (less than $2 \times$ width at base). Metatrochanter spine of males apex pointing parallel (or almost parallel) to leg, recurved dorsally without acute angle ventrally, with a sharp apex.

Aedeagus. Paramere ventral setal patch not overlapping with apicolateral patch. Parameres evenly curved.

Ovipositor. Spatula on proctiger (T10) apex narrow. Valvifer claw dentate.

Distribution

Oriental: Philippines: Mindanao (Fig. 29).

Remarks

There are only two known species of *Nicrophorus* in the Philippines: *N. nepalensis* and *N. apo*. This species, *N. apo*,

can be distinguished from *N. nepalensis* by its lack of black spots within the elytral fascia. Its elytral pattern (Fig. 8E) is most similar to that of *N. herscheli* (Fig. 8G) of Sumatra, and *N. trumboi* (Fig. 8F) of Nepal; it can be distinguished from these species by its dentate valvifer claw on the ovipositor (Fig. 10M) (*N. trumboi* has the claw lobed with a round apex (Fig. 11B)) and by having the inner margin of the metatibia of large males curved outwards with a prebasal bump (e.g. Fig. 15A,B), *N. herscheli* has the inner margin curved gradually outwards without a prebasal bump (e.g. Fig. 15C,D). Additionally, *N. apo* has the long, semi-erect setae of the third abdominal sternum interrupted medially whereas *N. trumboi* and *N. herscheli* have these setae uninterrupted (Fig. 19). No variation known except for secondary sexual characters, in which small males approach the condition of females.

Etymology

This is a modern place name, treated as a Latin noun in the nominative. Mount Apo, Mindanao, Republic of the Philippines is the type locality of the species.

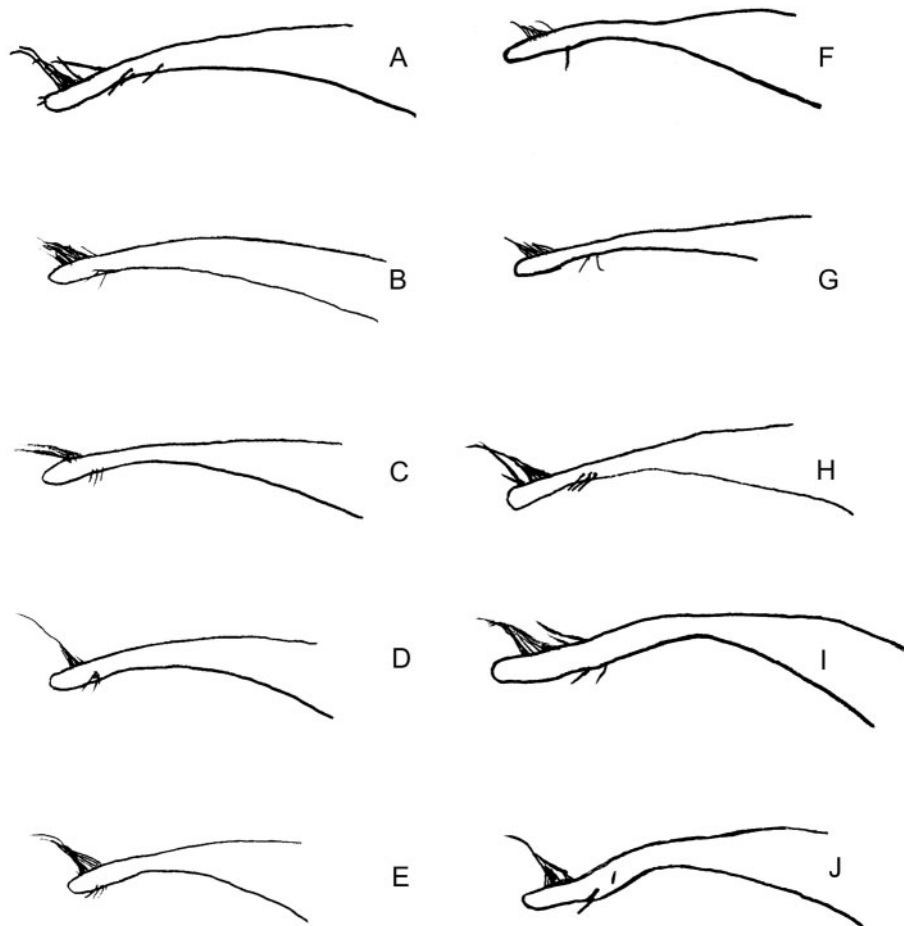


Fig. 17. Right paramere of aedeagus, lateral view: A, *Nicrophorus nepalensis*. B, *N. insignis*. C, *N. charon*. D, *N. melissae* (Nepal). E, *N. melissae* (Bhutan). F, *N. trumboi*. G, *N. reticulatus*. H, *N. insularis*. I, *N. schawalleri*. J, *N. maculifrons*.

***Nicrophorus charon* Sikes & Madge, sp. nov.**(Figs 8*N*, 10*R*, 14*A*, 17*C*, 22*B*, 23)*Nicrophorus* undescribed Hanski & Niemelä, 1990: 149.*Nicrophorus* undescribed Hanski & Krikken, 1991: 195.*Nicrophorus* sp. n. Peck, 2001: 94.**Material examined**

Holotype. ♀ labelled 'INDONESIA: Sulawesi, Tengah: Mt. Tambusisi, elev. 1219 m, 1°39'S, 121°21'E, 3–13.iv.1980 (coll. M. J. D. Brendell) BMNH006420Nic'. (London (BMNH)).

Paratypes. 10 ♂, 7 ♀: **INDONESIA: Sulawesi:** Utara, Gng. Amang F. R. nr. Kotamobagu, elev. 1200 m, [1°N, 123°E], 4.ii.1985, 3 ♂: BMNH83802Nic, BMNH83803Nic, BMNH83804Nic; same locality, 2.vi.1985, 1 ♂: BMNH83805Nic; Utara Dumoga-Bone N.P., lower montane, 2000 m pitfall trap / R. Ent. Soc. Lond., PROJECT WALLACE, B.M. 1985–10, 1985 (coll. P. Whilton), 2 ♂: BMNH122043Nic, BMNH122045Nic; Utara, Gng. Ambang F. R., Gng. Muajak, nr. Kotamobagu, 1780 m, 1–30.xi.1985, 1 ♀: BMNH122046Nic; 30 km NW Rantepao, Bulu-Bulu, elev. 1600 m, [2°59'S, 119°54'E], 9–15.v.1966 (coll. R. Straatman), 1 ♀: BPBM003389Nic; ~30 km NE of Enrekang. Gn. Rantemario. Borong Tangga Camp, 3°24'S, 120°0'E, 5.xi.1993 (coll. J. P. & M. J. Duffels), 2 ♀: ZMAN003702Nic, ZMAN003703Nic; Latimodiongeb., elev. 2200 m, 23.vi.1930 (coll. G. Heinrich), 1 ♂: BMNH006421Nic; Palu Central-Celebes, [0°54'S, 119°52'E], 1–30.iv.1991, 1 ♂: WBC080867Nic; Tengah Lore Lindu N.P., 10 km SE Poloka, Stat. 55 Disturbed lower montane forest ML-light, canopy, elev. 1900 m, 25.iii.1985 (coll. J.P. & M. J. Duffels), 2 ♂: ZMAN003740Nic, ZMAN003741Nic; Tengah Lore Lindu N.P., 10 km SE Poloka, Stat. 57 Disturbed lower montane forest ML-light, canopy, elev. 1900 m, 26.iii.1985 (coll. J.P. & M. J. Duffels), 1 ♀: ZMAN003690Nic; Tengah Lore Lindu N.P., Rano Rano 10 km NE Gimpu, Stat 41 lower montane forest MV-light, elev. 1600 m, [1°36'S, 120°2'E], 14.iii.1985 (coll. J.P. & M. J. Duffels), 2 ♀: ZMAN003688Nic, ZMAN003689Nic.

Measurements

(10 ♂, 8 ♀), pronotal width: ♂ 4.8–7.0, 5.66 ± 0.77 mm, ♀ 4.7–6.71, 5.65 ± 0.63 mm.

Diagnosis

Nicrophorus nepalensis-group taxon with epipleuron partially or entirely black; metasternal pubescence long and well developed medially; males (moderate to large individuals only): metatibiae with inner face not widened. Pale lunule at base of elytral epipleura very small (Fig. 22*B*); abdominal spiracle 1 with a large lobe at anterior end (Fig. 14*A*); abdominal sterna 3 to 6 with long setae along posterior margins (these setae are 5–8 × longer than the distance between adjacent setae). Elytral disc with strongly transverse microsculpturing (e.g. Figs 2, 13).

Description

Head. Antennal club basal segment black, apical three orange. Antennomeres of club weakly emarginate. Frons black, without orange spot. Post-ocular bulge of large males larger than females.

Thorax. Microsculpture of pronotum disc composed of many parallel transverse lines. Pronotum of large males

orbicular. Setae on posteroventral portion of hypomeron long, erect, sparse; filling region extending a third or less length between trochantin and posterior margin, restricted to upper region of sclerite. Pronotum with brown to light-brown, short (approximately < 0.1 mm), sparse, setae restricted to margins. Humerus immediately dorsal of epipleural ridge orange. Humeral setae short, not forming row. Epipleuron black throughout, medial (dorsal) half orange. Posterior epipleural ridge with isolated single-file row of contiguous preapical setae. Epipleuron and lateral margin of elytron with sparse, short, recumbent, yellow setae throughout. Region adjacent to apex of elytral suture black. Anterior black band (or spot) reaches 3rd costa. Anterior fascia of elytron with black spot completely surrounded by fascia, passing first costa but not reaching suture, anterior margin u-shaped between costae 1 and 2 (with bottom of u towards posterior), posterior margin u-shaped between costae 1 and 2 (with bottom of u towards posterior). Posterior fascia not touching lateral or posterior margins of elytron. Black spot of elytral posterior fascia near anterior margin of fascia present on callus. Black spot of elytral posterior fascia near anterior margin of fascia incomplete, joining black elytral disc. Black spot of elytral posterior fascia near posterior margin of fascia present between costa 1 and 2 and incompletely surrounded by fascia. Elytral posterior fascia reduced, interrupted before suture. Elytral microsculpture transverse straight, narrow with breaks (e.g. Figs 2, 13). Posterior margin of elytron with 5–10 clusters of long, dark or light brown setae. Metanotal subalare with sharply rising, internally margined ridge along anteriomedial edge. Metasternal pubescence medially long, well developed, dark brown. Metapimeral posterior lobe with long brown setae throughout lobe.

Abdomen. Posterior margin of abdominal ventrite 5 with long setae. Setae cluster on centre of sternite 3 between metacoxae light brown. Abdominal setae dark brown. Tergite 9 of males (pygidium) with brown setae.

Legs. Lateral margin of anterior of procoxae smooth, without ridge or bump. Meso- and metatibia apical angle produced into lobe. Inner margin of metatibia of large males gradually curved outwards. Middle of outer margin of metatibia slightly swollen in large males. Middle of inner face of metatibia (large males) not greatly widened (less than 2 × width at base). Metatrochanter spine of males with apex pointing parallel (or almost parallel) to leg, straight, not recurved dorsally.

Aedeagus. Paramere ventral setal patch overlaps at edge with apicolateral patch. Parameres evenly curved.

Ovipositor. Spatula on proctiger (T10) apex narrow. Valvifer claw dentate (Fig. 10*R*).

Distribution

Oriental: Indonesia: Sulawesi (Fig. 23).

Remarks

This species shares a pattern of colouration of the epipleura with only one other species in the subfamily, *N. heurni* of New Guinea; the dorsal (medial) half of the epipleura is orange (more so anteriorly) and the ventral (lateral) half is black (Figs 18, 22B). This species can be distinguished from *N. heurni* in that it has metasternal pubescence long and well developed medially whereas *N. heurni* has this pubescence short and fine medially. In addition, the middle of the inner face of the metatibia of large males is not greatly widened (less than $2 \times$ width at apex), unlike the state seen in *N. heurni*. Additionally, this species has a large lobe on the first abdominal spiracle (Fig. 14A) in contrast to a small lobe seen in *N. heurni*. No variation is known except for secondary sexual characters, in which small males approach the condition of females.

Etymology

This is a Latin/Greek mythological name in the nominative. In Greco-Roman religion, Charon was the ferryman who transported the spirits of the dead across the river Styx in the underworld. The name alludes to the species' association with dead bodies.

Nicrophorus herscheli Sikes & Madge, sp. nov.

(Figs 8G, 11A, 16G, 22C, 30)

Nicrophorus undescribed Hanski & Niemelä, 1990: 149.

Nicrophorus undescribed Hanski & Krikken, 1991: 195.

Nicrophorus sp. n. Peck, 2001: 94.

Material examined

Holotype. ♀, labelled '[INDONESIA]: Sumatra, N. Sumatra Gng Leuser NP Mt. Mamas, elev. 1630 m, 3°33'N, 97°39'E, 7–10.viii.1983 (coll. H. Räisänen) – MCZC73701Nic'. (Cambridge (MCZC)).

Paratypes. 3 ♂, 5 ♀. [INDONESIA]: Sumatra: N. Sumatra Gng Leuser NP Mt. Mamas, elev. 1630 m, 3°33'N, 97°39'E, 24–28.vii.1983 (coll. H. Räisänen), 2 ♀: DSSC73703Nic, MCZC73705Nic, 1 ♂: DSSC73699Nic; **same locality, 28.vii–7.viii.1983, 1 ♂: MZHF73698Nic; **same locality, 7–10.viii.1983, 1 ♀: MCZC73704Nic, 1 ♂: MCZC73700Nic; **same locality, elev. 1650–1680 m, 3°20'N, 97°46'E, 10–17.ix.1983 (coll. H. Räisänen), 1 ♀: MZHF73702Nic; **N. Sumatra Tele (south-west of lake Toba and Samosir Island; south-west of Mt. Belirang, approximately 1700 m elev.), [2°33'N, 98°35'E], 23–24.iii.1984 (coll. G. Hangay), 1 ♀: SMNS003361Nic.

Measurements

(3 ♂, 6 ♀), pronotal width: ♂: 5.27–6.54, 5.72 ± 0.71 mm, ♀ 4.66–6.14, 5.35 ± 0.51 mm.

Diagnosis

Nicrophorus nepalensis-group taxon with epipleuron entirely red-orange, posterior maculae usually widely separated at suture; posterior fascia not touching lateral or posterior margin of elytron (Fig. 8G), posterior margin of middle

black band without a dark finger projecting over the callus (bump near posterior of elytron); never with a completely surrounded black spot near humerus (e.g. Figs 8E, G, K; 22A, C, D); pronotum of large males subquadrate; metasternum with dark to light brown pubescence; apical procoxal setae very short, straight and very sparse; third abdominal sternum on basal half with band of long, semi-erect setae across middle, not interrupted at midline; moderate to large males: metatibiae with dorsal margin swollen near middle (e.g. Fig. 15A, C, D); females: valvifer claw with outer margin obviously toothed (Fig. 11A).

Description

Head. Antennal club basal segment black, apical three orange. Antennomeres of club weakly emarginate. Frons black, with orange spot. Post-ocular bulge of large males larger than females.

Thorax. Microsculpture of pronotum disc isodiametric. Pronotum of large males subquadrate. Setae on posteroventral portion of hypomeron long, erect, sparse; filling region extending a third or less length between trochantin and posterior margin, restricted to upper region of sclerite. Pronotum with brown to light-brown, short (approximately < 0.1 mm), sparse, setae restricted to margins. Humerus immediately dorsal of epipleural ridge orange. Humeral setae short, not forming row. Epipleuron entirely orange. Posterior epipleural ridge with isolated single-file row of contiguous preapical setae. Epipleuron and lateral margin of elytron with sparse, short, recumbent, yellow setae throughout. Region adjacent to apex of elytral suture black. Anterior black band reaches 3rd costa. Anterior fascia of elytron without black spot. Anterior fascia of elytron passing first costa but not reaching suture. Anterior fascia between costae, anterior margin u-shaped between costae 1 and 2 (with bottom of u towards posterior), posterior margin u-shaped between costae 1 and 2 (with bottom of u towards posterior). Posterior fascia not touching lateral or posterior margins of elytron. Black spot of elytral posterior fascia near anterior margin of fascia absent. Black spot of elytral posterior fascia near posterior margin of fascia absent, region black. Elytral posterior fascia reduced, interrupted before suture. Elytral microsculpture transverse straight, narrow with breaks (e.g. Figs 2, 13). Posterior margin of elytron with 5–10 clusters of long, dark or light brown setae. Metanotal subalare with sharply rising, internally margined ridge along anteriomedial edge. Metasternal pubescence medially long, well developed, light brown. Metapimeral posterior lobe with long brown setae throughout lobe.

Abdomen. Posterior margin of abdominal ventrite 5 with long setae. Setae cluster on centre of sternite 3 between metacoxae light brown. Abdominal setae dark brown or light brown. Tergite 9 of males (pygidium) with brown setae.

Legs. Lateral margin of anterior of procoxae smooth, without ridge or bump. Meso- and metatibia apical angle

produced into lobe. Inner margin of metatibia of large males with a prebasal bump. Middle of outer margin of metatibia slightly swollen in large males. Middle of inner face of metatibia (large males) not greatly widened (less than $2 \times$ width at base). Metatrochanter spine of males with apex pointing parallel (or almost parallel) to leg, recurved dorsally without acute angle ventrally, with a sharp apex.

Aedeagus. Paramere ventral setal patch not overlapping with apicolateral patch. Parameres evenly curved.

Ovipositor. Spatula on proctiger (T10) apex narrow. Valvifer claw dentate (Fig. 11A).

Distribution

Oriental: northern Sumatra (Fig. 30).

Remarks

The elytral pattern of this species (Fig. 8G) is most similar to that of *N. trumboi* of Nepal and *N. apo* of the Philippines. It can be distinguished from *N. trumboi* by its dentate (Fig. 11A) valvifer claw of the ovipositor whereas *N. trumboi* has the valvifer claw lobed with a round apex (Fig. 11B). It can be distinguished from *N. apo* by having long, semi-erect setae continuous across the third abdominal sternum whereas *N. apo* has these setae interrupted in the middle. No variation is known except for secondary sexual characters, in which small males approach the condition of females.

Etymology

This is a Latinised personal name in the genitive singular, meaning 'of Herschel.' It is given in honour of Johann Dietrich Herschel (1755–1827), Hanoverian musician / entomologist. Herschel revised the European species of *Nicrophorus* (Herschel 1807).

Nicrophorus heurni Portevin

(Figs 10J,Q, 16E, 21)

Nicrophorus Heurni Portevin, 1926: 209

Material examined

See Accessory Publication on *Invertebrate Systematics* website.

Measurements

(65 ♂, 78 ♀), pronotal width: ♂ 4.4–6.74, 5.55 ± 0.54 mm, ♀ 4.24–6.87, 5.61 ± 0.61 mm.

Diagnosis

Nicrophorus nepalensis-group taxon with epipleuron partially or entirely black; metasternal pubescence short and fine medially; males (moderate to large individuals only): metatibiae with inner face widened; pale lunule at base of elytral epipleura large; abdominal spiracle 1 with a small lobe at

anterior end (e.g. Fig. 14B); abdominal sterna 3 to 6 with long setae along posterior margins (these setae are $5\text{--}8 \times$ longer than the distance between adjacent setae); elytral disc with strongly transverse microsculpturing (e.g. Figs 2, 13).

Description

Head. Antennal club basal segment black, apical three orange. Antennomeres of club weakly emarginate. Frons black, without orange spot. Post-ocular bulge of large males larger than females.

Thorax. Microsculpture of pronotum disc composed of many parallel transverse lines. Pronotum of large males orbicular. Setae on posteroventral portion of hypomeron long, erect, sparse; filling region extending a third or less length between trochantin and posterior margin, restricted to upper region of sclerite. Pronotum with brown to light-brown, short (approximately < 0.1 mm), sparse, setae restricted to margins. Humerus immediately dorsal of epipleural ridge orange. Humeral setae short, not forming row. Epipleuron black throughout, medial (dorsal) half orange. Posterior epipleural ridge with isolated single-file row of contiguous preapical setae. Epipleuron and lateral margin of elytron with sparse, short, recumbent, yellow setae throughout. Region adjacent to apex of elytral suture black. Anterior black band (or spot) does not reach 3rd costa. Anterior fascia of elytron with black spot completely surrounded by fascia. Anterior fascia of elytron passing first costa but not reaching suture, between costae, anterior margin u-shaped between costae 1 and 2 (with bottom of u towards posterior), posterior margin u-shaped between costae 1 and 2 (with bottom of u towards posterior). Posterior fascia not touching lateral or posterior margins of elytron. Black spot of elytral posterior fascia near anterior margin of fascia present on callus. Black spot of elytral posterior fascia near anterior margin of fascia incomplete, joining black elytral disc. Black spot of elytral posterior fascia near posterior margin of fascia present between costa 1 and 2 and incompletely surrounded by fascia. Elytral posterior fascia reduced, interrupted before suture. Elytral microsculpture transverse straight, narrow with breaks (e.g. Figs 2, 13). Posterior margin of elytron with 5–10 clusters of long, dark or light brown setae. Metanotal subalare with sharply rising, internally margined ridge along anteriomedial edge. Metasternal pubescence medially short, fine, dark brown. Metapimeral posterior lobe with long brown setae throughout lobe.

Abdomen. Posterior margin of abdominal ventrite 5 with long setae. Setae cluster on centre of sternite 3 between metacoxae absent in centre but with long erect setae lateral of centre under coxae. Abdominal setae dark brown. Tergite 9 of males (pygidium) with brown setae.

Legs. Lateral margin of anterior of procoxae smooth, without ridge or bump. Meso- and metatibia apical angle produced into lobe. Inner margin of metatibia of large males gradually curved outwards. Middle of outer margin of meta-

tibia slightly swollen in large males. Middle of inner face of metatibia (large males) greatly widened (2.5 or greater × width at base). Metatrochanter spine of males with apex pointing parallel (or almost parallel) to leg, straight, not recurved dorsally.

Aedeagus. Paramere ventral setal patch not overlapping with apicolateral patch. Parameres evenly curved.

Ovipositor. Spatula on proctiger (T10) apex narrow. Valvifer claw dentate (Fig. 10J, Q).

Distribution

Australian: Papua New Guinea, Indonesia (Irian Jaya) (Fig. 21).

Remarks

This species, the only *Nicrophorus* species known from the island of New Guinea, shares a pattern of colouration of the epipleura with only one other species in the subfamily,

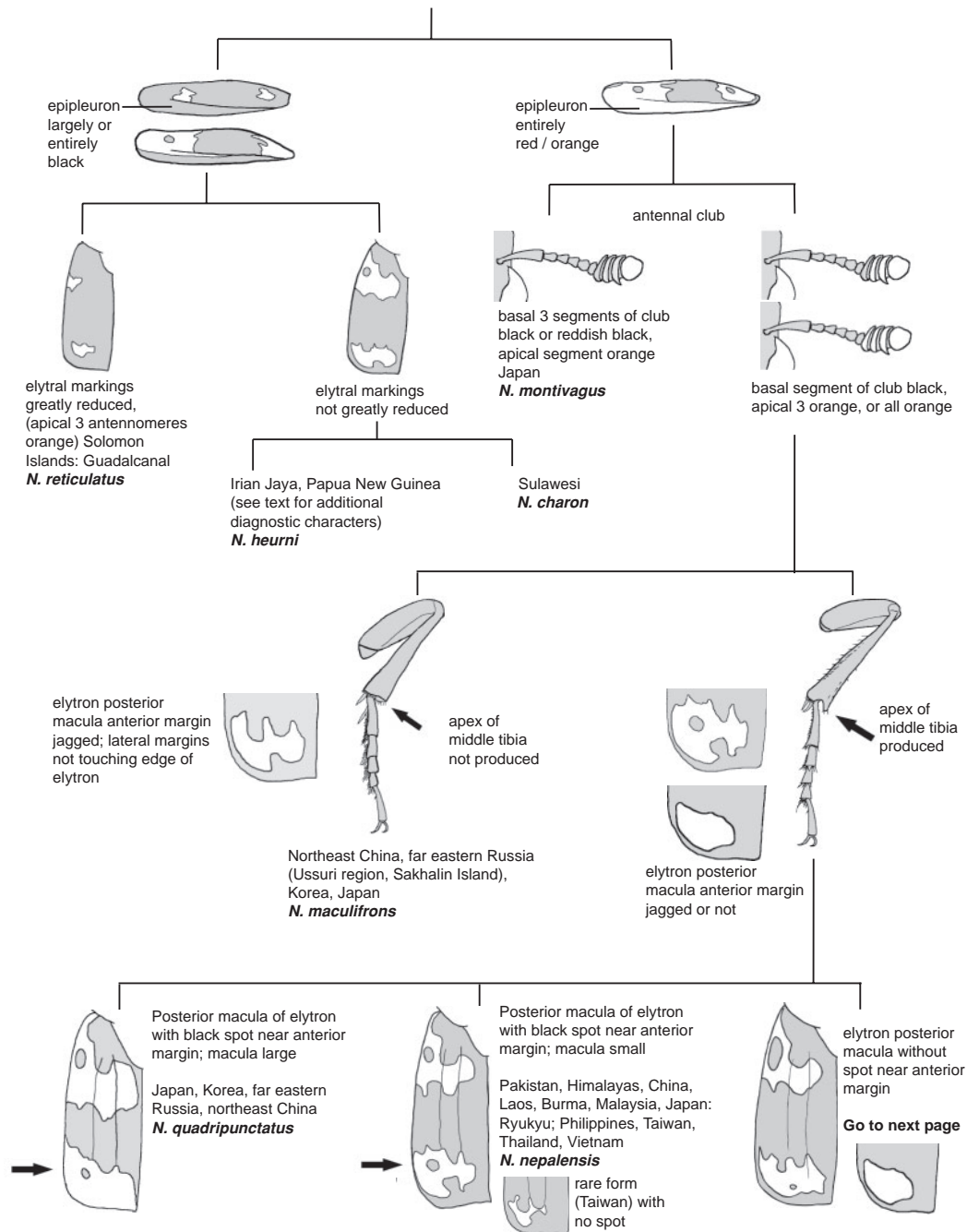


Fig. 18. Visual key to adults of species of *Nicrophorus* in the *nepalensis*-group, part 1. See also the dichotomous key for more detailed descriptions.

N. charon of Sulawesi; the dorsal (medial) half of the epipleura is orange and the ventral (lateral) half is black (Fig. 18, e.g. 22B). This species can be distinguished from *N. charon* by having metasternal pubescence that is short and fine medially whereas *N. charon* has this pubescence long and well developed medially, in addition to other characters listed in the key. No variation is known except for secondary sexual characters, in which small males approach the condition of females.

Etymology

The latinised form of Heurn. Named in honour of Willem Conelis van Heurn (1887–1972), Dutch entomologist; Heurn collected the type series.

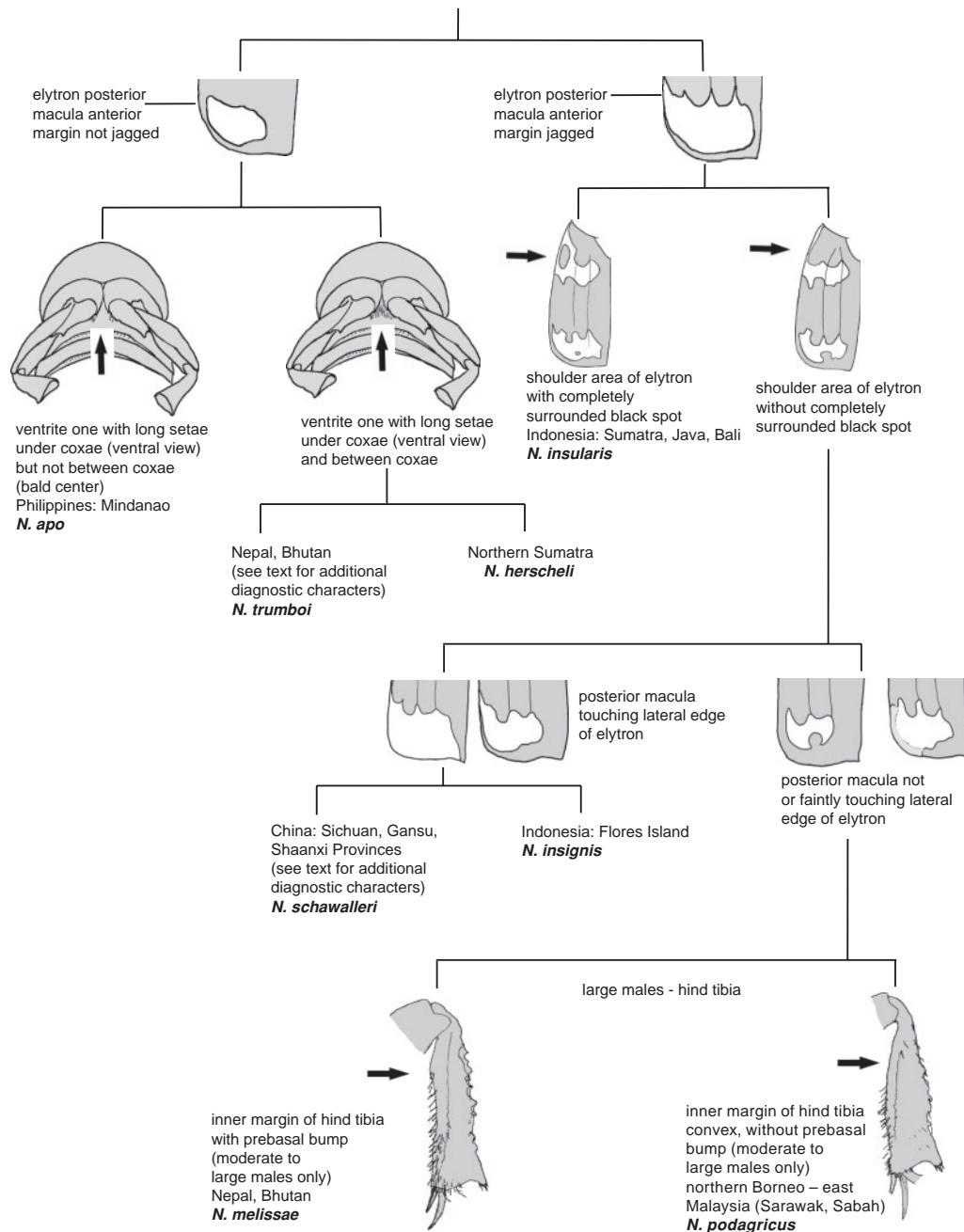


Fig. 19. Visual key to adults of species of *Nicrophorus* in the *nepalensis*-group, part 2. See also the dichotomous key for more detailed descriptions.

***Nicrophorus insignis* Sikes & Madge, sp. nov.**

(Figs 8K, 11E, 17B, 22D, 23)

Nicrophorus nepalensis Hope; Portevin, 1926: 208. [misidentification]*Nicrophorus* undescribed Hanski & Niemelä, 1990: 149.*Nicrophorus* undescribed Hanski & Krikken, 1991: 195.*Nicrophorus* sp. n. Peck, 2001: 94.**Material examined**

Holotype. ♀ labelled 'INDONESIA: Flores Island, Nusa Tenggara, Gunung Ranakah, elev. 1950 m, [8°37'S, 120°32'E] 26.vii.1991 (coll. M. Nishikawa) MCZC002506Nic', (Cambridge (MCZC)).

Paratypes. 8 ♂, 10 ♀: **INDONESIA: Flores Island:** same data as holotype. 1 ♀: NSMT002507Nic; same locality, elev. 1400 m, [8°37'S, 120°32'E] 1 ♀: MCZC70013Nic, 1 ♂: MCZC70012Nic; 2 ♂: BMNH002503Nic, BMNH002504Nic, 1 ♀: NSMT002505Nic, 1 ♂: NSMT002502Nic; same data as holotype, 1 ♂: MCZC70009Nic, 1 ♀: BMNH70010Nic; Island Nusa Tenggara, near Ruteng, elev. 1200 m, [8°35'S, 120°28'E] 23.vii.1991 (coll. C. U. Paukstadt), 1 ♀: MNC70011Nic, (Ebina (MNC) Nishikawa private coll); S. Flores, Dry S., 1.x–30.xi.1896 (coll. Everett.), 1 ♀: MNHN001082Nic; Golo; Lusang Mtns, S. of Ruteng; E of road, 5900' / 1829 m, 8°40'11"S, 120°28'2"E, ridge top forest, carrion trap, 23.v.2005 (coll. D. S. Sikes) – 3 ♂: DSSC123523Nic, DSSC123524Nic, DSSC123525Nic, 4 ♀: DSSC123521Nic, DSSC123522Nic, DSSC123526Nic, DSSC123526Nic.

Measurements

(8 ♂, 10 ♀), pronotal width: ♂ 4.74–6.42, 5.49 ± 0.56 mm, ♀ 4.31–5.42, 5.06 ± 0.36 mm.

Diagnosis

Nicrophorus nepalensis-group taxon with epipleuron entirely red-orange, elytra with posterior fascia typically not interrupted at suture, or if interrupted, then fascia narrowly separated, posterior fascia touching lateral and posterior margins of elytron (Fig. 22D), posterior margin of middle black band without a dark finger projecting over the callus (bump near posterior of elytron), never with a completely surrounded black spot near humerus (Figs 8K; 22D); pronotum of large males orbicular; metasternum with light brown to golden pubescence; apical procoxal hairs long, curved; third abdominal sternum on basal half with band of long, semi-erect setae across middle, not interrupted at midline; moderate to large males: metatibiae with dorsal margin swollen near middle (e.g. Fig. 15A, C, D); females: valvifer claw with outer margin obviously toothed (Fig. 11E).

Description

Head. Antennal club basal segment black, apical three orange. Antennomeres of club weakly or deeply emarginate. Frons black, with orange spot. Post-ocular bulge of large males larger than females.

Thorax. Microsculpture of pronotum disc isodiametric. Pronotum of large males orbicular. Setae on posteroventral portion of hypomeron long, erect, sparse; filling region extending a third or less length between trochantin and

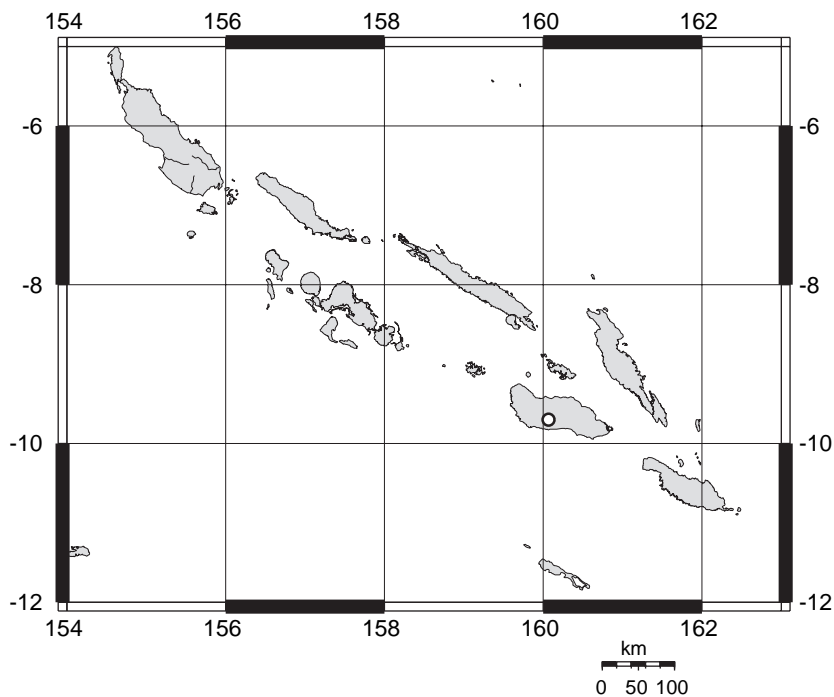


Fig. 20. Distribution of all geo-referenced specimens of *Nicrophorus reticulatus* Sikes and Madge, type locality: Solomon Islands: Guadalcanal: 'Popamasin' (= Mt Popomanaseu), 1524 m (9°42'S, 160°4'E).

posterior margin, restricted to upper region of sclerite. Pronotum with brown to light-brown, short (approximately < 0.1 mm), sparse, setae restricted to margins. Humerus immediately dorsal of epipleural ridge orange. Humeral setae short, not forming row. Epipleuron entirely orange. Posterior epipleural ridge with isolated single-file row of contiguous preapical setae. Epipleuron and lateral margin of elytron with sparse, short, recumbent, yellow setae throughout. Region adjacent to apex of elytral suture black. Anterior black band not reaching 3rd costa. Anterior fascia of elytron without black spot, passing first costa but not reaching suture, anterior margin u-shaped between costae 1 and 2 (with bottom of u towards posterior), posterior margin u-shaped between costae 1 and 2 (with bottom of u towards posterior). Posterior fascia touching lateral and posterior margins of elytron. Black spot of elytral posterior fascia near anterior margin of fascia absent. Black spot of elytral posterior fascia near posterior margin of fascia absent, region within fascia. Elytral posterior fascia enlarged, not interrupted. Elytral microsculpture transverse straight, narrow with breaks (Fig. 13A, B). Posterior margin of elytron with 5–10 clusters of long, dark or light brown setae. Metanotal subalare with sharply rising, internally margined ridge along anteriomedial edge. Metasternal pubescence medially long, well developed, light brown. Metapimeral posterior lobe with long brown setae throughout lobe.

Abdomen. Posterior margin of abdominal ventrite 5 with long setae. Setae cluster on centre of sternite 3 between metacoxae light brown. Abdominal setae dark brown. Tergite 9 of males (pygidium) with brown setae.

Legs. Lateral margin of anterior of procoxae smooth, without ridge or bump. Meso- and metatibia apical angle produced into lobe. Inner margin of metatibia of large males

with a prebasal bump. Middle of outer margin of metatibia slightly swollen in large males. Middle of inner face of metatibia (large males) not greatly widened (less than 2 × width at base). Metatrochanter spine of males with apex pointing parallel (or almost parallel) to leg, recurved dorsally without acute angle ventrally, with a sharp apex.

Aedeagus. Paramere ventral setal patch overlaps at edge with apicolateral patch. Parameres evenly curved.

Ovipositor. Spatula on proctiger (T10) apex narrow. Valvifer claw dentate (Fig. 11E).

Distribution

Oriental: Flores, Indonesia (Fig. 23).

Remarks

This species is one of 11 in the genus that has a small orange spot in the centre of the frons. It can be distinguished from these species by the following combination of states: humeral setae present, short, not forming row; anterior fascia of elytron without black spot; black spot of elytral posterior fascia near posterior margin of fascia absent, region within fascia (Fig. 8K). Additionally, this species is endemic to and the only known *Nicrophorus* on the island of Flores in the Lesser Sundas, Indonesia. No variation is known except for secondary sexual characters, in which small males approach the condition of females.

Etymology

Latin, *insignis*; referring to the well marked and distinctive elytral pattern. Based on first observation of this population from Flores island as having ‘coloration remarquable’ by Portevin (1926) in a footnote (p.208). The name is a Latin adjective, meaning ‘remarkable, distinguished by a mark’.

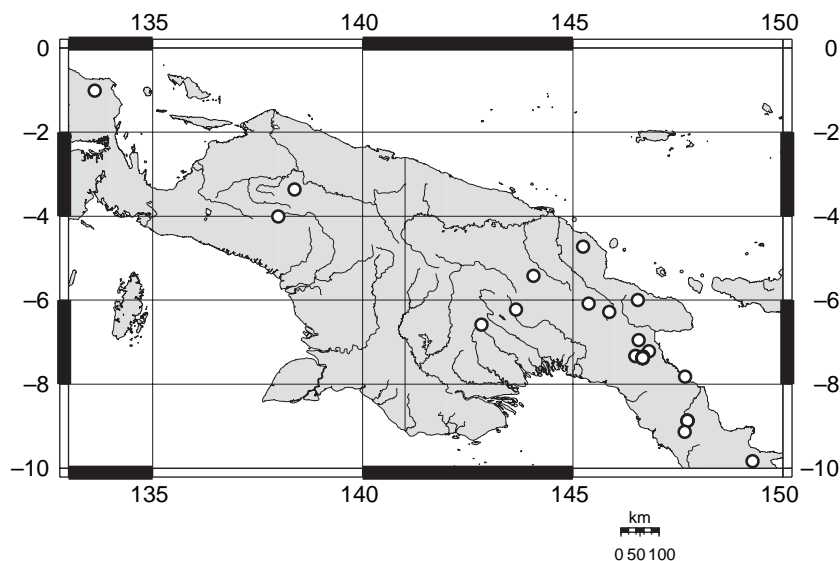


Fig. 21. Distribution of all geo-referenced specimens of *Nicrophorus heurni* Portevin.

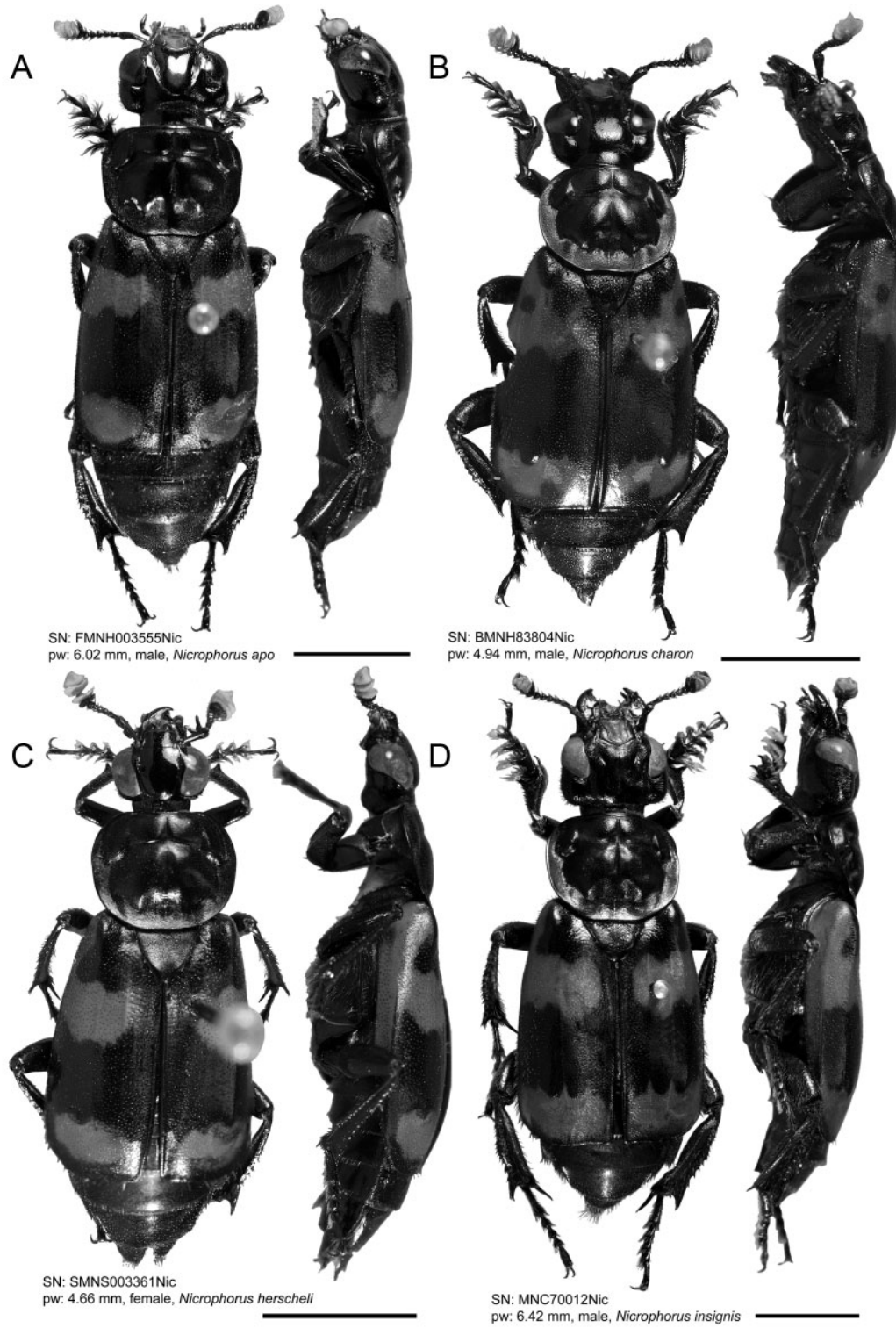


Fig. 22. Dorsal and lateral habitus. *A*, Male *Nicrophorus apo* Arnett. *B*, Male *Nicrophorus charon* Sikes and Madge (paratype, left elytron damaged). *C*, Female *Nicrophorus herscheli* Sikes and Madge (paratype). *D*, Male *Nicrophorus insignis* Sikes and Madge (paratype). Scale bar = 5 mm.

***Nicrophorus insularis* Grouvelle**
(Figs 8J, 9A, 10H, I, K, 15D, 17H, 32)

Nicrophorus insularis Grouvelle, 1893: 161

Material examined

See Accessory Publication on *Invertebrate Systematics* website.

Measurements

(45 ♂, 44 ♀), pronotal width: ♂ 4.44–6.36, 5.41 ± 0.53 mm, ♀ 4.23–6.45, 5.34 ± 0.59 mm.

Diagnosis

Nicrophorus nepalensis-group taxon with frons without an orange spot; elytra with epipleuron entirely red-orange, shoulder area of elytra with a completely surrounded black spot, separated from end of basal black band (Fig. 8J); posterior fascia interrupted at suture (Fig. 8J); not reaching dorsal ridge of epipleura (Fig. 22D), posterior margin of middle black band with a dark finger (rarely an isolated dark spot) projecting over the callus; moderate to large males with metatibiae expanded laterally, inner face convex, without a pre-basal bump (Fig. 15D), with dorsal margin swollen near middle (Fig. 15D); metasternum with dark brown pubescence; shoulder area of elytra with a row of short setae;

females: valvifer claw with outer margin obviously toothed (Fig. 10H, I, K).

Description

Head. Antennal club basal segment black, apical three orange. Antennomeres of club weakly emarginate. Frons black, without orange spot. Post-ocular bulge of large males larger than females.

Thorax. Microsculpture of pronotum disc composed of many parallel transverse lines. Pronotum of large males orbicular. Setae on posteroventral portion of hypomeron long, erect, sparse; filling region extending a third or less length between trochantin and posterior margin, restricted to upper region of sclerite. Pronotum with brown to light-brown, short (approximately < 0.1 mm), sparse, setae restricted to margins. Humerus immediately dorsal of epipleural ridge orange. Humeral setae long, not forming row. Epipleuron entirely orange. Posterior epipleural ridge with isolated single-file row of contiguous preapical setae. Epipleuron and lateral margin of elytron with sparse, short, recumbent, yellow setae throughout. Region adjacent to apex of elytral suture black. Anterior black band (or spot) does or does not reach 3rd costa. Anterior fascia of elytron with black spot completely surrounded by fascia. Anterior fascia of elytron passing first costa but not reaching suture, anterior margin u-shaped between costae 1 and 2 (with bottom of u towards

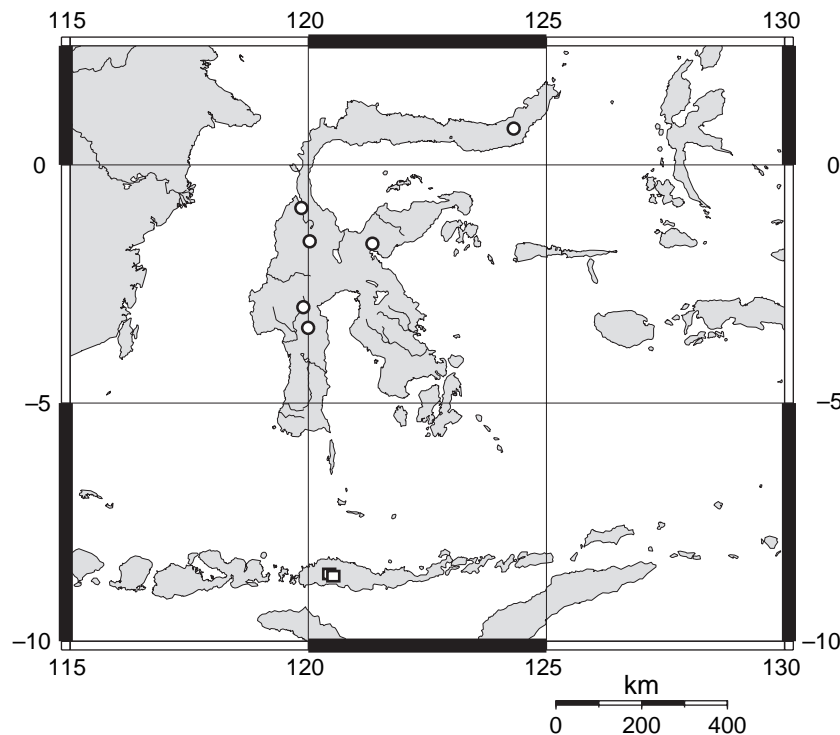


Fig. 23. Distribution of all geo-referenced specimens of *Nicrophorus charon* Sikes and Madge (circles), type locality: Indonesia: Sulawesi, Tengah: Mt. Tambusisi, 1219 m, 1°39'N, 121°21'E, and *Nicrophorus insignis* Sikes and Madge (squares). Type locality: Indonesia: Flores Island, Nusa, Tenggara, Gunung Ranakah' (8°37' 120°31'E).

posterior), posterior margin u-shaped between costae 1 and 2 (with bottom of u towards posterior). Posterior fascia not touching lateral or posterior margins of elytron. Black spot of elytral posterior fascia near anterior margin of fascia present on callus. Black spot of elytral posterior fascia near anterior margin of fascia incomplete, joining black elytral disc. Black spot of elytral posterior fascia near posterior margin of fascia present between costa 1 and 2 and incompletely surrounded by fascia. Elytral posterior fascia reduced, interrupted before suture. Elytral microsculpture transverse straight, narrow with breaks (e.g. Figs 2, 13). Posterior margin of elytron with 5–10 clusters of long, dark or light brown setae. Metanotal subalare with sharply rising, internally margined ridge along anteriomedial edge. Metasternal pubescence medially long, well developed, light brown. Metapimeral posterior lobe with long brown setae throughout lobe.

Abdomen. Posterior margin of abdominal ventrite 5 with long setae. Setae cluster on centre of sternite 3 between metacoxae light brown. Abdominal setae dark brown. Tergite 9 of males (pygidium) with brown setae.

Legs. Lateral margin of anterior of procoxae smooth, without ridge or bump. Meso- and metatibia apical angle produced into lobe. Inner margin of metatibia of large males gradually curved outwards or with a prebasal bump. Middle of outer margin of metatibia slightly swollen in large males. Middle of inner face of metatibia (large males) greatly widened (2.5 or greater \times width at base). Metatrochanter spine of males with apex pointing parallel (or almost paral-

lel) to leg, recurved dorsally without acute angle ventrally, with a sharp apex.

Aedeagus. Paramere ventral setal patch not overlapping with apicolateral patch. Parameres evenly curved.

Ovipositor. Spatula on proctiger (T10) apex narrow. Valvifer claw dentate (Fig. 10H, I, K).

Distribution

Oriental: Indonesia: Java, Sumatra, Bali. One questionable record from Borneo (Fig. 32).

Remarks

This species, the only *Nicrophorus* on the islands of Java, Bali, and most of Sumatra (*N. herscheli* is in the extreme north), is most similar to *N. podagricus*. Both have swollen metatibiae in moderate to large males, all red-orange elytral epipleura, and no row of long setae on the elytral shoulders. These characters distinguish both from all remaining species of the *nepalensis*-group. This species differs from *N. podagricus* by having an all black frons and a small black shoulder spot in the anterior fascia that is separate from the basal black band of the elytra. There is slight variation in the shape of the end of the basal black band. Sometimes it is simply oblique and sometimes it shows some concavity. Minor variation exists in the shape of the tooth on the valvifer claw of the ovipositor (Figs 10H, I, K).

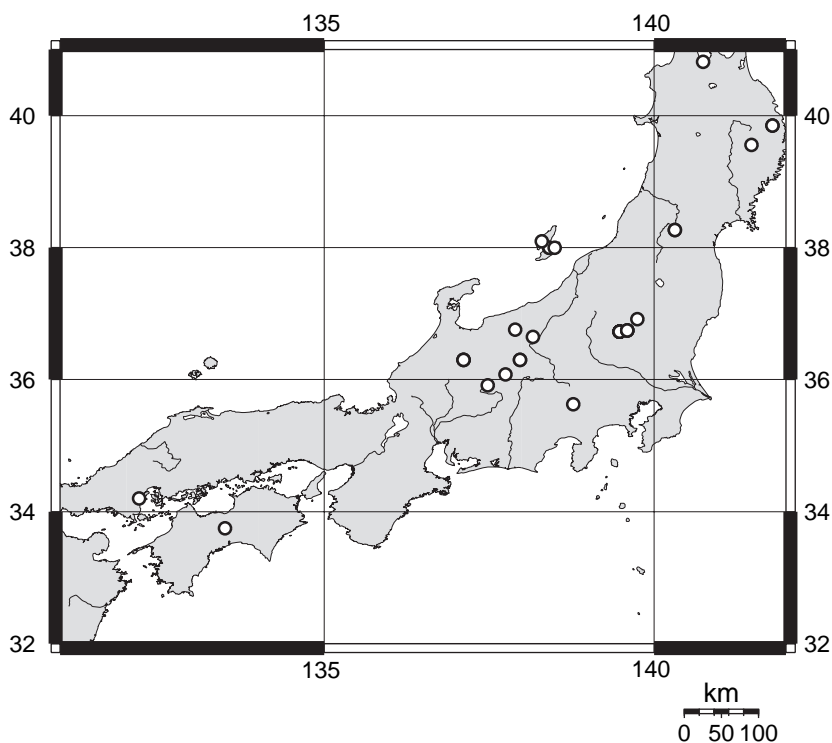


Fig. 24. Distribution of all geo-referenced specimens of *Nicrophorus montivagus* Lewis.

Etymology

The name is a Latin adjective, meaning 'insular, pertaining to islands.' It refers to the source of the type specimens, on the island of Sumatra, Indonesia.

Nicrophorus maculifrons Kraatz

(Figs 9B, 10O, 14B, 15B, 17J, 28)

Nicrophorus maculifrons Kraatz, 1877: 101.

Material examined

See Accessory Publication on *Invertebrate Systematics* website.

Measurements

(76 ♂, 138 ♀), pronotal width: ♂ 4.45–7.34, 5.71 ± 0.61 mm, ♀ 4.0–7.39, 5.60 ± 0.70 mm.

Diagnosis

Nicrophorus nepalensis-group taxon with antennal club with basal segment black, apical three orange; elytra with epipleuron entirely red-orange, with middle black band always reaching dorsal ridge of epipleuron (Fig. 9B), posterior fascia with anterior margin irregular; metasternum with golden pubescence; dorsal ridge of epipleuron with posterior setae dark brown; metafemora with apical setae dark brown; meso- and metatibiae with apical emargination small, not semicircular; the apical process thus broad; lower part of emargination with a row of setae (e.g. Fig. 15B); moderate to large males: metatibiae with inner face bearing a prebasal bump and then concave (Fig. 15B), with dorsal margin not swollen, simple as in female (Fig. 15B); females: valvifer claw with outer margin lobed but not toothed (Fig 10O).

Description

Head. Antennal club basal segment black, apical three orange. Antennomeres of club weakly emarginate. Frons black, with orange spot. Post-ocular bulge of large males larger than females.

Thorax. Microsculpture of pronotum disc absent (smooth, polished) or composed of many parallel transverse lines. Pronotum of large males subquadrate. Setae on posteroventral portion of hypomerion long, erect, sparse; filling region extending a third or less length between trochantin and posterior margin, restricted to upper region of sclerite. Pronotum with brown to light-brown, short (approximately < 0.1 mm), sparse, setae restricted to margins. Humerus immediately dorsal of epipleural ridge orange. Humeral setae long, forming row. Epipleuron entirely orange. Posterior epipleural ridge with isolated single-file row of contiguous preapical setae. Epipleuron and lateral margin of elytron with sparse, short, recumbent, yellow setae throughout. Region adjacent to apex of elytral suture black. Anterior black band (or spot) not reaching 3rd costa. Anterior fascia

of elytron with black spot completely or incompletely surrounded by fascia, joined to basal band, passing first costa and reaching suture or not, anterior margin u-shaped between costae 1 and 2 (with bottom of u towards posterior), posterior margin u-shaped between costae 1 and 2 (with bottom of u towards posterior). Posterior fascia not touching lateral or posterior margins of elytron. Black spot of elytral posterior fascia near anterior margin of fascia present on callus and incomplete, joining black elytral disc. Black spot of elytral posterior fascia near posterior margin of fascia present between costa 1 and 2 and incompletely surrounded by fascia. Elytral posterior fascia reduced, interrupted before suture. Elytral microsculpture transverse straight, narrow with breaks (e.g. Figs 2, 13). Posterior margin of elytron with 5–10 clusters of long, dark or light brown setae. Metanotal subalare with sharply rising, internally margined ridge along anteriomedial edge. Metasternal pubescence medially long, well developed, golden. Metapimeral posterior lobe with long brown setae throughout lobe.

Abdomen. Posterior margin of abdominal ventrite 5 with long setae. Setae cluster on centre of sternite 3 between metacoxae light brown. Abdominal setae dark brown. Tergite 9 of males (pygidium) with brown setae.

Legs. Lateral margin of anterior of procoxae smooth, without ridge or bump. Meso- and metatibia apical angle not produced into spine or lobe. Inner margin of metatibia of large males with a prebasal bump. Middle of outer margin of metatibia not swollen. Middle of inner face of metatibia (large males) not greatly widened (less than $2 \times$ width at base). Metatrochanter spine of males apex pointing perpendicular to leg. Metatrochanter spine of males recurved dorsally without acute angle ventrally, with a sharp apex.

Aedeagus. Paramere ventral setal patch not overlapping with apicolateral patch. Parameres sinuate.

Ovipositor. Spatula on proctiger (T10) apex narrow. Valvifer claw lobed with round apex.

Distribution

Palearctic: Russia: eastern Siberia, Amur, Ussuri reg., Kuriles, Sakhalin; north-eastern China, Japan, Korea (Fig. 28).

Remarks

This species is one of only four in the genus *Nicrophorus* with a small orange spot on the frons, and with the meso- and metatibial apical angles not produced into a spine or a lobe. It can be distinguished from these species by the following combination of character states: antennal club basal segment black, apical three orange; humeral setae forming a long row; elytra with middle black band always reaching dorsal ridge of epipleuron; epipleural ridge short, reaching to tip of scutellum but not beyond; region immediately adjacent to apex of elytral suture black; metasternal pubescence golden. The black spot on the shoulders varies in size from small and isolated to large and broadly joined to the basal black band.

Etymology

The name is a Modern Latin compound noun (from *macula* (spot) and *frons* (front)) in the nominative, meaning 'a spotted front'. It refers to the red spot on the frons of this species.

Nicrophorus melissae Sikes & Madge, sp. nov.

(Figs 8C, D, 9C, 11C, D, 13C, D, 36)

Nicrophorus nepalensis ab. *immaculatus* Emetz & Schawaller, 1975: 230; Schawaller, 1977: 260 [infrasubspecific, unavailable, name].

Material examined

Holotype. ♀, labelled 'NEPAL: Ganesh Himal, 7 km W Godlang, elev. 2950 m, 28°10'N, 85°14'E, 20.ix.1995 (coll. B. Herczig Gy. M. Laszló) HNHM003464Nic'. (Budapest (HNHM)).

Paratypes. 20 ♂, 32 ♀. **BHUTAN**: Chelaila, elev. 3200 m, [27°24'N, 89°30'E] 22.v.1986 (coll. Schmutzenhofer), 1 ♀: SBPC004510Nic; same locality, 9.vi.1986, 4 ♂: SBPC004509Nic, WBC080870Nic, DSSC080873Nic, DSSC080877Nic, 9 ♀: JRC003454Nic, JRC003455Nic, JSC003440Nic, DSSC080869Nic, DSSC080871Nic, WBC080872Nic, WBC080874Nic, WBC080875Nic, WBC080876Nic; China, Bhutan, Chelaila, [27°24' N, 89°30'E] 9.vi.1986, 1 ♀: JHC001846Nic; West Bhutan, Paro Distr., Chiley. La, elev. 3000 m, [27°24'N, 89°24'E] 21.vi.1988 (coll. C. Holzschuh), 3 ♂

JSC003441Nic, JSC003442Nic, JSC003443Nic; [**NEPAL**]: 172 Parbat Dist., zwischen Chitre und Ghandrung, Chitre-Seite des Passes, Tsuga Rhodod., elev. 2800–2900 m, 4–7.v.1980 (coll. Martens & Ausobsky), 1 ♂: SMFC16405; 233 Gorkha Distr. Chuling Khola, Meme Kharka, Wald/ Moräne, 5–6.viii.1983 (coll. Martens & Schawaller), 1 ♀: SMNS003338Nic; Annapurna Himal, between Ghorepani and Geirigan, elev. 1300–2600 m, 25–27.vii.1995 (coll. Gy. M. László, G. Ronkay & G. Csorba), 1 ♀: HNHM000628Nic; centr. Nepal: Birethanti Goropani, 4–9.vi.1992 (coll. Ivo Jenis), 1 ♂: NHMW002021Nic; Ganesh Himal, 7 km W Godlang, elev. 2950 m, 28°10'N, 85°14'E, 20.ix.1995 (coll. B. Herczig Gy. M. Laszló), 2 ♀: HNHM003463Nic, HNHM003465Nic; Ganesh Himal, 8 km W Godlang, elev. 3050 m, 28°10' N, 85°17'E, 14 × 1995 (coll. L. Peregovits & L. Ronkay), 1 ♀: HNHM000691Nic; Ganesh Himal, Nesukharka, 12km S Somdang, elev. 2700 m, 28°9'N, 85°11'E, 21.v.1995 (coll. Gy. Fábrián & L. Ronkay), 2 ♂: HNHM003469Nic, SMNS003335Nic; Kalobeni Kali Gandaki Valley, elev. 2400 m, [28°N, 83°E,] 1–31.v.1984 (coll. Holzechuh), 1 ♂: WBC080881Nic; Kangchenjunga Himal Mts. Ghunsa vill., elev. 3375 m, 27°24'N, 87°34'E, 6–10.vii.2000 (coll. Jan Schneider), 1 ♀: JSC080898Nic, 1 ♂: JSC080899Nic; Karnali, Bachtal bel Pahada, elev. 3100–3400 m, 29°4'N, 82°42'E, 2.vi.1997 (coll. J. Weipert), 1 ♀: SMNS080941Nic; Karnali, Hochtal Gothichaur, elev. 2900 m, 29°12'N, 82°18'E, 3.vi.1997 (coll. J. Weipert), 1 ♀: SMNS080940Nic, 1 ♂: SMNS080942Nic; Karnali Prov., Distr. Jumla, 2 km W Gothichaur, elev. 2700 m, 20–21.v.1995 (coll. M. Hartmann), 1 ♂: SMNS003337Nic; Kaski Dist., Birethanti, Gandaki Zone, elev. 2620 m, [28°10'N, 84°30'E] 16 × 1981 (coll. S. Uéno), 1 ♀: NSMT003075Nic;

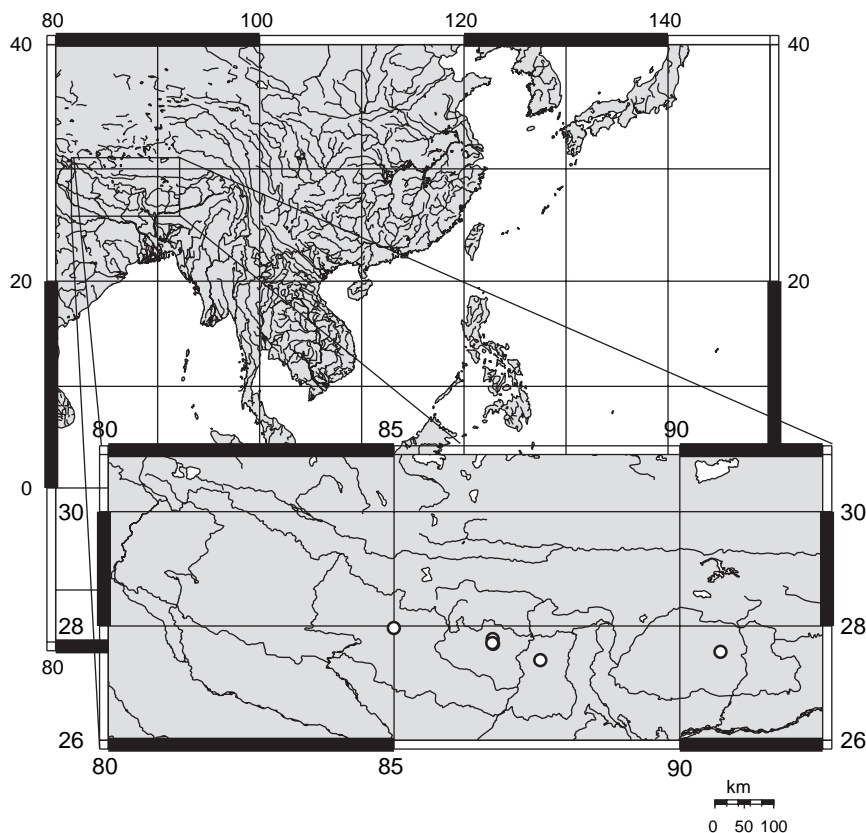


Fig. 25. Distribution of all geo-referenced specimens of *Nicrophorus trumboi* Sikes & Madge. Type locality: Nepal: Solu Khumbu Dist., Mtns east of Lukla, moist cloud forest, 2840–2900m, 27°41'15"N, 86°44'9"E.

Mustang Dist., Mtns. west of Marpha, 10,850', elev. 3307m, 28°44'38"N, 83°39'54"E, 9.viii.1999 (coll. D. S. Sikes), DNA-voucher 03, ♀: DSSC006475Nic; same locality, 11.viii.1999 (coll. D. S. Sikes), DNA-voucher 02, ♀: DSSC006377Nic, DNA-voucher 04, ♀: DSSC006476Nic; nördl. Dhaulagiri Gompa / Tarakot, elev. 3300–3400 m, [28°50'N, 83°30'E] 2–6.vi.1973 (coll. Jochen Martens), 3 ♀ SMFC16407, DSSC006684Nic, SMFC16408, 3 ♂: DSSC006685Nic, DSSC006686Nic, SMNS003340Nic; Solu Khumbu Dist., Mtns east of Lukla, moist cloud forest, elev. 2840–2900 m, 27°41'15"N, 86°44'9"E, 20.viii.1999 (coll. D. S. Sikes), DNA-voucher 01, ♂: DSSC006376Nic; südl. Dhaulagiri, Dhorpatan, elev. 3000 m, [28°29'N, 83°4'E] 5–13.v.1973 (coll. Jochen Martens), 1 ♀: HNHM002402Nic; same locality, elev. 3000–3200 m, (coll. Jochen Martens), 2 ♀: SMFC16406, DSSC006682Nic; same locality, 7–25.v.1973 (coll. Jochen Martens), 1 ♀: SMNS003339Nic; Thakkhola, Chadziuo-Khola bei Ghassa, elev. 2600 m, 1 vi–30.vii.1970 (coll. Jochen Martens), 1 ♀: SMFC16403, 1 ♂: SMFC16404; Thakkhola, Tukche Thaksang, elev. 3100–3300 m, 1–5.vii.1973 (coll. Jochen Martens), 1 ♀: HNHM002401Nic.

Literature record. **BHUTAN:** Gogono, elev. 3100 m, 10–12.vi.1972, (Schawaller 1977: 260).

Measurements

(19 ♂, 28 ♀), pronotal width: ♂ 3.66–6.26, 5.03 ± 0.77, ♀ 4.52–6.25, 5.27 ± 0.46 mm.

Diagnosis

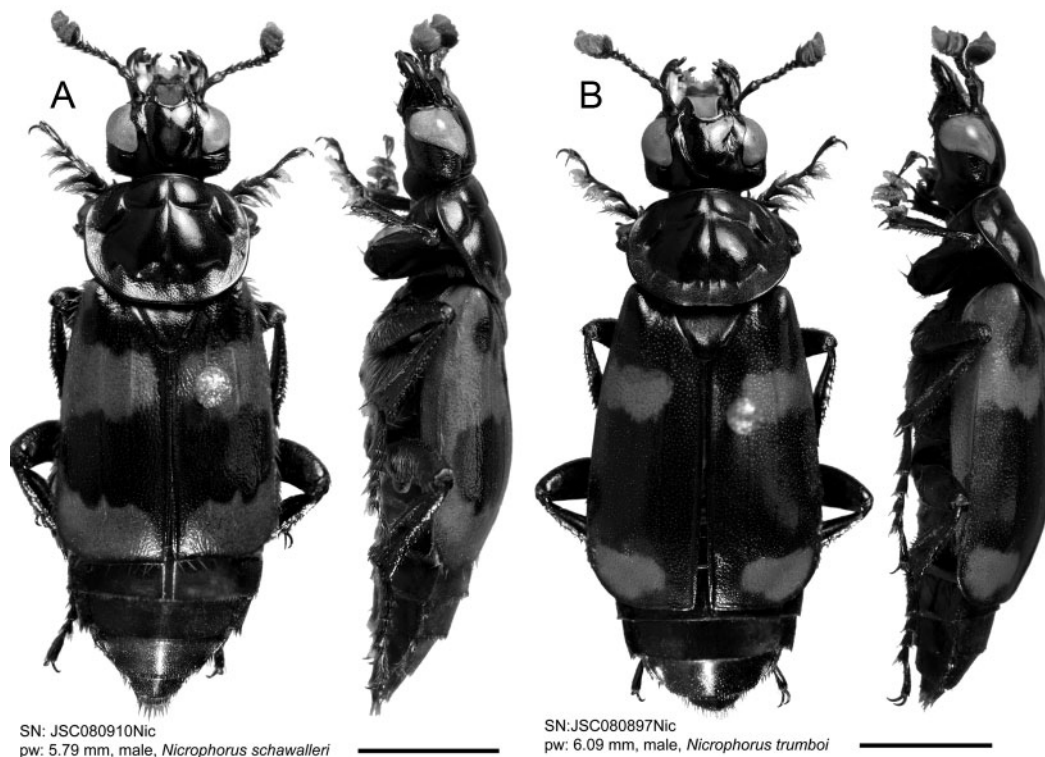
Nicrophorus nepalensis-group taxon with epipleuron entirely red-orange; moderate to large males with metatibiae not expanded laterally, with inner face not convex but with a prebasal bump (e.g. Fig. 15A, B), with dorsal margin swollen

near middle (e.g. Fig. 15A, C, D); shoulder area of elytra with black spot connected to basal black band, not separated (e.g. Fig. 8C, D), posterior margin of middle black band with a dark finger (rarely an isolated dark spot) projecting over the callus; females: valvifer claw with outer margin obviously toothed (Fig. 11C, D).

Description

Head. Antennal club basal segment black, apical three orange. Antennomeres of club weakly emarginate. Frons black, with orange spot. Post-ocular bulge of large males larger than that of females.

Thorax. Microsculpture of pronotum disc composed of many parallel transverse lines. Pronotum of large males orbicular. Setae on posteroventral portion of hypomeron long, erect, sparse; filling region extending a third or less length between trochantin and posterior margin, restricted to upper region of sclerite. Pronotum with brown to light-brown, short (approximately < 0.1 mm), sparse, setae restricted to margins. Humerus immediately dorsal of epipleural ridge orange. Humeral setae long or short, not forming row. Epipleuron entirely orange. Posterior epipleural ridge with isolated single-file row of contiguous preapical setae. Epipleuron and lateral margin of elytron with sparse, short, recumbent, yellow setae throughout. Region adjacent to apex of elytral suture black. Anterior black band (or spot) not reaching 3rd costa. Anterior fascia of elytron without black



SN: JSC080910Nic
pw: 5.79 mm, male, *Nicrophorus schawalleri*

SN: JSC080897Nic
pw: 6.09 mm, male, *Nicrophorus trumboi*

Fig. 26. Dorsal and lateral habitus. A, Male *Nicrophorus schawalleri* Sikes & Madge (paratype). B, Male *Nicrophorus trumboi* Sikes & Madge (paratype). Scale bar = 5 mm.

spot or with black spot incompletely surrounded by fascia, joined to basal band. Anterior fascia of elytron passing first costa but not reaching suture and stopping at or just before first costa as a wide band, anterior margin u-shaped between costae 1 and 2 (with bottom of u towards posterior), posterior margin u-shaped between costae 1 and 2 (with bottom of u towards posterior). Posterior fascia not touching lateral or posterior margins of elytron. Black spot of elytral posterior fascia near anterior margin of fascia present on callus, incomplete, joining black elytral disc. Black spot of elytral posterior fascia near posterior margin of fascia present between costa 1 and 2 and incompletely surrounded by fascia. Elytral posterior fascia reduced, interrupted before suture. Elytral microsculpture transverse straight, narrow with breaks (Fig. 13C, D). Posterior margin of elytron with 5–10 clusters of long, dark or light brown setae. Metanotal subalare with sharply rising, internally margined ridge along anteriomedial edge. Metasternal pubescence medially long, well developed, light brown. Metapimeral posterior lobe with long brown setae throughout lobe.

Abdomen. Posterior margin of abdominal ventrite 5 with long setae. Setae cluster on centre of sternite 3 between metacoxae light brown. Abdominal setae dark brown. Tergite 9 of males (pygidium) with brown setae.

Legs. Lateral margin of anterior of procoxae smooth, without ridge or bump. Meso- and metatibia apical angle produced into lobe. Inner margin of metatibia of large males with a prebasal bump. Middle of outer margin of metatibia slightly swollen in large males. Middle of inner face of metatibia (large males) not greatly widened (less than $2 \times$ width at base). Metatrochanter spine of males apex pointing parallel (or almost parallel) to leg, straight, not recurved dorsally or recurved dorsally without acute angle ventrally, with a sharp apex.

Aedeagus. Paramere ventral setal patch overlaps at edge with apicolateral patch. Parameres evenly curved.

Ovipositor. Spatula on proctiger (T10) apex narrow. Valvifer claw dentate (Fig. 11C, D).

Distribution

Oriental: Bhutan, Nepal (Fig. 36).

Remarks

This species, from Nepal and Bhutan, is similar to *N. nepalensis* in structure and elytral pattern. In both species the metatibiae in moderate to large males are not swollen except for a medial enlargement on the dorsal face. The middle black band of the elytra extends over the posterior

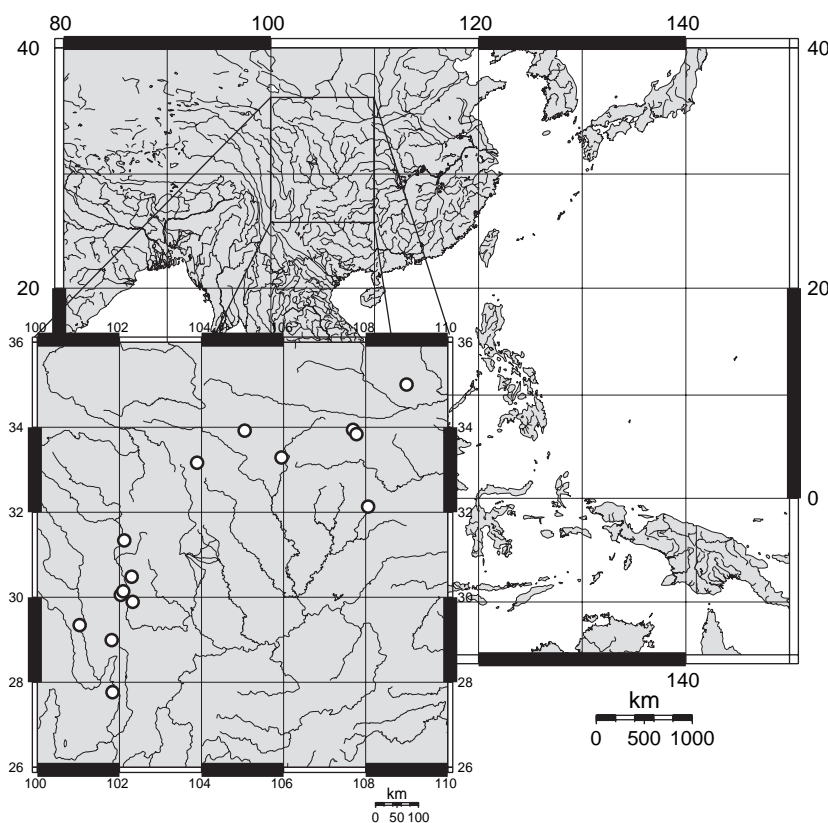


Fig. 27. Distribution of all geo-referenced specimens of *Nicrophorus schawalleri* Sikes & Madge. Type locality: CHINA, Taibai Shan above Houshenzi, elev. 2500–2600 m, ($33^{\circ}58'N$, $107^{\circ}42'E$).

callus. They differ in that the elytral shoulder spot in the anterior fascia of *N. melissae* is connected to the basal black band (Figs 8C, D) while *N. nepalensis* has a separate shoulder spot isolated from the black band (Figs 8H, I).

See the section above, 'New species', for discussion of phylogenetic results supporting this species' status as new. Specimens from further east in the distribution, from Bhutan, have somewhat reduced elytral maculations (e.g. Fig. 8C). However, the two forms intergrade. We hope to study this species' molecular variation if we can obtain DNA data from the Bhutan population.

Etymology

This is a personal name, treated as Latin, in the genitive singular and meaning 'of Melissa'. It is given in honour of the first author's wife, Melissa Sikes (with her permission) who endured a month without her husband while he was in Nepal and who has never complained about being married to a carrion beetle taxonomist.

Nicrophorus montivagus Lewis

(Figs 9D, 11F, 16C, 24)

Nicrophorus montivagus Lewis, 1887: 340

Material examined

See Accessory Publication on *Invertebrate Systematics* website.

Measurements

(63 ♂, 60 ♀), pronotal width: ♂ 2.96–5.21, 4.18 ± 0.49 mm, ♀ 3.24–4.96, 4.12 ± 0.39 mm.

Diagnosis

Antennal club with basal three segments black or reddish black, apical segment orange.

Description

Head. Antennal club basal three segments black, apical orange. Antennomeres of club weakly emarginate. Frons black, with or without orange spot. Post-ocular bulge of large males larger than or equal to size of females.

Thorax. Microsculpture of pronotum disc composed of many parallel transverse lines. Pronotum of large males subquadrate. Setae on posteroventral portion of hypomeron long, erect, sparse; filling region extending a third or less length between trochantin and posterior margin, restricted to upper region of sclerite. Pronotum with brown to light-brown, short (approximately < 0.1 mm), sparse, setae restricted to margins. Humerus immediately dorsal of epipleural ridge orange. Humeral setae long, not forming row. Epipleuron entirely orange. Posterior epipleural ridge with isolated single-file row of contiguous preapical setae.

Epipleuron and lateral margin of elytron with sparse, short, recumbent, yellow setae throughout. Region adjacent to apex of elytral suture black. Anterior black band (or spot) reaches 3rd costa. Anterior fascia of elytron with or without black spot incompletely surrounded by fascia, joined to basal band. Anterior fascia of elytron passing first costa but not reaching suture, anterior margin u-shaped between costae 1 and 2 (with bottom of u towards posterior), posterior margin u-shaped between costae 1 and 2 (with bottom of u towards posterior). Posterior fascia not touching lateral or posterior margins of elytron. Black spot of elytral posterior fascia near anterior margin of fascia present on callus. Black spot of elytral posterior fascia near anterior margin of fascia incomplete, joining black elytral disc. Black spot of elytral posterior fascia near posterior margin of fascia present between costa 1 and 2 and incompletely surrounded by fascia. Elytral posterior fascia reduced, interrupted before suture. Elytral microsculpture transverse straight, narrow with breaks (e.g. Figs 2, 13). Posterior margin of elytron with 5–10 clusters of long, dark or light brown setae. Metanotal subalare with sharply rising, internally margined ridge along anteriomedial edge. Metasternal pubescence medially long, well developed, golden. Metapimeral posterior lobe with long brown setae throughout lobe.

Abdomen. Posterior margin of abdominal ventrite 5 with long setae. Setae cluster on centre of sternite 3 between metacoxae light brown. Abdominal setae dark brown. Tergite 9 of males (pygidium) with brown setae.

Legs. Lateral margin of anterior of procoxae smooth, without ridge or bump. Meso- and metatibia apical angle not produced into spine or lobe. Inner margin of metatibia of large males with a prebasal bump. Middle of outer margin of metatibia not swollen. Middle of inner face of metatibia (large males) not greatly widened (less than 2 × width at base). Metatrochanter spine of males apex pointing perpendicular to leg, recurved dorsally without acute angle ventrally, with a sharp apex.

Aedeagus. Paramere ventral setal patch not overlapping with apicolateral patch. Parameres sinuate.

Ovipositor. Spatula on proctiger (T10) apex narrow. Valvifer claw weakly dentate (Fig. 11F).

Distribution

Palearctic: Japan: Honshu, Shikoku (Fig. 24).

Remarks

This is the only species in the subfamily with the basal three segments of the antennal club black, or reddish black, and the apical segment orange. It is also endemic to Japan and is the smallest species in the genus *Nicrophorus*, being the only species with a mean pronotal width less than 4.5 mm. The red spot on the frons is sometimes absent.

Etymology

The name is a Latin adjective meaning ‘mountain-roaming’. It refers to the species’ distribution in the mountains of Japan.

Nicrophorus nepalensis Hope

(Figs 2, 8H, I, 10A, B, C, D, E, F, G, 15A, 33A, 34)

Nicrophorus Nepalensis Hope, 1831: 21.

Material examined

See Accessory Publication on *Invertebrate Systematics* website.

Measurements

(207 ♂, 288 ♀), pronotal width: ♂ 3.77–6.87, 5.30 ± 0.64 mm, ♀ 3.59–7.07, 5.22 ± 0.69 mm.

Diagnosis

Nicrophorus nepalensis-group taxon with frons usually with an orange spot; with epipleuron entirely red-orange; elytra with posterior fascia interrupted at suture (Fig. 8H, I), usually reaching dorsal ridge of epipleura (Figs. 8H, 33A), shoulder area of elytra with a row of short setae and a completely surrounded black spot, separated from end of basal black band (e.g. Fig. 8H, I); posterior margin of middle black band with a dark finger (rarely an isolated dark spot) projecting over the callus; moderate to large males with meta-

tibiae not expanded laterally, inner face not convex but with a prebasal bump (Fig. 15A), with dorsal margin swollen near middle (e.g. Fig. 15A); metasternum with dark brown pubescence. females: valvifer claw with outer margin obviously toothed (Figs 10A, B, C, D, E, F, G)

Description

Head. Antennal club basal segment black, apical three orange. Antennomeres of club weakly emarginate. Frons black, with orange spot. Post-ocular bulge of large males larger than females.

Thorax. Microsculpture of pronotum disc composed of many parallel transverse lines. Pronotum of large males orbicular or subquadrate. Setae on posteroventral portion of hypomeron long, erect, sparse; filling region extending a third or less length between trochantin and posterior margin, restricted to upper region of sclerite. Pronotum with brown to light-brown, short (approximately < 0.1 mm), sparse, setae restricted to margins. Humerus immediately dorsal of epipleural ridge orange. Humeral setae long, forming row or not. Epipleuron entirely orange. Posterior epipleural ridge with isolated single-file row of contiguous preapical setae. Epipleuron and lateral margin of elytron with sparse, short, recumbent, yellow setae throughout. Region adjacent to apex of elytral suture black. Anterior black band (or spot) not reaching 3rd costa or reaches 3rd costa. Anterior fascia of elytron with black spot completely surrounded by fascia. Anterior fascia of elytron passing first costa but not reaching suture, anterior margin u-shaped between costae 1 and 2

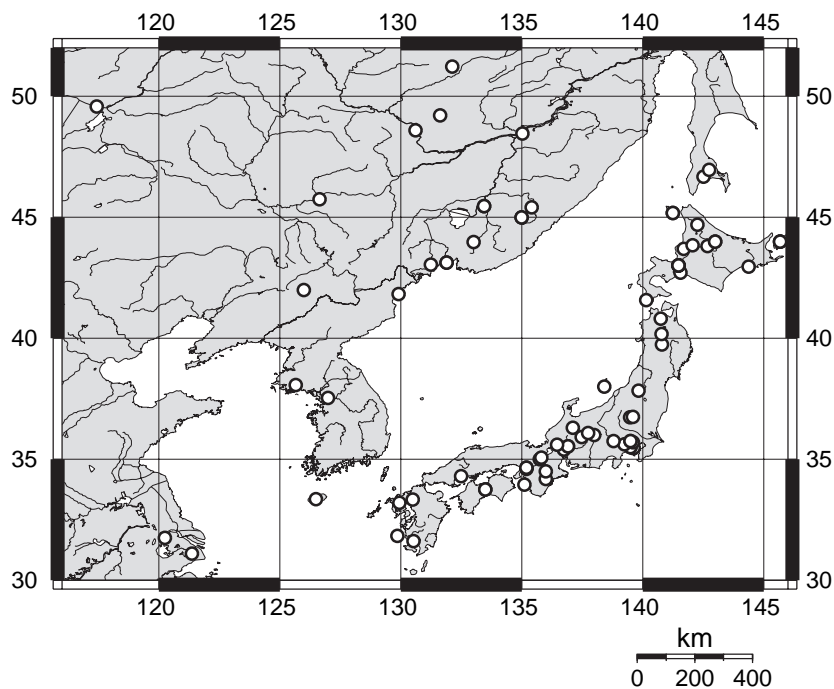


Fig. 28. Distribution of all geo-referenced specimens of *Nicrophorus maculifrons* Kraatz.

(with bottom of u towards posterior), posterior margin u-shaped between costae 1 and 2 (with bottom of u towards posterior). Posterior fascia touching lateral and posterior margins of elytron. Black spot of elytral posterior fascia near anterior margin of fascia present on callus, complete, surrounded by fascia. Black spot of elytral posterior fascia near posterior margin of fascia present between costa 1 and 2 and incompletely surrounded by fascia. Elytral posterior fascia reduced, interrupted before suture. Elytral microsculpture transverse straight, narrow with breaks (Fig. 2). Posterior margin of elytron with 5–10 clusters of long, dark or light brown setae. Metanotal subalare with sharply rising, internally margined ridge along anteriomedial edge. Metasternal pubescence medially long, well developed, light brown. Metapimeral posterior lobe with long brown setae throughout lobe.

Abdomen. Posterior margin of abdominal ventrite 5 with long setae. Setae cluster on centre of sternite 3 between metacoxae light brown. Abdominal setae dark brown. Tergite 9 of males (pygidium) with brown setae.

Legs. Lateral margin of anterior of procoxae smooth, without ridge or bump. Meso- and metatibia apical angle produced into lobe. Inner margin of metatibia of large males with a prebasal bump. Middle of outer margin of metatibia slightly swollen in large males. Middle of inner face of metatibia (large males) not greatly widened (less than $2 \times$ width at base). Metatrochanter spine of males apex pointing parallel (or almost parallel) to leg, recurved dorsally without acute angle ventrally, with a sharp apex.

Aedeagus. Paramere ventral setal patch not overlapping with apicolateral patch. Parameres evenly curved.

Ovipositor. Spatula on proctiger (T10) apex narrow. Valvifer claw dentate (Fig. 10A, B, C, D, E, F, G).

Larva. Length of projection lateral to urogomphus not reduced, proportionate to length of projections on tergite 8.

Distribution

Oriental: Pakistan, Himalayas, India, China, Laos, Burma, Malaysia, Japan: Ryukyu; Philippines, Taiwan, Thailand, Vietnam (Fig. 34).

Remarks

This is one of only four species in the genus *Nicrophorus* that have both a small orange spot on the frons and a black spot in the anterior fascia of the elytron that is, typically, completely surrounded by the fascia. It can be distinguished from these taxa by the following combination of character states: clypeal membrane not black; region adjacent to apex of elytral suture black (Fig. 8H, I).

Despite this species' wide geographic range, the examination of hundreds of specimens indicates this species shows very little polymorphism. Characters such as the valvifer claw of the ovipositor (Figs 10A, B, C, D, E, F, G) and the elytral pattern show virtually no variation in specimens taken

from widely distant sites. Rarely, for example, are seen examples in which the anterior spot of the posterior fascia is incompletely surrounded. This is in great contrast to the level of polymorphism seen in the *investigator* species-group, in which the most widespread species, *N. investigator*, among others, shows considerable elytral pattern polymorphism (Anderson and Peck 1986). Two exceptions to this constancy are noted: Arnett (1946) described a new species of *Nicrophorus* from the Philippines (*N. benguentensis*) which differed subtly from the typical form of *N. nepalensis*. These differences were deemed too subtle to warrant separate species status and this name was synonymised under *N. nepalensis* by Sikes *et al.* (2002). We hope to investigate the status of this form using molecular data which will act as a test of our morphologically-based hypothesis.

The second exception involves a single, possibly melanistic, specimen collected in Taiwan. This form was remarkable in being the only example among hundreds of examined specimens showing a strong deviation from the typical elytral pattern of *N. nepalensis* (Fig. 8I). However, the differences between this form and typical *N. nepalensis* involved only characters of colouration and no structural features. This fact, combined with the limited sample size, suggests this specimen is only an aberrant *N. nepalensis*.

Etymology

The name is a Modern Latin adjective, meaning 'Nepalese, pertaining to Nepal'. It refers to the source of the original specimen(s), from Nepal.

Nicrophorus podagricus Portevin

(Figs 8L, 10L, 15C, 16F, 33B, 35)

Nicrophorus (Nicrophorus) podagricus Portevin, 1920: 400.

Material examined

See Accessory Publication on *Invertebrate Systematics* website.

Measurements

(52 ♂, 58 ♀), pronotal width: ♂ 4.35–7.14, 5.86 ± 0.72 mm, ♀ 4.47–7.35, 5.98 ± 0.61 mm.

Diagnosis

Nicrophorus nepalensis-group taxon with epipleuron entirely red-orange; shoulder area of elytra with black spot connected to basal black band, not separated (Fig. 8L), posterior margin of middle black band with a dark finger (rarely an isolated dark spot) projecting over the callus; moderate to large males: metatibiae with dorsal margin swollen near middle (Fig. 15C), expanded laterally, with inner face convex (Fig. 15C); females: valvifer claw with outer margin obviously toothed (Fig 10L)

Description

Head. Antennal club basal segment black, apical three orange. Antennomeres of club weakly emarginate. Frons black, usually with orange spot. Post-ocular bulge of large males larger than females.

Thorax. Microsculpture of pronotum disc absent (smooth, polished) or isodiametric. Pronotum of large males orbicular. Setae on posteroventral portion of hypomeron long, erect, sparse; filling region extending a third or less length between trochantin and posterior margin, restricted to upper region of sclerite. Pronotum with brown to light-brown, short (approximately < 0.1 mm), sparse, setae restricted to margins. Humerus immediately dorsal of epipleural ridge orange. Humeral setae short, not forming row. Epipleuron entirely orange. Posterior epipleural ridge with isolated single-file row of contiguous preapical setae. Epipleuron and lateral margin of elytron with sparse, short, recumbent, yellow setae throughout. Region adjacent to apex of elytral suture black. Anterior black band (or spot) reaches 3rd costa. Anterior fascia of elytron with black spot incompletely surrounded by fascia, joined to basal band, passing first costa but not reaching suture, anterior margin u-shaped between costae 1 and 2 (with bottom of u towards posterior), posterior margin u-shaped between costae 1 and 2 (with bottom of u towards posterior). Posterior fascia not

touching lateral or posterior margins of elytron. Black spot of elytral posterior fascia near anterior margin of fascia present on callus, incomplete, joining black elytral disc. Black spot of elytral posterior fascia near posterior margin of fascia present between costa 1 and 2 and incompletely surrounded by fascia. Elytral posterior fascia reduced, interrupted before suture. Elytral microsculpture transverse straight, narrow with breaks (e.g. Figs 2, 13). Posterior margin of elytron with 5–10 clusters of long, dark or light brown setae. Metanotal subalare with sharply rising, internally margined ridge along anteriomedial edge. Metasternal pubescence medially long, well developed, light brown. Metapimeral posterior lobe with long brown setae throughout lobe.

Abdomen. Posterior margin of abdominal ventrite 5 with long setae. Setae cluster on centre of sternite 3 between metacoxae light brown. Abdominal setae dark brown. Tergite 9 of males (pygidium) with brown setae.

Legs. Lateral margin of anterior of procoxae smooth, without ridge or bump or with elongate, low ridge. Meso- and metatibia apical angle produced into lobe. Inner margin of metatibia of large males gradually curved outwards. Middle of outer margin of metatibia slightly swollen in large males. Middle of inner face of metatibia (large males) greatly widened (2.5 or greater \times width at base). Meta-

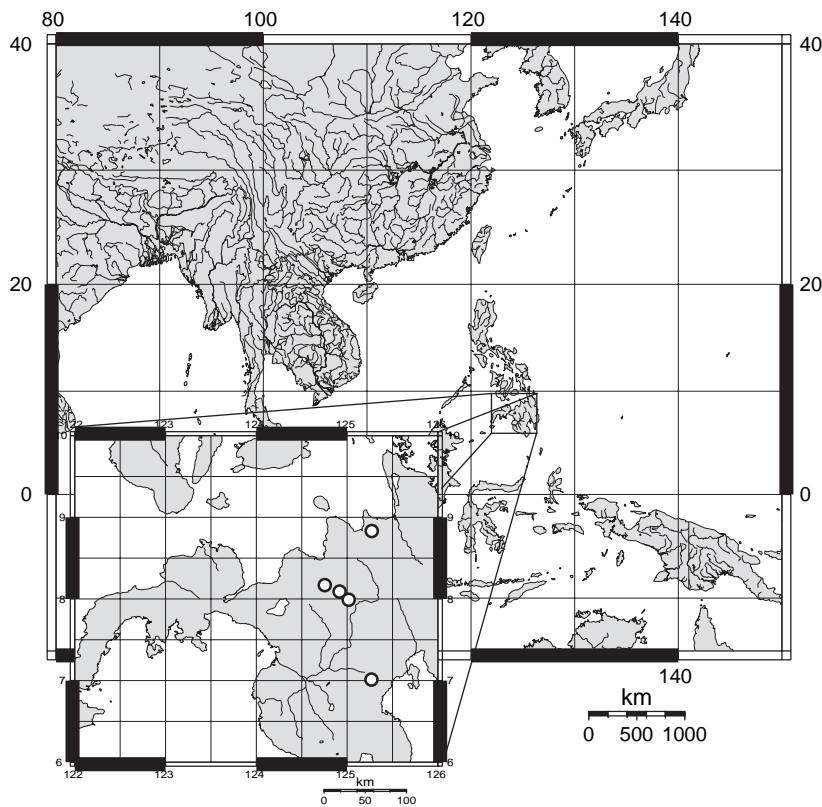


Fig. 29. Distribution of all geo-referenced specimens of the species *Nicrophorus apo* Arnett.

trochanter spine of males apex pointing parallel (or almost parallel) to leg, recurved dorsally without acute angle ventrally, with a sharp apex.

Aedeagus. Paramere ventral setal patch overlaps at edge with apicolateral patch. Parameres evenly curved.

Ovipositor. Spatula on proctiger (T10) apex narrow. Valvifer claw dentate (Fig 10L).

Distribution

Oriental: northern Borneo (Fig. 35).

Remarks

This species, the only *Nicrophorus* on the northern part of the island of Borneo, is one of six species in the genus with both a small orange spot on the frons (usually) and a black spot that is incompletely surrounded by the anterior fascia of the elytra. It can be distinguished from these taxa by the following combination of character states: meso- and metatibia angle produced into a lobe; all red / orange epipleura; no row of long humeral setae; inner margin of metatibia of large males gradually curved outwards (Fig. 15C). No variation is known except for secondary sexual characters, in which small males approach the condition of females.

Etymology

The name is a Latin adjective, meaning 'gouty'. It refers to the enlarged metatibiae in the male of this species.

Nicrophorus quadripunctatus Kraatz

(Figs 8M, 10N, 16B, 31, 33)

Nicrophorus maculifrons var. *quadripunctatus* Kraatz, 1877: 101.

Material examined

See Accessory Publication on *Invertebrate Systematics* website.

Measurements

(154 ♂, 247 ♀), pronotal width: ♂ 3.4–6.48, 5.08 ± 0.56 mm, ♀ 3.44–6.77, 5.05 ± 0.60 mm.

Diagnosis

Nicrophorus nepalensis-group taxon with epipleuron entirely red-orange; elytra with posterior fascia not interrupted at suture (Fig. 8M); shoulder area of elytra with a completely surrounded black spot, separated from end of basal black band (e.g. Fig. 8H, I, J, M, N), with a row of long erect setae; metasternum with golden pubescence; moderate to large males: metatibiae expanded laterally, inner face convex, without a prebasal bump (Fig. 15C, D), with dorsal margin swollen near middle (e.g. Fig. 15A, C, D); females: valvifer claw with outer margin obviously toothed (Fig. 10N).

Description

Head. Antennal club basal segment black, apical three orange. Antennomeres of club weakly emarginate. Frons

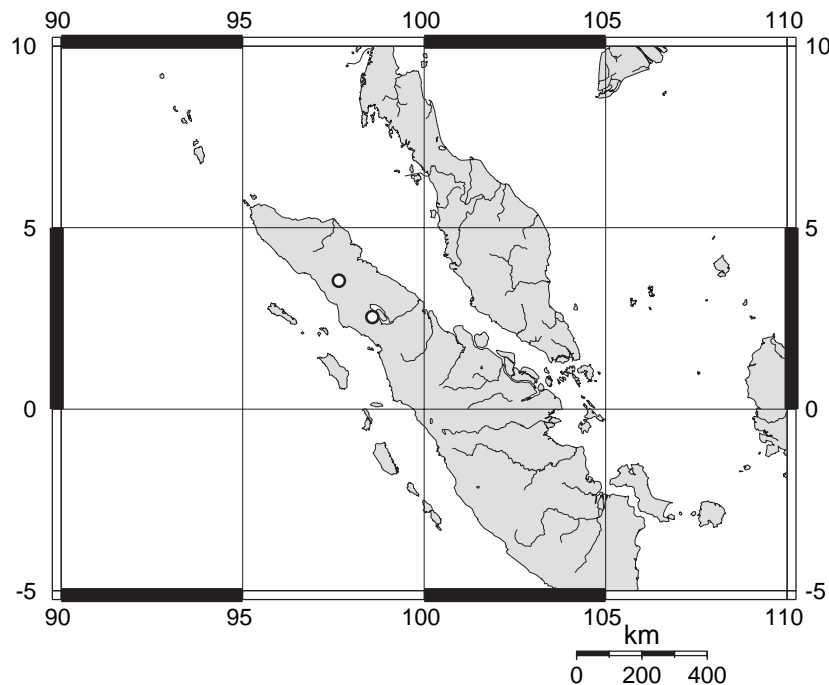


Fig. 30. Distribution of all geo-referenced specimens of *Nicrophorus herscheli* Sikes and Madge. Type locality: INDONESIA: 'Sumatra, N. Sumatra Gng Leuser NP Mt. Mamas, elev. 1630 m, 3°33'N, 97°39'E'.

black, with orange spot. Post-ocular bulge of large males larger than females.

Thorax. Microsculpture of pronotum disc composed of many parallel transverse lines. Pronotum of large males subquadrate. Setae on posteroventral portion of hypomeron long, erect, sparse; filling region extending a third or less length between trochantin and posterior margin, restricted to upper region of sclerite. Pronotum with brown to light-brown, short (approximately < 0.1 mm), sparse, setae restricted to margins. Humerus immediately dorsal of epipleural ridge orange. Humeral setae long, forming row. Epipleuron entirely orange. Posterior epipleural ridge with isolated single-file row of contiguous preapical setae. Epipleuron and lateral margin of elytron with sparse, short, recumbent, yellow setae throughout. Region adjacent to apex of elytral suture orange or yellow. Anterior fascia near suture and scutellum curving anteriorly between first costa and scutellum. Anterior fascia reaching posterior edge of scutellum. Anterior black band (or spot) not reaching 3rd costa. Anterior fascia of elytron with black spot completely surrounded by fascia, reaching suture, anterior margin u-shaped

between costae 1 and 2 (with bottom of u towards posterior), posterior margin u-shaped between costae 1 and 2 (with bottom of u towards posterior). Posterior fascia touching lateral and posterior margins of elytron. Black spot of elytral posterior fascia near anterior margin of fascia present on callus. Black spot of elytral posterior fascia near anterior margin of fascia complete, surrounded by fascia. Black spot of elytral posterior fascia near posterior margin of fascia absent, region within fascia. Elytral posterior fascia enlarged, not interrupted. Elytral microsculpture transverse straight, narrow with breaks (e.g. Figs 2, 13). Posterior margin of elytron with 5–10 clusters of long, dark or light brown setae. Metanotal subalare with sharply rising, internally margined ridge along anteriomedial edge. Metasternal pubescence medially long, well developed, light brown. Metapimeral posterior lobe with long brown setae throughout lobe.

Abdomen. Posterior margin of abdominal ventrite 5 with long setae. Setae cluster on centre of sternite 3 between metacoxae light brown. Abdominal setae dark brown. Tergite 9 of males (pygidium) with brown setae.

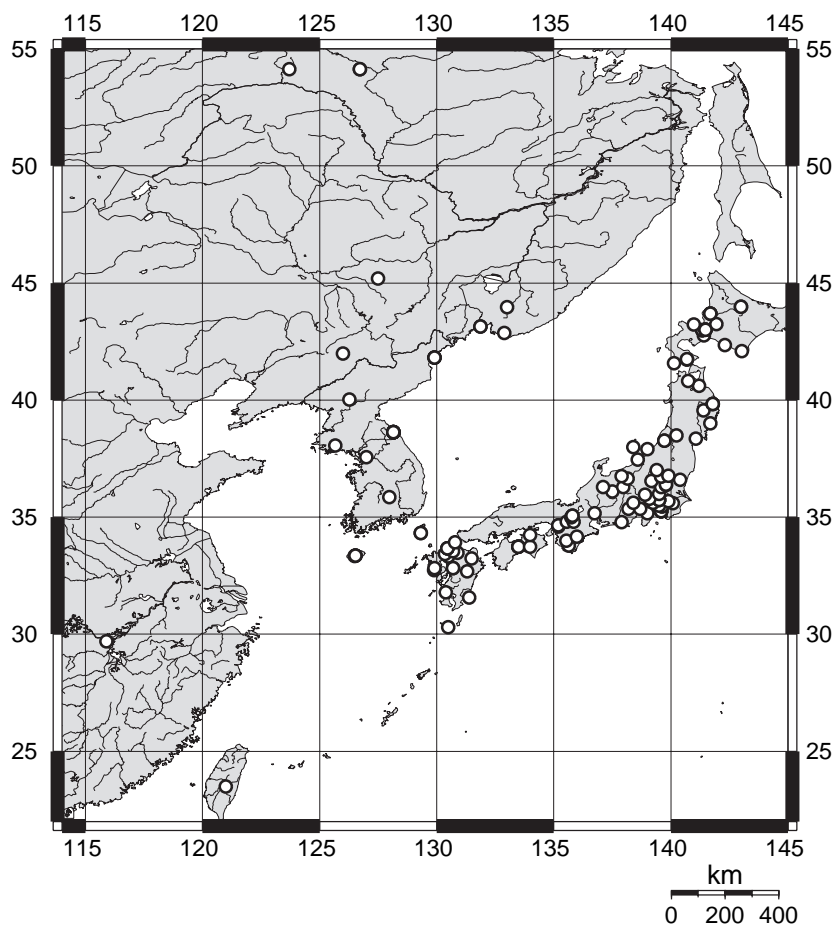


Fig. 31. Distribution of all geo-referenced specimens of *Nicrophorus quadripunctatus* Kraatz.

Legs. Lateral margin of anterior of procoxae smooth, without ridge or bump. Meso- and metatibia apical angle not produced into spine or lobe or produced into lobe. Inner margin of metatibia of large males gradually curved outwards. Middle of outer margin of metatibia slightly swollen in large males. Middle of inner face of metatibia (large males) greatly widened (2.5 or greater \times width at base). Metatrochanter spine of males apex pointing parallel (or almost parallel) to leg, recurved dorsally without acute angle ventrally, with a sharp apex.

Aedeagus. Paramere ventral setal patch not overlapping with apicolateral patch. Parameres evenly curved.

Ovipositor. Spatula on proctiger (T10) apex narrow. Valvifer claw dentate (Fig. 10N).

Larvae. Length of projection lateral to urogomphus reduced, not proportionate to length of projections on tergite 8.

Distribution

Palearctic: China, Japan, Korea, Russia: Ussuri region and Amur, Taiwan (Fig. 31).

Remarks

This is the only species in the genus *Nicrophorus* with both of the following two character states: frons black with a small orange spot and region adjacent to apex of elytral suture orange or yellow, region within posterior fascia (Figs 8M, 33). Unlike most *Nicrophorus*, in this species there is no apparent sexual dimorphism in the size and quantity of fore-

tarsal setae. Of hundreds of specimens examined only two were noted as showing a slight interruption of the posterior fascia at the suture; less so than *N. nepalensis*, but atypical for this species.

Etymology

The name is a Modern Latin compound adjective (from the Latin prefix *quadri* (four) and *punctum* (puncture, spot)), meaning 'four-spotted'. It refers to the four, small black spots on the species' bifasciate elytra.

Nicrophorus reticulatus Sikes & Madge, sp. nov.

(Figs 8O, 12A, B, 17G, 20, 33D)

Nicrophorus undescribed Hanski & Niemelä, 1990: 149.

Nicrophorus undescribed Hanski & Krikken, 1991: 195.

Nicrophorus sp. n. Peck, 2001: 94.

Material examined.

Holotype. ♂, labelled 'SOLOMON ISLANDS: Guadalcanal, Popamanasin, elev. 5000' (1524 m), [9°42'S, 160°4'E] 20 \times 1965 (coll. P. Greenslade) BMNH000895Nic'. (London (BMNH)).

Paratypes. 3 ♂. SOLOMON ISLANDS: Guadalcanal, Beomahat?, elev. 1417 m, 19.vi.1965, 1 ♂: BMNH000898Nic; same locality as holotype, 24.x.1965 (coll. P. Greenslade), 1 ♂: BMNH000826Nic; Guadalcanal, Vununalekama, elev. 1341 m, 9.xi.1965, 1 ♂: BMNH000899Nic.

Measurements

(4 ♂); pronotal width: ♂: 4.87–6.60, 5.99 ± 0.78 mm.

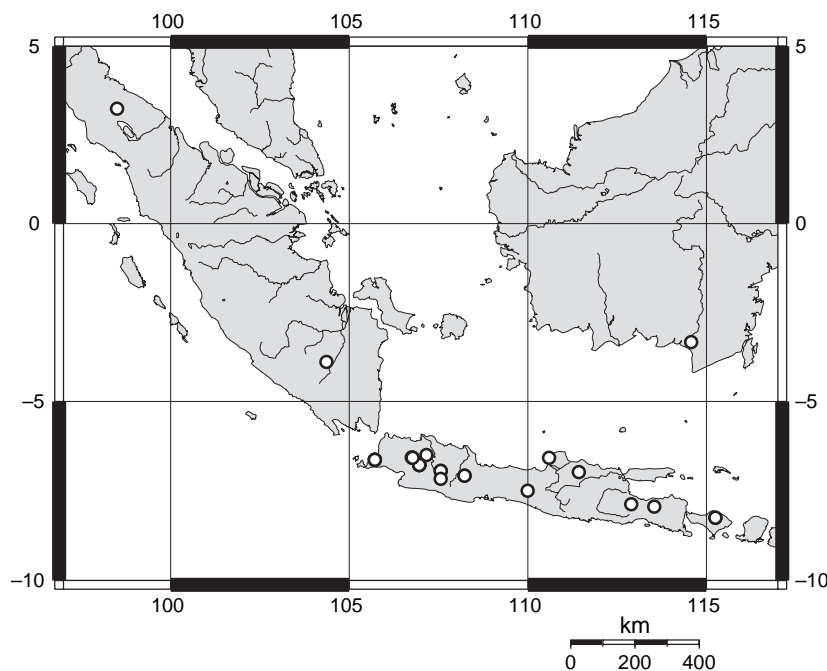


Fig. 32. Distribution of all geo-referenced specimens of *Nicrophorus insularis* Grouvelle (Borneo record is questionable).

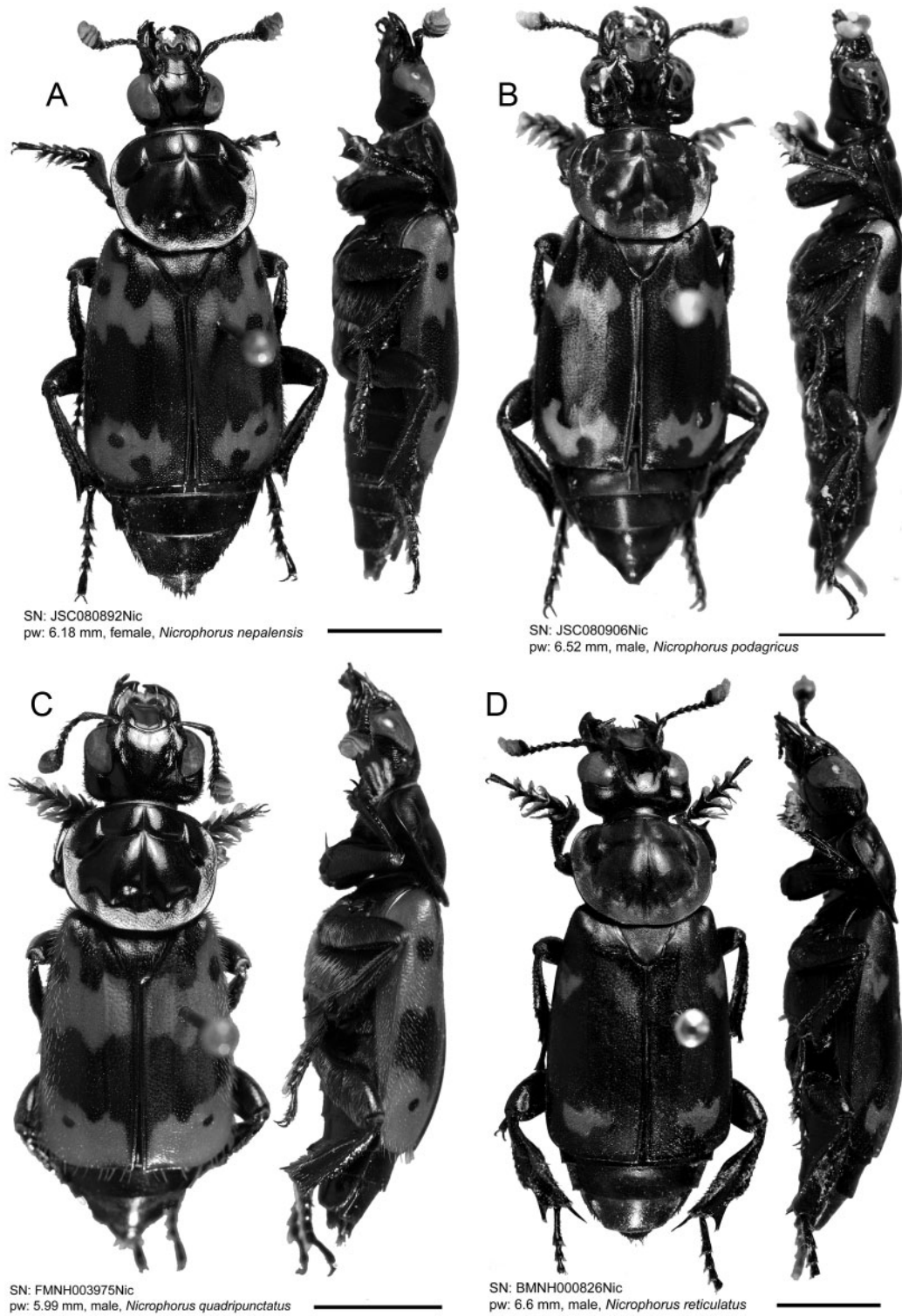


Fig. 33. Dorsal and lateral habitus. *A*, Female *Nicrophorus nepalensis* Hope. *B*, Male *Nicrophorus podagricus* Portevin. *C*, Male *Nicrophorus quadripunctatus* Kraatz. *D*, Male *Nicrophorus reticulatus* Sikes & Madge (paratype). Scale bar = 5 mm.

Diagnosis

Nicrophorus nepalensis-group taxon with epipleuron partially or entirely black; abdominal sterna 3 to 6 with very short setae along posterior margins (these setae are 2–3 × longer than the distance between adjacent setae); elytral disc with isodiametric microsculpturing (Fig. 12).

Description

Head. Antennal club basal segment black, apical three orange. Antennomeres of club weakly emarginate. Frons black, without orange spot. Post-ocular bulge of large males larger than females.

Thorax. Microsculpture of pronotum disc isodiametric. Pronotum of large males orbicular. Setae on posteroventral portion of hypomeron absent. Pronotum glabrous. Humeral setae short, not forming row. Epipleuron entirely black. Posterior epipleural ridge without isolated single-file row of contiguous preapical setae. Epipleuron glabrous, or with very sparse, extremely small setae (approximately the size of a puncture). Lateral margin of elytron glabrous, or with very sparse, extremely small setae (approximately the size of a puncture). Region adjacent to apex of elytral suture black. Anterior fascia of elytron without black spot, small, triangular-square, just reaching 2nd costa, anterior margin u-shaped between costae 3 and 4 (with bottom of u towards posterior). Black spot of elytral posterior fascia near anterior margin of fascia absent. Black spot of elytral posterior fascia near posterior margin of fascia absent, region black. Elytral posterior fascia greatly reduced, far from suture, jagged. Elytral microsculpture isodiametric (Fig. 12A, B). Posterior margin of elytron glabrous. Metanotal subalare with gradually rising ridge along anteriomedial edge. Metasternal pubescence medially long, well developed, light brown. Metapimeral posterior lobe with short brown setae throughout lobe.

Abdomen. Posterior margin of abdominal ventrite 5 with very short, (micro)setae. Setae cluster on centre of sternite 3 between metacoxae absent in centre but with long erect setae lateral of centre under coxae. Abdominal setae light brown. Tergite 9 of males (pygidium) with golden setae.

Legs. Lateral margin of anterior of procoxae smooth, without ridge or bump. Meso- and metatibia apical angle produced into lobe. Inner margin of metatibia of large males gradually curved outwards. Middle of outer margin of metatibia slightly swollen in large males. Middle of inner face of metatibia (large males) greatly widened (2.5 or greater × width at base). Metatrochanter spine of males apex pointing parallel (or almost parallel) to leg, straight, not recurved dorsally.

Aedeagus. Paramere ventral setal patch not overlapping with apicolateral patch. Parameres evenly curved.

Ovipositor. Females unknown.

Distribution

Australian: Solomon Islands: Guadalcanal (Fig. 20).

Remarks

This species and *N. kieticus* are endemic to and the only nicrophorines known from the Solomon Islands. This species is easily distinguished from *N. kieticus*, which has black antennal clubs, by its orange antennal clubs, among various other characters. Additionally, this species is unique among the *nepalensis*-group in having isodiametric microsculpturing (Fig. 12A, B) and greatly reduced elytral maculations (Figs 8O, 33D). However, in both *N. reticulatus* and *N. kieticus*, setae throughout the body are reduced or absent.

These three aspects (isodiametric microsculpturing of the elytra, greatly reduced elytral maculations, great reduction or loss of setae throughout the body) make this an unusual member of the *nepalensis*-group. The elytral pattern reduction appears most similar to that of *N. kieticus*, not currently considered to be a member of the *nepalensis*-group, which also shares reduced pubescence. *Nicrophorus kieticus* shares few *nepalensis*-group traits although it does bear a microsculpturing typical of the group. These two species represent ‘long’ morphological branches in all analyses and a more thorough investigation into their unusual character evolution than presented here is under way.

Etymology

Referring to the reticulate (*retic*, a Latin adjective, meaning ‘made like a net’), or isodiametric, elytral microsculpturing of this species, which is unique in this respect among species of the *nepalensis*-group. The name is a Latin adjective.

Nicrophorus schawalleri Sikes & Madge, sp. nov.

(Figs 8A, B, 10P, 17I, 26A, 27)

Material examined.

Holotype. ♀, labelled ‘[CHINA] Taibai Shan above Houshenzi, elev. 2500–2600 m, [33°58′N, 107°42′E] 9 vi–3.vii.1998 (coll. P. Jager & J. Martens) SMNS080911Nic’. (Stuttgart (SMNS)).

Paratypes. 39 ♂, 40 ♀, 2 adults. **CHINA: Gansu prov.,** S, Venxian env., 18–26 June 1995 (coll. Benes), ♂: JSC003452Nic, (Praha, priv.coll (JSC)); South Gansu Prov., Min Shan Mountains, 70 km NW of Wudu, elev. 2100 m, [34°0′N, 104°57′E] 1 June 1997 (coll. A. Gorodinski), 3 ♀: MNC122659Nic, MNC122660Nic, MNC122661Nic, 10 ♂: MNC122649Nic, MNC122650Nic, MNC122651Nic, MNC122652Nic, MNC122653Nic, MNC122654Nic, MNC122655Nic, MNC122656Nic, MNC122657Nic, MNC122658Nic, (Ebina (MNC) Nishikawa private coll); **Shaanxi prov.,** Qin Ling Mountains, Mt. Taibai Shan, elev. 2200 m, [33°55′N, 107°44′E] 1–31 August 2004 (coll. V. Simiaev *et al.*), 1 ♀: MNC122662Nic, (Ebina (MNC) Nishikawa private coll); Qinling mts. Xunyangba (12km SW), elev. 2000–2250 m, [35°N, 109°E] 14–18 June 1998 (coll. I. H. Marshal), 1 ♀: JSC080911Nic, 2 ♂: JSC080909Nic, JSC080910Nic, (Praha, priv.coll (JSC)); 5 ♀: SMNS080912Nic, SMNS080914Nic, SMNS080915Nic, SMNS080916Nic, SMNS080917Nic, 7 ♂: SMNS080913Nic, SMNS080918Nic, SMNS080919Nic, SMNS080920Nic, SMNS080921Nic, SMNS080922Nic, SMNS080923Nic, (Stuttgart (SMNS)); Tschingling Mts. Taibeichan Nat. Res. [Qinling Mountains – Taibaishan Nature Reserve], elev. 2000 m, [33°53′N,

107°49'E] 5–15 August 2005, 1 ♀: BMNH123518Nic, 2 ♂: BMNH123519Nic, BMNH123520Nic, (London (BMNH)); **Sichuan Prov.**, Bashan (Chengjiao Xian) Daba Shan Mts., elev. 1600–1900 m, 32°9'N, 108°4'E, 1 May–31 July 1995 (coll. 'Native collector'), 3 ♀: DSSC006248Nic, DSSC006249Nic, DSSC006250Nic, 2 ♂: DSSC006246Nic, DSSC006247Nic, (Calgary (DSSC)); Daxue Shan Gongga Shan Mt. Hailuogou, Glacier Park env. Camp 2, elev. 2650 m, [29°21'N, 101°1'E] 30 May 1997 (coll. A. Putz), 1 ♂: JSC080908Nic, (Praha, priv.coll (JSC)); Ganzi prefecture, Kangding Co., Pengta town, Tongling village, elev. 2585 m, 30°29'31"N, 102°18'15"E, 30 August 2005 (coll. D. S. Sikes), DNA-voucher 01 adult: DSSC123375Nic, DNA-voucher 02 adult: DSSC123376Nic, 8 ♀: DSSC123541Nic, DSSC123542Nic, DSSC123543Nic, DSSC123544Nic, DSSC123545Nic, DSSC123547Nic, DSSC123549Nic, DSSC123553Nic, 6 ♂: DSSC123546Nic, DSSC123548Nic, DSSC123550Nic, DSSC123551Nic, DSSC123552Nic, DSSC123554Nic, (Calgary (DSSC)); 2 ♀ IOZ-CAS123557Nic, IOZ-CAS123558Nic 2 ♂ IOZ-CAS123555Nic, IOZ-CAS123556Nic (Beijing (IOZ-CAS)); Gongga Shan mt. Moxi, [31°22'N, 102°7'E] 21–24 July 1992 (coll. J. Schneider), 2 ♂: JSC003450Nic, JSC003451Nic, (Praha, priv.coll (JSC)); Kangding [Kangding], elev. 3000 m, [30°5'N, 102°4'E] 23–27 July 1995 (coll. J. Schneider), 1 ♂: JSC003449Nic, (Praha, priv.coll (JSC)); ****Lu Ding Chiao, elev. 1524 m, [29°54'N, 102°19'E] 20 August 1937 (coll. (D. C. Graham)), 1 ♀: SBPC004504Nic, (Ottawa, priv. coll. (SBPC)); N, Jiuzhaigou, [33°17'N, 105°55'E] 12–16 June 1995 (coll. Benes), 1 ♀: JHC001845Nic, (Praha, priv.coll (JHC)); **Szechuan, Mukue Tatsienlu, [30°2'N, 102°2'E], 2 ♀ NMPC082224Nic, NMPC082225Nic, (Praha (NMPC)); **same locality, [30°3'N, 102°2'E] (coll. Em. Reitter), 1 ♀: JSC003453Nic, (Praha, priv.coll (JSC)); ****Szechuan, Wassuland, Chungwa, (coll. Reitter), 1 ♀: NMPC082185Nic, (Praha (NMPC)); **Szechwan, MuSangTsai, 10 mi NW WeiChow, elev. 2713 m, 26–28 July 1933 (coll. D C Graham), 1 ♀: USNM083614Nic, (USNM); **Tatsienlu Kiulung [Jiulong], [29°N, 101°48'E] (coll. Reitter), 1 ♀: NMPC082226Nic, 1 ♂: NMPC082223

Nic, (Praha (NMPC)); W, Daxue Shan Hailuogou, Glacier Park (Gongga Shan) Camp 2, elev. 2500–2700 m, [29°21'N, 101°1'E] 30–31 May 1997 (coll. Wrase), 3 ♀: SMNS080937Nic, SMNS080938Nic, SMNS080939Nic, (Stuttgart (SMNS)); W Sichuan, Aba pref. Nanping count. (regio silv.), elev. 2500 m, 33°12'N, 103°54'E, 28 May–6 June 1990 (coll. Görgner & Kleinfeld), 2 ♂: SMNS003348Nic, SMNS003349Nic, (Stuttgart (SMNS)); Wolong, elev. 1800–2700 m, [27°50'N, 101°50'E] 20–21 July 1990, 1 ♀: MNHN001305Nic, (Paris (MNHN)); *(unknown prov.), Hai - tsi - pin, elev. 3962 m, 1 July–31 August 1937 (coll. D. C. Graham), 3 ♀: SBPC004505Nic, SBPC004506Nic, SBPC004508Nic, (Ottawa, priv. coll. (SBPC)); ****same locality, elev. 3962 m, 1–31 August 1937 (coll. D. C. Graham), 1 ♀ SBPC004507Nic, (Ottawa, priv. coll. (SBPC)).

Measurements

(37 ♂, 40 ♀), pronotal width: ♂ 4.15–6.49, 5.21 ± 0.48 , ♀ 4.16–6.24, 5.13 ± 0.59 mm.

Diagnosis

Nicrophorus nepalensis-group taxon with frons with orange spot; elytra with epipleuron entirely red–orange; antennal club with basal segment black, apical three orange; meso- and metatibiae with apical emargination not semicircular, lower part of emargination with a row of setae (e.g. Fig. 15B); posterior fascia with anterior margin irregular, with elytra with middle black band usually not reaching the dorsal ridge of the epipleuron (Figs 8A, B; 26A); moderate to large males: metatibiae with inner face bearing a prebasal bump and then concave (Fig. 15A, B), with dorsal margin not swollen, simple as in female (Fig. 15B, E); pubescence of metasternum golden (when middle black band shortened,

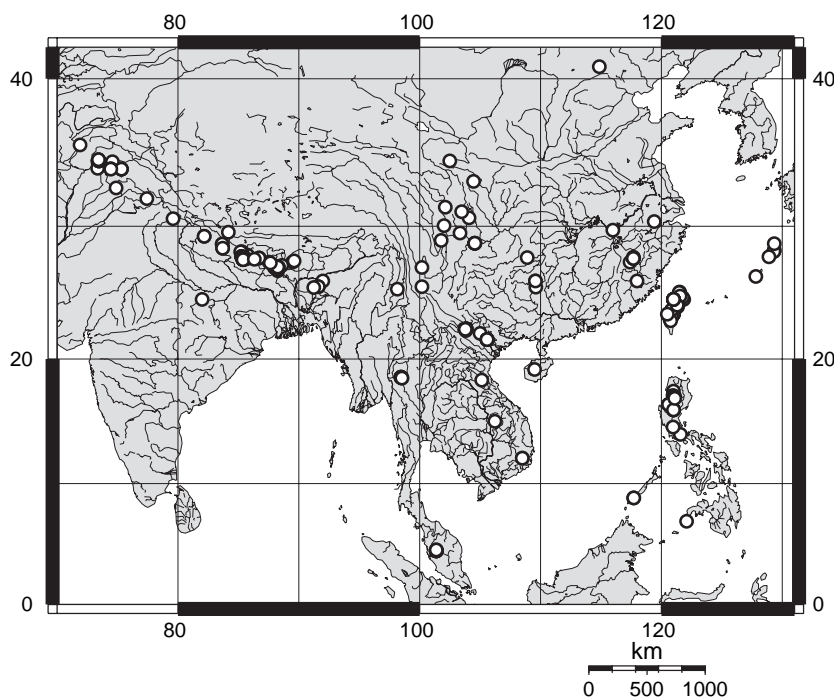


Fig. 34. Distribution of all geo-referenced specimens of *Nicrophorus nepalensis* Hope (record north of 40° is questionable).

e.g. Fig. 8A) or dark brown (when middle black band reaches or almost reaches the dorsal ridge, and sometimes when it almost does, e.g. Fig. 8B); dorsal ridge of epipleuron with posterior setae golden in palest forms but grading to dark brown in others; metafemora with apical setae golden in palest forms but grading to dark brown – apparently the first sign of darkening; females: valvifer claw with outer margin lobed but not toothed (Figs 10P).

Description

Head. Antennal club basal segment black, apical three orange. Antennomeres of club weakly emarginate. Frons black, with orange spot. Post-ocular bulge of large males larger than females.

Thorax. Microsculpture of pronotum disc isodiametric. Pronotum of large males subquadrate. Setae on postero-ventral portion of hypomeron long, erect, sparse; filling region extending a third or less length between trochantin and posterior margin, restricted to upper region of sclerite. Pronotum with brown to light-brown, short (approximately < 0.1 mm), sparse, setae restricted to margins. Humerus immediately dorsal of epipleural ridge orange. Humeral setae long, forming row. Epipleuron entirely orange. Posterior epipleural ridge with isolated single-file row of contiguous preapical setae. Epipleuron and lateral margin of elytron with sparse, short, recumbent, yellow setae throughout. Region adjacent to apex of elytral suture black. Anterior black band (or spot) not reaching 3rd costa. Anterior fascia

of elytron without black spot, passing first costa but not reaching suture, anterior margin u-shaped between costae 1 and 2 (with bottom of u towards posterior), posterior margin u-shaped between costae 1 and 2 (with bottom of u towards posterior). Posterior fascia touching lateral or posterior margins of elytron or not. Black spot of elytral posterior fascia near anterior margin of fascia present on callus or absent. Black spot of elytral posterior fascia near anterior margin of fascia incomplete, joining black elytral disc. Black spot of elytral posterior fascia near posterior margin of fascia absent, region black or region within fascia. Elytral posterior fascia reduced, interrupted before suture. Elytral microsculpture transverse straight, narrow with breaks (e.g. Figs 2, 13). Posterior margin of elytron with 5–10 clusters of long, dark or light brown setae. Metanotal subalare with sharply rising, internally margined ridge along anteriomedial edge. Metasternal pubescence medially long, well developed, golden or light brown. Metapimeral posterior lobe with long brown setae throughout lobe.

Abdomen. Posterior margin of abdominal ventrite 5 with long setae. Setae cluster on centre of sternite 3 between metacoxae light brown. Abdominal setae dark brown. Tergite 9 of males (pygidium) with brown setae.

Legs. Lateral margin of anterior of procoxae smooth, without ridge or bump. Meso- and metatibia apical angle produced into lobe. Inner margin of metatibia of large males with a prebasal bump. Middle of outer margin of metatibia not swollen. Middle of inner face of metatibia (large males)

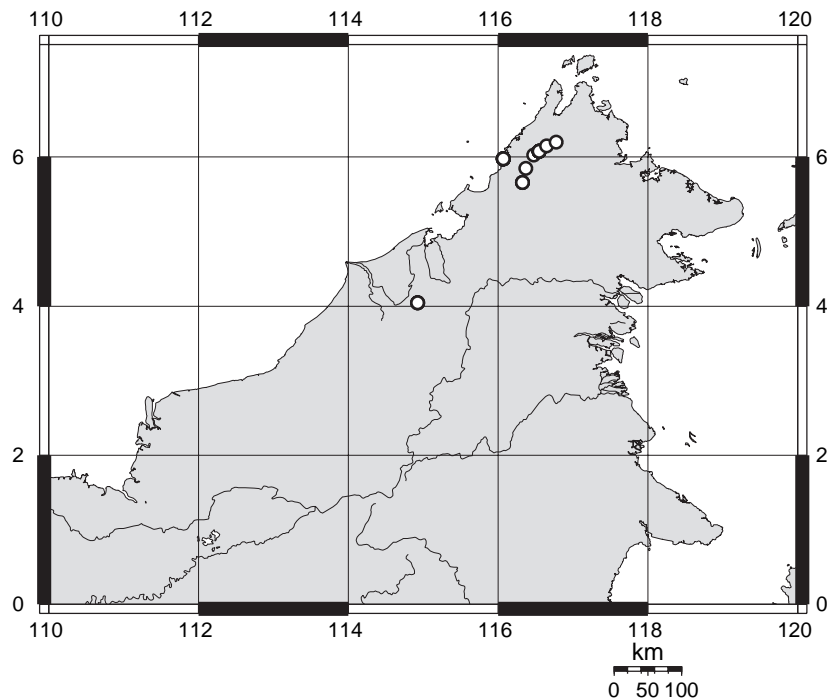


Fig. 35. Distribution of all geo-referenced specimens of *Nicrophorus podagricus* Portevin.

not greatly widened (less than $2 \times$ width at base). Metatrochanter spine of males apex pointing parallel (or almost parallel) to leg, recurved dorsally without acute angle ventrally, with a sharp apex.

Aedeagus. Paramere ventral setal patch overlaps at edge with apicolateral patch. Parameres evenly curved or sinuate.

Ovipositor. Spatula on proctiger (T10) apex narrow. Valvifer claw lobed with round apex (Fig. 10P).

Distribution

Oriental: China: Sichuan, Gansu, Shaanxi Provinces (Fig. 27).

Remarks

This species of south-west China is one of only three in the *nepalensis*-group that have a row of long setae on the elytral shoulders but lack dorsal swelling on the metatibiae of moderate to large males. Of the other two, *N. montivagus* has a uniquely coloured antennal club, with the basal three segments black and only the apical segment red. In *N. maculifrons* the metasternum always has golden pubescence and the middle black band of the elytra always reaches the epipleuron, a character combination not found in *N. schawalleri*. The only member of the *nepalensis*-group that is sympatric with this species is *N. nepalensis* itself and the latter always has a free shoulder spot, lacks a row of long

humeral setae and has male metatibiae modified with a dorsal swelling

The middle black band of the elytra in some specimens fails to reach the dorsal ridge of the epipleuron (e.g. Fig. 8A), in others, it broadly reaches it (Fig. 8B). This darkening of the middle black band is closely associated with darkening of the row of setae at the posterior end of the epipleuron, the setae at the end of the femora, and the metasternal pubescence. In addition, this change is associated with a reduction in size of the posterior fascia (e.g. Fig. 8B).

Etymology

This is a Latinised personal name in the genitive singular, meaning 'of Schawaller'. It is given in honour of Wolfgang Schawaller, a German entomologist with a particular interest in the Silphidae. Schawaller first recognised the possibility that this might be a distinct species.

Nicrophorus trumboi Sikes & Madge, sp. nov.

(Figs 8F, 11B, 12C, D, 15E, 17F, 25, 26B)

Material examined

Holotype. ♀ labelled: 'Nepal, Solu Khumbu Dist., Mtns east of Lukla, moist cloud forest, elev. 2840–2900 m, 27°41'15"N, 86°44'9"E,

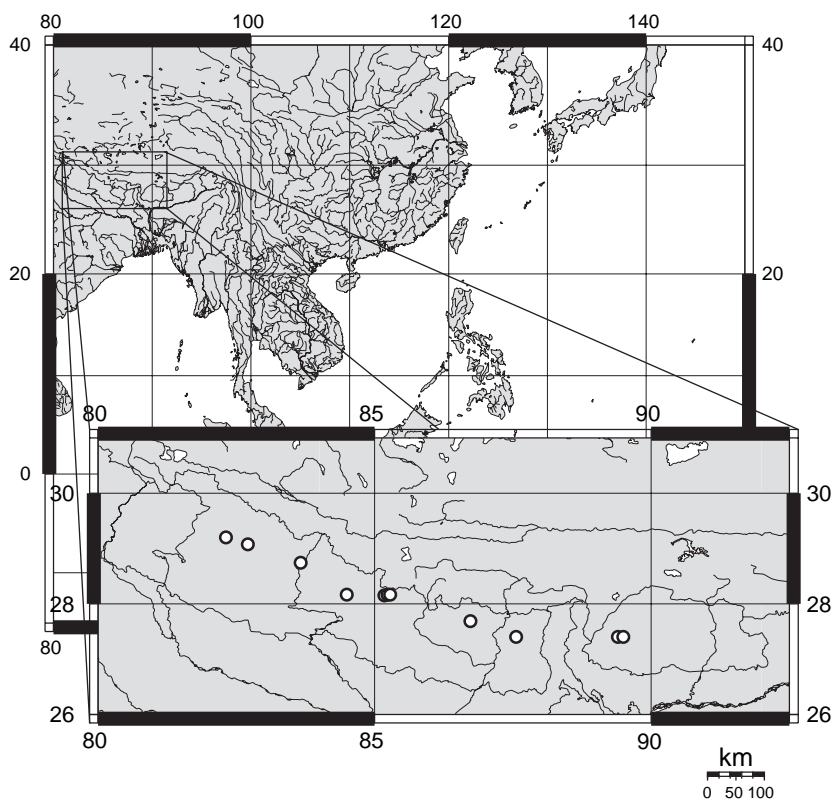


Fig. 36. Distribution of all geo-referenced specimens of *Nicrophorus melissae* Sikes & Madge. Type locality: Nepal, Ganesh Himal, 7 km W Godlang, 2950 m, 28°10'N, 85°14'E.

20.viii.1999 (coll. D. S. Sikes) MCZC100197Nic'. (Cambridge (MCZC)).

Paratypes. 7 ♂, 9 ♀. **BHUTAN:** Lame gumpa [walking distance from Bumtang], [27°33'N, 90°43'E] 1–30.ix.1977 (coll. W. Roder & L. Caminada), 1 ♀: SMNS003360Nic; **NEPAL:** elev. 3383 m, 31.v.1967, 1 ♂: CNCI000702Nic; 18.vi.1967, 1 ♂: CNCI000703Nic; 27.vi.1967, 1 ♂: CNCI000705Nic; Ganesh Himal betw. Golzong and Somathang, No. 13, elev. 1500–3600 m, 12–15.vii.1993 (coll. G. Csorba & M. Hreblay), 3 ♀: SMNS003355Nic, SMNS003356Nic, SMNS003357Nic, 1 ♂: SMNS003359Nic; Kangchenjunga Himal Mts. Ghunsa vill., elev. 3375 m, 27°24'N, 87°34'E, 6–10.vii.2000 (coll. Jan Schneider), 1 ♀: JSC080894Nic, 4 ♂: JSC080893Nic, JSC080895Nic, JSC080896Nic, JSC080897Nic; **Mal. tr., elev. 3383 m, 27°58'N, 85°0'E, 2.vi.1967, 1 ♂: CNCI000704Nic; Solu Khumbu Dist., Monju, moist pine 1° and 2° growth, elev. 2900 m, 27° 46'18"N, 86°43'47"E, 25.viii.1999 (coll. D. S. Sikes), DNA-voucher 02, ♀: DSSC006325Nic; same data as holotype- 2 ♀: DSSC100198Nic, DSSC100199Nic, DNA-voucher 01, ♂: DSSC006345Nic, 1 ♂: MCZC100196Nic; surroundings of Lukla, elev. 2800–4000 m, [27°42'N, 86°43'E] 26 vi–2.vii.1993 (coll. G. Csorba & M. Hreblay), 2 ♀: SMNS003354Nic, SMNS003358Nic, 1 ♂: SMNS003353Nic.

Measurements

(7 ♂, 10 ♀), pronotal width: ♂ 5.08–6.09, 5.39 ± 0.35, ♀ 4.56–6.35, 5.72 ± 0.52 mm.

Diagnosis

Nicrophorus nepalensis-group taxon with antennal club usually all orange, sometimes basal segment darkened; meso- and metatibiae with apical emargination very large, semicircular; the apical process thus very narrow; lower part of emargination without a row of setae (Fig. 15E); posterior fascia with anterior margin smooth; moderate to large males: metatibiae with inner face convex (Fig. 15E).

Description

Head. Antennal club entirely orange or basal segment black, apical three orange. Antennomeres of club weakly emarginate. Frons black, with orange spot. Post-ocular bulge of large males larger than females.

Thorax. Microsculpture of pronotum disc isodiametric. Pronotum of large males subquadrate. Setae on posterior-ventral portion of hypomeron long, erect, sparse; filling region extending a third or less length between trochantin and posterior margin, restricted to upper region of sclerite. Pronotum with brown to light-brown, short (approximately < 0.1 mm), sparse, setae restricted to margins. Humerus immediately dorsal of epipleural ridge orange. Humeral setae short, not forming row. Epipleuron entirely orange. Posterior epipleural ridge with isolated single-file row of contiguous preapical setae. Epipleuron and lateral margin of elytron with sparse, short, recumbent, yellow setae throughout. Region adjacent to apex of elytral suture black. Anterior black band (or spot) not reaching 3rd costa. Anterior fascia of elytron without black spot, passing first costa but not reaching suture, anterior margin u-shaped between costae 1 and 2 (with bottom of u towards posterior), posterior margin

u-shaped between costae 1 and 2 (with bottom of u towards posterior). Posterior fascia not touching lateral or posterior margins of elytron. Black spot of elytral posterior fascia near anterior margin of fascia absent. Black spot of elytral posterior fascia near posterior margin of fascia absent, region black. Elytral posterior fascia reduced, interrupted before suture. Elytral microsculpture transverse straight, narrow with breaks (Figs 12C, D). Posterior margin of elytron without 5–10 clusters of long, dark or light brown setae – shorter setae may be visible. Metanotal subalare with sharply rising, internally margined ridge along anteriomedial edge. Metasternal pubescence medially long, well developed, light brown. Metapimeral posterior lobe with long brown setae throughout lobe.

Abdomen. Posterior margin of abdominal ventrite 5 with long setae. Setae cluster on centre of sternite 3 between metacoxae light brown. Abdominal setae dark brown or light brown. Tergite 9 of males (pygidium) with brown setae.

Legs. Lateral margin of anterior of procoxae smooth, without ridge or bump. Meso- and metatibia apical angle produced into lobe. Inner margin of metatibia of large males gradually curved outwards. Middle of outer margin of metatibia not swollen. Middle of inner face of metatibia (large males) greatly widened (2.5 or greater × width at base). Metatrochanter spine of males apex pointing parallel (or almost parallel) to leg, recurved dorsally without acute angle ventrally, with a sharp apex.

Aedeagus. Paramere ventral setal patch overlaps at edge with apicolateral patch. Parameres sinuate.

Ovipositor. Spatula on proctiger (T10) apex wide. Valvifer claw lobed with round apex.

Distribution

Oriental: Himalayas: Nepal and Bhutan (Fig. 25).

Remarks

This species is known only from Nepal and Bhutan and is distinct. It is the only *Nicrophorus* with a large semicircular emargination at the apex of the meso- and metatibiae (Fig. 15E). Also, the anterior margin of the posterior fascia of the elytra is very smooth (Fig. 26B), not at all ragged as in *N. nepalensis* and *N. melissae*, the other species of this region. The basal segment of the antennal club is usually all or partially orange. The metatibiae of moderate to large males are unusual in that the dorsal margin is not swollen but the lower face is convex. The antennal club shows variation in the basal segment ranging from dark, almost brown, to lighter orange. See the section above, 'New species', for discussion of phylogenetic results supporting this species' status as new.

Etymology

This is a Latinised personal name in the genitive singular, meaning 'of Trumbo'. It is given in honour of the third author, Stephen T. Trumbo, a behavioural ecologist and

specialist on the genus *Nicrophorus*. Stephen's vision is to understand the evolution of the nicrophorines, thus, he began our molecular and behavioural (Trumbo *et al.* 2001) investigations into these Himalayan, and other Asian, species.

Acknowledgments

We thank the multitude of curators and collections managers who assisted with loans of study material including: N. Berti (MNHN), M. Brendell & M. Barclay (BMNH), R. W. Brooks (SEMC), B. Brugge (ZMAN), M.-L. Chan (NMNS), L.-y. Chou (TARI), R. Danielsson (MZLU), A. Davis (CNCI), F. Génier (CMNC), W. J. Hanson (EMUS), J. Háva (JHC), L. H. Herman (AMNH), E. R. Hoebeke (CUIC), G. N. House (NMNH, USNM), M. Jäch (NHMW), O. Jäger (SMTD), J. Jelínek (NMPC), D. Kavanaugh (CASC), A. G. Kireitshuk (ZMAS), K. Konishi (ITLJ), S. Krauth (IRCW), W. Wehling (MSUC), O. Martin (ZMUC), O. Merkl (HNHM), M. Nishikawa (MNC), S. Nomura (NSMT), G. R. Noonan (MCPM), M. Ôhara (EIHU), P. Parrillo (FMNH), S. B. Peck (SBPC), P. Perkins (MCZC), E. G. Riley (TAMU), G. A. Samuelson (BPBM), W. Schawaller (SMNS), J. Schneider (JSC), H. Silfverberg (MZHF), R. W. Sites (UMRM), M. Uhlig (ZMHB), T. W. Pietsch (TAMU2), A. Vesmanis (SMFD), B. Viklund (NHRs), K. Walker (MVMA), T. Wier (ANIC), and L.-y. Zheng (NKUM). We thank those who helped us obtain specimens with preserved DNA: A. Riede, S. Suzuki, M. Kon, K. Araya, M. Maruyama, J. Horák, S. B. Peck, D. Mohagan, B. D. Gill. Numerous faculty in the Ecology and Evolutionary Biology department at the University of Connecticut have assisted this project in various ways, including Janine Caira, Paul Lewis, Chris Simon, Jim Slater, and David Wagner. Expeditions to Nepal and Japan were wonderfully successful thanks to the generosity and assistance of Dhruva Manandhar (Nepal) and Masahiro Kon, Seizi Suzuki, Masahiro Ôhara, Tomoyosi Nisimura, Munetoshi Maruyama, and Masahiro Nagano (Japan). DSS thanks his good friend Piotr Naskrecki for countless hours of taxonomic, computer, and photography related discussions (and for tolerating all the carrion). This research was enormously simplified by use of Piotr's custom-built database MANTIS (A Manager of Taxonomic Information and Specimens (Naskrecki 2001)). Derek thanks his wonderful wife Melissa for her support and love. This project was supported by an Ernst Mayr grant and NSERC Discovery grant to Derek Sikes and a National Science Foundation Grant (DEB-9981381), a University of Connecticut Research Council grant, and a National Geographic Society grant to Stephen Trumbo.

References

Akaike, H. (1974). A new look at the statistical model identification. *IEEE Transactions on Automatic Control* **19**, 716–723. doi:10.1109/TAC.1974.1100705

- Anderson, R. S. (1982). Resource partitioning in the carrion beetle (Coleoptera: Silphidae) fauna of southern Ontario: ecological and evolutionary considerations. *Canadian Journal of Zoology* **60**, 1314–1325.
- Anderson, J. S. (2001). The phylogenetic trunk: maximal inclusion of taxa with missing data in an analysis of the lepospondyli (Vertebrata, Tetrapoda). *Systematic Biology* **50**, 170–193.
- Anderson, R. S., and Peck, S. B. (1986). Geographic patterns of colour variation in North American *Nicrophorus* burying beetles (Coleoptera: Silphidae). *Journal of Natural History* **20**, 283–297.
- Anduaga, S., and Huerta, C. (2001). Effect of parental care on the duration of larval development and offspring survival in *Nicrophorus mexicanus* Matthews (Coleoptera: Silphidae). *Coleopterists Bulletin* **55**, 264–271.
- Arnett, R. H., Jr (1946). A new species of *Nicrophorus* from the Philippine Islands (Coleoptera, Silphidae). *Proceedings of the Entomological Society of Washington* **48**, 207–209.
- Arnett, R. H., Jr (1950). The Silphidae of the Philippine Islands (Coleoptera). *Proceedings of the Entomological Society of Washington* **52**, 63–69.
- Arnett, R. H., Jr, Samuelson, G. A., and Nishida, G. M. (1993). 'The Insect and Spider Collections of the World.' 2nd edn. (Sandhill Crane Press, Inc.: Gainesville, FL, USA.)
- Bliss, R. Q. (1949). Studies on the Silphidae, I. Secondary sexual differences in the genus *Nicrophorus* (Coleoptera). *Entomological News* **60**, 197–204.
- Buckley, T. R., and Cunningham, C. W. (2002). The effects of nucleotide substitution model assumptions on estimates of non-parametric bootstrap support. *Molecular Biology and Evolution* **19**, 394–405.
- Bull, J. J., Huelsenbeck, J. P., Cunningham, C. W., Swofford, D. L., and Waddell, P. J. (1993). Partitioning and combining data in phylogenetic analysis. *Systematic Biology* **42**, 384–397.
- Darlu, P., and Lecointre, G. (2002). When does the incongruence length difference test fail? *Molecular Biology and Evolution* **19**, 432–437.
- de Pinna, M. C. C. (1991). Concepts and test of homology in the cladistic paradigm. *Cladistics* **7**, 317–338.
- Easton, C. (1980). A method of sexing three species of *Nicrophorus* (Col., Silphidae). *Entomologist's Monthly Magazine* **115**, 121–123.
- Emetz, V., and Schawaller, W. (1975). Silphidae aus dem Nepal-Himalaya (Ins.: Col.). *Senckenbergiana Biologica* **56**, 221–231.
- Erixon, P., Sennblad, B., Britton, T., and Oxelman, B. (2003). Reliability of Bayesian posterior probabilities and bootstrap frequencies in phylogenetics. *Systematic Biology* **52**, 665–673. doi:10.1080/10635150390235485
- Farris, J. S., Källersjö, M., Kluge, A. G., and Built, C. (1994). Testing significance of incongruence. *Cladistics* **10**, 315–319. doi:10.1111/j.1096-0031.1994.tb00181.x
- Giribet, G., and Wheeler, W. C. (1999). On gaps. *Molecular Phylogenetics and Evolution* **13**, 132–143. doi:10.1006/mpev.1999.0643
- Green, P. J. (1995). Reversible jump Markov chain Monte Carlo computation and Bayesian model determination. *Biometrika* **82**, 711–732.
- Grouvelle, A. H. (1893). Espèce nouvelle du genre *Nicrophorus* de l'archipel Indo-Néerlandais. *Notes from the Leyden Museum* **15**, 161–162.
- Gu, X., Fu, Y.-X., and Li, W.-H. (1995). Maximum likelihood estimation of the heterogeneity of substitution rare among nucleotide sites. *Molecular Biology and Evolution* **12**, 546–557.
- Gustincich, S., Manfioletti, G., Del Sal, G., Schneider, C., and Carnichi, P. (1991). A fast method for high quality genomic DNA extraction from whole human blood. *BioTechniques* **11**, 298–301.

- Hanski, I. (1983). Distributional ecology and abundance of dung and carrion-feeding beetles (Scarabaeidae) in tropical rain forests in Sarawak, Borneo. *Acta Zoologica Fennici* **167**, 1–45.
- Hanski, I., and Krikken, J. (1991). Dung beetles in tropical forests of south-east Asia. In 'Dung Beetle Ecology'. (Eds I. Hanski and Y. Camberfort.) pp. 179–197. (Princeton University Press: Princeton, NJ, USA.)
- Hanski, I., and Niemelä, J. (1990). Elevational distributions of dung and carrion beetles in northern Sulawesi. In 'Insects and the Rainforests of South East Asia (Wallacea)'. (Eds W. J. Knight and J. D. Holloway.) pp. 145–152. (Royal Entomological Society: London, UK.)
- Hastings, W. K. (1970). Monte Carlo sampling methods using Markov chains and their applications. *Biometrika* **57**, 97–109.
- Hatch, M. H. (1927). Studies on the Silphinae. *Journal of the New York Entomological Society* **35**, 331–370.
- Háva, J., Schneider, J., and Růžička, J. (1999). Four new species of carrion beetles from China (Coleoptera: Silphidae). *Entomological Problems* **30**, 67–83.
- Hawkins, J. A., Hughes, C. E., and Scotland, R. W. (1997). Primary Homology Assessment, Characters and Character States. *Cladistics* **13**, 275–283. doi:10.1111/j.1096-0031.1997.tb00320.x
- Herschel, J. D. (1807). Die Europäischen Arten von *Nicrophorus* mit Unterscheidung einer neuen Art: *Nicrophorus Vestigator*. *Magazin für Insektenkunde* **6**, 268–276.
- Hillis, D. M., and Wiens, J. J. (2000). Molecules versus morphology in systematics: conflicts, artifacts, and misconceptions. In 'Phylogenetic Analysis of Morphological Data'. (Ed. J. Wiens.) pp. 1–19. (Smithsonian Institution Press: Washington, DC, USA.)
- Hope, F. W. (1831). Synopsis of the new species of Nepaul insects in the collection of Major General Hardwicke. In 'The Zoological Miscellany. Vol. 1'. (Ed. J. E. Gray) pp. 21–32. (Treuttel, Wurtz & Co., London, UK.)
- Huelsenbeck, J. P., and Bollback, J. P. (2001). Empirical and hierarchical Bayesian estimation of ancestral states. *Systematic Biology* **50**, 351–366. doi:10.1080/106351501300317978
- Huelsenbeck, J. P., and Ronquist, F. (2001). MRBAYES: Bayesian inference of phylogeny. *Bioinformatics (Oxford, England)* **17**, 754–755. doi:10.1093/bioinformatics/17.8.754
- Huelsenbeck, J. P., Ronquist, F., Nielsen, R., and Bollback, J. P. (2001). Bayesian inference of phylogeny and its impact on evolutionary biology. *Science* **294**, 2310–2314. doi:10.1126/science.1065889
- Huelsenbeck, J. P., Larget, B., Miller, R. E., and Ronquist, F. (2002). Potential applications and pitfalls of Bayesian inference of phylogeny. *Systematic Biology* **51**, 673–688. doi:10.1080/10635150290102366
- Hufford, L. (1992). Rosidae and their relationships to other nonmagnoliid dicotyledons: A phylogenetic analysis using morphological and chemical data. *Annals of the Missouri Botanical Garden* **79**, 218–248.
- ICZN (1999). 'International Code of Zoological Nomenclature, Fourth Edition, adopted by the International Union of Biological Sciences.' (International Trust for Zoological Nomenclature: London, UK.)
- Kamimura, K., Nakane, T., and Koyama, N. (1964). Seasonal and altitudinal distribution of beetles in Mt. Jōnen, the Japan Alps, with descriptions of new species, I (Studies on the insects of high mountains, III). *Scientific Reports of the Kyoto Prefectural University (Natural Science, Living Science, Welfare Science) (A)* **15**, 17–38.
- Kass, R. E., and Raftery, A. E. (1995). Bayes factors. *Journal. American Statistical Association* **90**, 773–795.
- Kearney, M. (2002). Fragmentary taxa, missing data, and ambiguity: mistaken assumptions and conclusions. *Systematic Biology* **51**, 369–381. doi:10.1080/10635150252899824
- Kluge, A. G. (1989). A concern for evidence and a phylogenetic hypothesis among *Epicrates* (Boidae, Serpentes). *Systematic Zoology* **38**, 7–25.
- Kraatz, G. (1877). Beiträge zur Käferfauna von Japan, meist auf R. Hiller's Sammlungen basirt *Deutsche Entomologische Zeitschrift* **21**, 81–128.
- Kress, W. J. (1990). The phylogeny and classification of the Zingiberales. *Annales of the Missouri Botanical Garden* **77**, 698–721.
- Larget, B., and Simon, D. (1999). Markov chain Monte Carlo algorithms for the Bayesian analysis of phylogenetic trees. *Molecular Biology and Evolution* **16**, 750–759.
- Leaché, A. D., and Reeder, T. W. (2002). Molecular systematics of the Eastern Fence lizard (*Sceloporus undulatus*): A comparison of parsimony, likelihood, and Bayesian approaches. *Systematic Biology* **51**, 44–68. doi:10.1080/106351502753475871
- Lewis, G. (1887). A list of the Japanese Silphidae. *Annals and Magazine of Natural History* **5**, 338–342.
- Lewis, P. O. (2001). A likelihood approach to estimating phylogeny from discrete morphological character data. *Systematic Biology* **50**, 913–925. doi:10.1080/106351501753462876
- Li, S. (1996). Phylogenetic tree construction using Markov chain Monte Carlo. Ph.D. Thesis, Ohio State University, Columbus, OH, USA.
- Liu, H., and Beckenbach, A. T. (1992). Evolution of the mitochondrial cytochrome oxidase II gene among 10 orders of insects. *Molecular Phylogenetics and Evolution* **1**, 41–52. doi:10.1016/1055-7903(92)90034-E
- Livezey, B. C. (1989). Phylogenetic relationships and incipient flightlessness of the extinct Auckland Islands Merganser. *The Wilson Bulletin* **101**, 410–435.
- Lutzoni, F., Wagner, P., Reeb, V., and Zoller, S. (2000). Integrating ambiguously aligned regions of DNA sequences in phylogenetic analyses without violating positional homology. *Systematic Biology* **49**, 628–651. doi:10.1080/106351500750049743
- Maddison, W. (1993). Missing data versus missing characters in phylogenetic analysis. *Systematic Biology* **42**, 576–581.
- Maddison, W. P. (1997). Gene trees in species trees. *Systematic Biology* **46**, 523–536.
- Maddison, W. P., and Maddison, D. R. (2001). 'MacClade: Interactive Analysis of Phylogeny and Character Evolution, ver. 4.01.' (Sinauer, Sunderland, MA, USA.)
- Martin, S. J. (1989). Altitudinal distribution of burying beetles (Coleoptera, Silphidae) in the Southern Alps of Japan. *Japanese Journal of Entomology* **57**, 876–879.
- Mau, B. (1996). Bayesian phylogenetic inference via Markov chain Monte Carlo methods. Ph.D. Thesis, University of Wisconsin, Madison, WI, USA.
- Mau, B., and Newton, M. (1997). Phylogenetic inference for binary data on dendrograms using Markov chain Monte Carlo. *Journal of Computational and Graphical Statistics* **6**, 122–131.
- Mau, B., Newton, M., and Larget, B. (1999). Bayesian phylogenetic inference via Markov chain Monte Carlo methods. *Biometrics* **55**, 1–12. doi:10.1111/j.0006-341X.1999.00001.x
- Metropolis, N., Rosenbluth, A. W., Rosenbluth, M. N., Teller, A. H., and Teller, E. (1953). Equations of state calculations by fast computing machines. *The Journal of Chemical Physics* **21**, 1087–1091. doi:10.1063/1.1699114
- Minin, V., Abdo, Z., Joyce, P., and Sullivan, J. (2003). Performance-based selection of likelihood models for phylogeny estimation. *Systematic Biology* **52**, 674–683. doi:10.1080/10635150390235494
- Moore, W. S. (1995). Inferring phylogenies from mtDNA variation: mitochondrial gene trees versus nuclear-gene trees. *Evolution* **49**, 718–726.

- Naskrecki, P. (2001). 'MANTIS: A Manager of Taxonomic Information and Specimens. FileMakerPro Database.' Available online at: <http://140.247.119.145/Mantis/> [verified March 2006]
- Newton, M., Mau, B., and Larget, B. (1999). Markov chain Monte Carlo for the Bayesian analysis of evolutionary trees from aligned molecular sequences. In 'Monograph Series of the Institute of Mathematical Statistics. Statistics in Molecular Biology'. (Eds F. Seillier-Moseiwitch, T. P. Speed and M. Waterman.)
- Nishikawa, M. (1986). A review of the grouping within the tribe Nicrophorini, with a check-list of world species. *Kanagawa-Chuho, Kawasaki* **80**, 93–100.
- Nisimura, T., Kon, M., and Numata, H. (2002). Bimodal life cycle of the burying beetle *Nicrophorus quadripunctatus* in relation to its summer reproductive diapause. *Ecological Entomology* **27**, 220–228. doi:10.1046/j.1365-2311.2002.00400.x
- Nixon, K. C., and Carpenter, J. M. (1993). On outgroups. *Cladistics* **9**, 413–426. doi:10.1111/j.1096-0031.1993.tb00234.x
- Nixon, K., and Davis, J. (1991). Polymorphic taxa, missing values and cladistic analysis. *Cladistics* **7**, 233–241. doi:10.1111/j.1096-0031.1991.tb00036.x
- Nylander, J. A., Ronquist, F., Huelsenbeck, J. P., and Nieves-Aldrey, J. L. (2004). Bayesian phylogenetic analysis of combined data. *Systematic Biology* **53**, 47–67. doi:10.1080/10635150490264699
- Ôhara, M. (1992). Notes on the insects fauna of the Nagahashi Naeba area, Otaru, central Hokkaido, Japan, No. 1. -Coleoptera. *Bulletin of the Otaru Museum* **6**, 1–21.
- Ôhara, M. (1994a). On the beetles in Otaru, Hokkaido. *Hokkaido no Shizen to Seibutsu (Nature and Organisms of Hokkaido)* **9**, 59–65.
- Ôhara, M. (1994b). Notes of Insect in Mt. Yotei, Hokkaido. *Kutchansosyo* **14**, 1–89.
- Ôhara, M. (1995a). Notes on the insect fauna of the Nagahashi Naeba area, Otaru, central Hokkaido, Japan, No. 9. - Survey of the research in 1992 and 1993, and on the beetles collected by bait trap with dead chicken. *Bulletin of the Otaru Museum* **8**, 19–42.
- Ôhara, M. (1995b). Notes on insect fauna of the Okusawa-Suigenchi area, Otaru, central Hokkaido, Japan, No. 1. Coleoptera. *Bulletin of the Otaru Museum* **8**, 1–13.
- Ôhara, M. (1997). Notes on the insect fauna of the Niseko Mountains, central Hokkaido, Japan, No. 1. Survey of the research and records of beetles. *Bulletin of the Otaru Museum* **10**, 97–110.
- Ôhara, M., and Higashi, S. (1987). Interference by ground beetles with the dispersal by ants of seeds of *Trillium* species (Liliaceae). *Journal of Ecology* **75**, 1091–1098.
- Ôhara, M., and Yabuki, T. (1992). Insect faunal survey of Mt. Yotei, Hokkaido. - Coleoptera. *Bulletin of the Otaru Museum* **6**, 55–62.
- Ôhara, M., Miyashita, K., and Yabuki, T. (1995). Insect faunal survey of Mt. Yotei, Hokkaido. Coleoptera. *Bulletin of the Otaru Museum* **8**, 65–80.
- Patterson, C. (1982). Morphological characters and homology. In 'Problems in Phylogenetic Reconstruction'. (Eds K. A. Joysey and A. E. Friday.) pp. 21–74. (Academic press: London, UK.)
- Peck, S. B. (2001). Review of the carrion beetles of Australia and New Guinea (Coleoptera: Silphidae). *Australian Journal of Entomology* **40**, 93–101. doi:10.1046/j.1440-6055.2001.00216.x
- Peck, S. B., and Anderson, R. S. (1985). Taxonomy, phylogeny and biogeography of the carrion beetles of Latin America (Coleoptera: Silphidae). *Quaestiones Entomologicae* **21**, 247–317.
- Platnick, N. I., Griswold, C. E., and Coddington, J. A. (1991). On missing entries in cladistic analysis. *Cladistics* **7**, 337–343. doi:10.1111/j.1096-0031.1991.tb00042.x
- Portevin, G. (1920). Revision des Silphini et Nicrophorini de la région indo-malaise. *Bulletin du Muséum National d'Histoire Naturelle* **26**, 395–401.
- Portevin, G. (1923). Revision des Nicrophorini du globe. *Bulletin du Muséum National d'Histoire Naturelle* **29**, 64–309.
- Portevin, G. (1926). 'Les Grands Nérophages du Globe. Silphini – Necrodini – Nicrophorini. Encyclopédie Entomologique (A), Vol. 6.' (Lechevalier: Paris, France.)
- Posada, D., and Buckley, T. R. (2004). Model selection and model averaging in phylogenetics: Advantages of Akaike Information Criterion and Bayesian approaches over likelihood ratio tests. *Systematic Biology* **53**, 793–808. doi:10.1080/10635150490522304
- Posada, D., and Crandall, K. A. (1998). MODELTEST: Testing the model of DNA substitution. *Bioinformatics (Oxford, England)* **14**, 817–818. doi:10.1093/bioinformatics/14.9.817
- Rannala, B., and Yang, Z. (1996). Probability distribution of molecular evolutionary trees: a new method of phylogenetic inference. *Journal of Molecular Evolution* **43**, 304–311. doi:10.1007/PL00006090
- Rauter, C. M., and Moore, A. J. (2002). Quantitative genetics of growth and development time in the burying beetle *Nicrophorus pustulatus* in the presence and absence of post-hatching parental care. *Evolution* **56**, 96–110.
- Root, T. L., Price, J. T., Hall, K. R., Schneider, S. H., Rosenzweig, C., and Pounds, J. A. (2003). Fingerprints of global warming on wild animals and plants. *Nature* **421**, 57–60. doi:10.1038/nature01333
- Růžička, J., Háva, J., and Schneider, J. (2000). Taxonomical and distributional notes on Oriental Silphidae, with description of *Nicrophorus sausai* sp. n. (Insecta: Coleoptera). *Reichenbachia* **33**, 377–384.
- Sambrook, J., Fritsch, E. F., and Maniatis, T. (1989). 'Molecular Cloning: A Laboratory Manual.' 2nd edn. (Cold Spring Harbor Laboratory Press: Cold Spring Harbor, NY, USA.)
- Satou, A., Nisimura, T., and Numata, H. (2001). Cost and necessity of parental care in the burying beetle *Nicrophorus quadripunctatus*. *Zoological Science* **18**, 975–979. doi:10.2108/zsj.18.975
- Schawaller, W. (1977). Ergebnisse der Bhutan-Expedition 1972 des Naturhistorischen Museums in Basel. Coleoptera: Fam. Silphidae. *Entomologica Basiliensia* **2**, 259–260.
- Schawaller, W. (1982). Die Aaskäfer des Himalaya (Insecta: Coleoptera: Silphidae s. str.). *Senckenbergiana Biologica* **62**, 237–260.
- Scott, M. P. (1998). The ecology and behavior of burying beetles. *Annual Review of Entomology* **43**, 595–618. doi:10.1146/annurev.ento.43.1.595
- Semenov-Tian-Shanskij, A. (1933). De tribu Nicrophorini (Coleoptera, Silphidae) classificanda et de ejus distributione geographica. *Trudy Zoologicheskogo Instituta Akademii Nauk SSSR* **1**, 149–160.
- Serb, J. M., Phillips, C. A., and Iverson, J. B. (2001). Molecular phylogeny and biogeography of *Kinosternon flavescens* based on complete mitochondrial control region sequences. *Molecular Phylogenetics and Evolution* **18**, 149–162. doi:10.1006/mpev.2000.0858
- Sikes, D. S. (2003). A revision of the subfamily Nicrophorinae Kirby (Insecta: Coleoptera: Silphidae). Ph.D. Thesis, Department of Ecology and Evolutionary Biology, University of Connecticut, Storrs, CT, USA.
- Sikes, D. S., and Peck, S. B. (2000). Description of *Nicrophorus hispaniola*, new species, from Hispaniola (Coleoptera: Silphidae) and a key to the species of *Nicrophorus* of the New World. *Annals of the Entomological Society of America* **93**, 391–397.
- Sikes, D. S., Madge, R. B., and Newton, A. F. (2002). A catalog of the Nicrophorinae (Coleoptera: Silphidae) of the world. *Zootaxa* **65**, 1–304.
- Simmons, M. P., and Ochoterena, H. (2000). Gaps as characters in sequence-based phylogenetic analyses. *Systematic Biology* **49**, 369–381. doi:10.1080/10635159950173889

- Simon, C., Frati, F., Beckenbach, A., Crespi, B., Liu, H., and Flook, P. (1994). Evolution, weighting and phylogenetic utility of mitochondrial gene sequences and a compilation of conserved polymerase chain reaction primers. *Annals of the Entomological Society of America* **87**, 651–701.
- Smiseth, P. T., Darwell, C. T., and Moore, A. J. (2003). Partial begging: an empirical model for the early evolution of offspring signaling. *Proceedings of the Royal Society of London. Series B. Biological Sciences* **270**, 1773–1777. doi:10.1098/rspb.2003.2444
- Steppan, S. J. (1998). Phylogenetic relationships and species limits within *Phyllotis* (Rodentia: Sigmodontinae): Concordance between mtDNA sequences and morphology. *Journal of Mammalogy* **79**, 573–593.
- Stickney, F. S. (1923). The head-capsule of Coleoptera. *Illinois Biological Monographs* **8**, 1–104.
- Strong, E. E., and Lipscomb, D. (1999). Character coding and inapplicable data. *Cladistics* **15**, 363–371. doi:10.1111/j.1096-0031.1999.tb00272.x
- Swofford, D. L. (2002). 'PAUP*. Phylogenetic Analysis using Parsimony (*And Other Methods), version 4.0b10.' (Sinauer: Sunderland, MA, USA.)
- Trumbo, S. T., and Sikes, D. S. (2000). Sexual selection and leg morphology in *Nicrophorus orbicollis* and *Ptomascopus morio*. *Entomological Science* **3**, 585–589.
- Trumbo, S. T., Kon, M., and Sikes, D. (2001). The reproductive biology of *Ptomascopus morio*, a brood parasite of *Nicrophorus*. *Journal of Zoology* **255**, 543–560.
- Tuffley, C., and Steel, M. A. (1997). Links between maximum likelihood and maximum parsimony under a simple model of site substitution. *Bulletin of Mathematical Biology* **59**, 581–607. doi:10.1016/S0092-8240(97)00001-3
- Wiens, J. J. (1998). Does adding characters with missing data increase or decrease phylogenetic accuracy? *Systematic Biology* **47**, 625–640. doi:10.1080/106351598260635
- Wiens, J. J., and Penkrot, T. A. (2002). Delimiting species using DNA and morphological variation and discordant species limits in spiny lizards (*Sceloporus*). *Systematic Biology* **51**, 69–91. doi:10.1080/106351502753475880
- Wiens, J. J., and Reeder, T. W. (1995). Combining data sets with different numbers of taxa for phylogenetic analysis. *Systematic Biology* **44**, 548–558.
- Wilkinson, M. (1995a). Arbitrary resolutions, missing entries, and the problem of zero-length branches in parsimony analysis. *Systematic Biology* **44**, 108–111.
- Wilkinson, M. (1995b). Coping with abundant missing entries in phylogenetic inference using parsimony. *Systematic Biology* **44**, 501–514.
- Xu, H., and Suzuki, N. (2001). Effects of carcass size and parental feeding on reproductive success of the burying beetle *Nicrophorus quadripunctatus* (Coleoptera: Silphidae). *Entomological Science* **4**, 217–222.
- Yang, Z. (1993). Maximum likelihood estimation of phylogeny from DNA sequences when substitution rates differ over sites. *Molecular Biology and Evolution* **10**, 1396–1401.
- Yang, Z. (1994). Maximum likelihood phylogenetic estimation from DNA sequences with variable rates over sites: Approximate methods. *Journal of Molecular Evolution* **39**, 306–314. doi:10.1007/BF00160154
- Yang, Z., and Rannala, B. (1997). Bayesian phylogenetic inference using DNA sequences: a Markov chain Monte carlo method. *Molecular Biology and Evolution* **14**, 717–724.

Manuscript received 13 May 2005, revised and accepted 22 February 2006.

Appendix 1. Specimens from which DNA was extracted for sequencing of the *COII* mitochondrial gene

DNA voucher specimens are stored in the first author's collection at -80°C . Specimen ID codes correspond to specimen records in the project database and the labels associated with the specimens

| Species | Specimen ID | Country | GenBank No. |
|------------------------------------|---------------|----------|-------------|
| <i>Nicrophorus humator</i> | DSSC006372Nic | RUSSIA | AY825261 |
| <i>Nicrophorus humator</i> | DSSC006497Nic | RUSSIA | AY825262 |
| <i>Nicrophorus maculifrons</i> | DSSC006368Nic | JAPAN | AY826808 |
| <i>Nicrophorus maculifrons</i> | DSSC007293Nic | JAPAN | AY826809 |
| <i>Nicrophorus melissae</i> | DSSC006376Nic | NEPAL | AY826801 |
| <i>Nicrophorus melissae</i> | DSSC006377Nic | NEPAL | AY826802 |
| <i>Nicrophorus melissae</i> | DSSC006475Nic | NEPAL | AY826803 |
| <i>Nicrophorus montivagus</i> | DSSC006350Nic | JAPAN | AY826810 |
| <i>Nicrophorus nepalensis</i> | DSSC006374Nic | NEPAL | AY826804 |
| <i>Nicrophorus nepalensis</i> | DSSC006375Nic | NEPAL | AY826807 |
| <i>Nicrophorus nepalensis</i> | DSSC006463Nic | MALAYSIA | AY826805 |
| <i>Nicrophorus nepalensis</i> | DSSC006486Nic | MALAYSIA | AY826806 |
| <i>Nicrophorus podagricus</i> | DSSC006332Nic | MALAYSIA | AY826800 |
| <i>Nicrophorus podagricus</i> | DSSC006354Nic | MALAYSIA | AY826799 |
| <i>Nicrophorus quadripunctatus</i> | DSSC006198Nic | JAPAN | AY826813 |
| <i>Nicrophorus quadripunctatus</i> | DSSC006371Nic | RUSSIA | AY826814 |
| <i>Nicrophorus sayi</i> | DSSC006190Nic | USA | AY826797 |
| <i>Nicrophorus sayi</i> | DSSC006472Nic | USA | AY826798 |
| <i>Nicrophorus trumboi</i> | DSSC006325Nic | NEPAL | AY826811 |
| <i>Nicrophorus trumboi</i> | DSSC006345Nic | NEPAL | AY826812 |

Appendix 2. Museums and collections from which specimens were borrowed

| | |
|-----------------|--|
| AMNH | American Museum of Natural History, Central Park West at 79th St. New York, NY 10024–5192, USA |
| ANIC | Australian National Insect Collection CSIRO Division of Entomology, GPO Box 1700, Canberra, ACT 2601, AUSTRALIA |
| BMNH | Department of Entomology, The Natural History Museum, Cromwell Rd, London, SW7 5BD, UNITED KINGDOM |
| BPBM | Bishop Museum, 1525 Bernice St, Honolulu, HI 96817–0916, USA |
| CASC | California Academy of Sciences, Department of Entomology, San Francisco, CA 94118, USA |
| CMNC | Canadian Museum of Nature, Insects–Collection Division, PO Box 3443, Station ‘D’Ottawa, ON K1P 6P4, CANADA |
| CNCI | Canadian National Collection of Insects, Crop Protection Program, Eastern Cereal and Oilseeds Research Centre, K. W. Neatby Bldg, C.E.F. Ottawa, K1A 0C6, CANADA |
| CUIC | Cornell University Insect Collections, Dept. of Entomology, Cornell University, Ithaca, NY 14853, USA |
| DSSC | Private collection of Derek S. Sikes, Dept. Biological Sciences, University of Calgary, Calgary, AB, T2N 1N4 CANADA |
| EIHU (= SEHU) | Systematic Entomology, Faculty of Agriculture, Hokkaido University, Kita 9 Nisi 9, Kitaku, Sapporo 060, JAPAN |
| EMUS | Department of Biology, Utah State University, College of Science, Logan, UT 84322–5305, USA |
| FMNH | The Field Museum of Natural History, Roosevelt Rd at Lake Shore Drive Chicago, IL 60605–2496, USA |
| HNHM | Coleoptera Collection, Department of Zoology, Hungarian Natural History Museum, H-1088, Budapest, Baross u. 13, HUNGARY |
| ITLJ | Laboratory of Insect Systematics, National Institute of Agro-Environmental Sciences, Kannondai 3–1–1, Tsukuba Ibaraki, 305, JAPAN |
| IZCAS (IOZ-CAS) | Chinese Academy of Sciences, Institute of Zoology, Beijing, CHINA |
| JHC | Private collection of Jirí Háva, Branická 13, CZ-147 00, Praha 4, CZECH REPUBLIC |
| JRC | Private collection of Jan Růžička, Pod Královkou 7, CZ-169 00 Praha 6, Praha, CZECH REPUBLIC |
| JSC | private collection of Jan Schneider, Lipová 15, CZ-120 00, Praha 5, CZECH REPUBLIC |
| MCPM | Milwaukee Public Museum 800 West Wells St., Milwaukee, WI 53233, USA |
| MCZC | Museum of Comparative Zoology Harvard University, 26 Oxford St. Cambridge, MA 02138, USA |
| MNC | private collection of Masaaki Nishikawa, 27–1–115, Higashi-kashiwagaya 1, Ebina 243–04, JAPAN |
| MNHN | Museum National D’Histoire Naturelle, Laboratoire D’Entomologie, 45 rue Buffon, F-75005, Paris, FRANCE |
| MOC | Systematic Entomology, Faculty of Agriculture, Hokkaido University, Kita 9 Nisi 9 Kitaku, Sapporo 060, JAPAN |
| MSUC | Center for Insect Diversity Study, Museum Department of Entomology, 243 Natural Science, Michigan State University, East Lansing, MI 48824, USA |
| MVMA | Dept. of Natural Sciences Museum of Victoria, 71 Victoria Crescent, Abbotsford, Victoria, 3067, AUSTRALIA |
| MZHF | Zoological Museum, PO Box 17, FIN-00014 University of Helsinki, Helsinki, FINLAND |
| MZLU | Museum of Zoology, Department of Zoology, Division of Systematics, Lund University, Helgonavagen 3, S-233 62 Lund, SWEDEN |
| NHMW | Naturhistorisches Museum Wien, Zweite Zoologische Abteilung-Insekten, Burgring 7 A-1014, Wien, AUSTRIA |
| NHRS | Naturhistoriska Riksmuseet of Natural History, Sektion För entomologi Box 50007, 104 05 Stockholm, SWEDEN |
| NKUM | Dept. of Biology, Nankai University, Tianjin 300071, P. R. CHINA |
| NMNH (= USNM) | National Museum of Natural History, Smithsonian Institution, Dept. Entomology, Collections Management Unit, NHB MRC 165; 10th & Constitution Ave. N. W. Washington, D. C. 20560, USA |
| NMNS | National Museum of Natural Science1, Kuan-Chein Rd., Taichung, Taiwan, R.O.C. TAIWAN |
| NMPC | Národní Muzeum, Entomologicke Odd. PM, Golcova 1, Kunratice 148 00 Praha 4, CZECH REPUBLIC |
| NSMT | National Science Museum, Hyakunin-cho 3–23–1, Shinjuku-ku, Tokyo, JAPAN |
| SBPC | private collection of Stewart Peck, Department of Biology, Carleton University, 1125 Colonel By Drive, Ottawa, Ontario K1S 5B6 Ottawa, CANADA |
| SEMC | Snow Entomological Museum, Natural History Museum, University of Kansas, Lawrence, KS 66045, USA |
| SMFD (= SMFC) | Forschungsinstitut Senckenberg, Entomologie I, Senckenberganlage 25 D-60325 Frankfurt /M., F. R. GERMANY |
| SMNS | Staatliches Museum für Naturkunde in Stuttgart, Rosenstein 1, D-70191, Stuttgart 1, F. R. GERMANY |
| SMTD | Staatliches Museum für Tierkunde, Augustusstraße 2, D-01067 Dresden, F. R. GERMANY |
| TAMU (= UWFC) | Insect Collection, Dept. of Entomology, Texas A&M University, College Station, TX 77843, USA |
| TARI | Insect Collection, Taiwan Agricultural Research Institute, 189 Chungcheng Rd. Wufeng, Taichung Hsien, Taiwan 431, Taiwan, R. O. CHINA |
| UCDC | R. M. Bohart Museum of Entomology, University of California, 1124 Academic Surge, Davis, California, 95616, USA |
| UMRM | Wilbur R. Enns Entomology Museum, Dept. of Entomology, University of Missouri, Columbia, MO 65211, USA |
| WBC | private collection of Wolfgang Barries. Kinzerplatz 10–11/3/3/9, A – 1 2 1 0, Wien, AUSTRIA |
| ZMAN | Instituut voor Taxonomische Zoölogie, Zoölogisch Museum, Universiteit van Amsterdam, Afdeling Entomologie, Plantage Middenlaan 64, 1018 DH, Amsterdam, The NETHERLANDS |
| ZMAS | Russian Academy of Sciences, Zoological Institute, 199034, Universitetskaya nab., 1, St. Petersburg, RUSSIA |
| ZMHB | Museum für Naturkunde der Humboldt-Universität zu Berlin, D-10115 Berlin, Invalidenstr. 43, Berlin, F. R. GERMANY |
| ZMUC | Zoologisk Museum, Universitetsparken 15, DK 2100 Kobenhavn O., Kobenhavn, DENMARK |
| ZSMC | Zoologische Staatssammlung Münchhausenstraße 21, D-81247, München, München, F. R. GERMANY |
